HOLOCENE STRATIGRAPHY AND SEDIMENTATION OFF THE GREAT WHALE RIVER ENTRANCE, SOUTHEASTERN HUDSON BAY

by

Nicole Gonthier

Department of Geological Sciences McGill University, Montreal

March, 1992

A Thesis submitted to the Faculty of Graduate Studies and Research in partial fulfillment of the requirements for the degree of Master in Science (Geology).

ABSTRACT

The regional distribution of Holocene sediments of eastern Hudson Bay off the Great Whale River mouth was mapped using a grid of reflection seismic lines over 60 km long and covering an area of approximately 800 km² and data from eight piston cores. A larger data base and a greater area of study than that used in previous studies significantly increases our understanding of the sedimentation and deglaciation processes that have occurred in the area since the last deglaciation. Based on the seismic records and piston cores, four stratigraphic units overlying the Proterozoic bedrock (unit 1) were defined and interpreted: unit 2, glacial till deposited by a westward flowing ice sheet; unit 3, glaciolacustrine stratified muds deposited in glacial Lake Ojibway; unit 4, postglacial marine muds deposited in Tyrrell Sea; unit 5, distal fluvio-deltaic sediments from the Great Whale River. Textural and geochemical analyses of individual laminae suggest that unit 3 rhythmites are true varves; dark "summer" laminae were deposited mainly by underflows during the open water season, and light "winter" laminae were deposited by overflows-interflows under a seasonal ice cover. Unit 5 covers approximately 400 km² and occurs as a deltaic constructional wedge which reaches 11 km offshore of the Great Whale River entrance. It was deposited between 3500 BP and 2800 BP from material supplied by the erosion of the Sakami Moraine and of glaciolacustrine and marine muds exposed along the river banks.

RÉSUMÉ

La distribution régionale des sédiments holocènes de l'est de la baie d'Hudson face à l'embouchure de la Grande rivière de la Baleine a été cartographiée à l'aide d'une grille de lignes de relevés sismiques de plus de 60 km et couvrant une surface d'environ 800 km², ainsi que de huit carottes à pistons. Une plus grande base de données et une plus grande aire d'étude que celles utilisées dans les études antérieures ont augmenté de façon significative notre compréhension des processus de de sedimentation et de déglaciation qui se sont produits dans la région depuir la dernière déglaciation. A partir des relevés sismiques et des carottes à pistons, quatre unités stratigraphiques reposant sur le socle protérozoïque (unité 1) ont été définies et interprétées unité 2, un till déposé par un glacier ayant progressé vers l'ouest; unité 3, des boues glaciolacustres stratifiées déposées dans le lac glaciaire Ojibway; unité 4, des boues marines postglaciaires déposées dans la mer de Tyrrell, unité 5, des sédiments fluvio-deltaiques distants provenant de la Grande rivière de la Baleine. Des analyses granulométriques et géochimiques faites sur des laminations individuelles suggèrent que les rhythmites de l'unité 3 sont des varves; les couches foncés d'"été" ayant été déposées principalement par des courants de densité s'écoulant le long du fond durant la saison d'eau libre, et les couches pâle d'"hiver" ayant été transportée en suspension le long d'interfaces thermiques sous un couvert de glace saisonnier L'unité 5 couvre approximativement 400 km² et forme un prisme de déposition s'étendant jusqu'à 11 km de l'embouchure de la Grande rivière de la Baleine. Sa déposition s'est produite entre 3500 BP et 2800 BP à partir d'une source de sédiments fournis par l'érosion en amont de la moraine de Sakami ainsi que de boues glaciolacustres et marines exposées le long du chenal de la rivière.



AKNOWLEDGEMENTS

First, I thank my thesis adviser Dr. Bruno d'Anglejan for his supervision, guidance, and advice rendered during this study, and his critical review of the thesis. I also thank the other member of the thesis committee, Heiner Josenhans, for his helpful comments, suggestions, and guidance with the seismic records interpretation.

I sincerely thank the officers and crew of CSS Hudson and CCGS Narwhal for their assistance at sea and the technicians from the Atlantic Geoscience Centre who helped with sampling and equipment operation during the cruise.

I am grateful to Mark Fay for doing the X-ray photographs of the slab and to R. Ramesh who performed the X-ray diffractogram analyses. I am also grateful to CSSA Consultants Ltée for financing the drafting of the isopach maps. Daniel R. Suchy contributed in a large part to the drafting of the other figures.

I would like to thank Stéphane Lorrain for his assistance at sea and at the department, and Marlène Charland for her friendship and encouragment. Finally, I would like to thank my husband Daniel R. Suchy for his precious moral support, love and caring during the whole project without which the realization of this thesis would not have been possible. I dedicate this thesis to Martine Gonthier and to Arianne Suchy. Financial support for this project was provided by grants from Energy Mines and Resources Canada and the National Sciences and Research Council to B. d'Anglejan.

PREFACE

1. STATEMENT OF ORIGINALITY

This work represents the first comprehensive study on the seismostratigraphy and sedimentology of the region fronting the Great Whale River mouth. Chapter 2 provides an overview of the distribution, acoustic properties, and physical characteristics of the Quaternary sediments in this area, and allows a better understanding of the depositional processes of the different units. It also makes it possible to extend offshore the stratigraphy of Quaternary deposits previously established onshore. Chapter 3 attemps to provide a better understanding of the depositional environment and processes of unit 3. Collectively, the two main chapters contribute new knowledge to our understanding of the last deglaciation period of the southeastern Hudson Bay region.

2. HISTORICAL BACKGROUND OF PREVIOUSLY RELEVANT WORK

An extensive historical background can be found in the the General Introduction.

3. THESIS FORMAT

The thesis consists of a general introduction, two main chapters, and general conclusions. Chapter 2 has been written in a format suitable for publication in the journal <u>Géographie physique et Quaternaire</u> and is to be submitted soon. It therefore contains its own introduction and presentation of the Regional Geology and Physiography, Instruments and Methods. Results, Discussion, and Conclusions. Because of the thesis format adopted, some information within Chapter 2 is repeated in the General Introduction and in other parts of the thesis. However, efforts were made to reduce duplication to a minimum. References cited in Chapter 2 have been included in the list of references cited at the end of the thesis

TABLE OF CONTENTS

Pa	ge
ABSTRACT RÉSUMÉ ACKNOWLEDGEMENTS FREFACE	i ii N
CHAPTER 1. GENERAL INTRODUCTION	1
REGIONAL DESCRIPTION	15
CHAPTER 2. SEISMO-STRATIGRAPHY AND SEDIMENTOLOGY OF HOLOCENE SEDIMENTS OFF THE GREAT WHALE RIVER	4.6
(SOUTHEASTERN HUDSON BAY)	16
INTRODUCTION REGIONAL GEOLOGY AND PHYSIOGRAPHY INSTRUMENTS AND METHODS ACOUSTIC STRATIGRAPHIC UNITS Unit 1: Bedrock Unit 2: Ice Contact Sediments Unit 3: Ice Proximal Sediments Unit 4: Ice Distal Sediments Unit 5: Distal Fluvio-Deltaic Sediments LITHOSTRATIGRAPHIC CHARACTERISTICS OF THE UNITS Unit 2: Ice Contact Sediments Unit 3. Ice Proximal Sediments Unit 4. Ice Distal Sediments Unit 5: Distal Fluvio-Deltaic Sediments	16 18 21 22 26 37 40 48 57 62 63 72 76
CHAPTER 3. THE ICE PROXIMAL SEDIMENTS OF UNIT 3	79
INTRODUCTION	79 82 82 88 88

Core 69	92
DISCUSSION	95
Depositional Environment	95
Depositional Processes	102
CONCLUSIONS	104
CHAPTER 4. GENERAL CONCLUSIONS	107
REFERENCES CITED	111
APPENDIX 1	120
APPENDIX 2	128

LIST OF FIGURES

FIGU	PRE	Page
1.	Locality and bathymetry map	3
2.	Generalized map of bedrock geology	5
3.	Map of surface water circulation in Hudson Bay	7
4.	Map of maximal sea level altitude of Tyrrell Sea	12
5.	Map of seismic reflection tracks and core sites	13
6.	Total Quaternary sediment isopach map	23
7.	Seismic profile A-A'	27
8.	Seismic profile B-B'	29
9.	Seismic profile C-C'	31
10.	Seismic profile D-D'	33
11.	Isopach map of unit 2 (ice-contact sediments)	35
12.	Isopach map of unit 3 (ice proximal sediments)	38
13.	Isopach map of unit 4 (ice distal sediments)	41
14.	Isopach map of unit 5 (distal fluvio-deltaic sediments)	43
15.	Seismic profile E-E'	46
16.	Lithostratigraphy of core 47	49
17.	Lithostratigraphy of core 48	51
18.	Lithostratigraphy of core 69	53
19.	Lithostratigraphy of core 43	55
20.	Graph of grain size variations in laminae of unit 3 in core 18	59



21.	Deltaic sand distribution along lower Great Whale River	68			
22.	Correlation between onshore and offshore stratigraphy	73			
23.	Lithostratigraphy of unit 3 in core 43	83			
24.	Graph of grain size variations in laminae of unit 3 in core 43	85			
25.	Lithostratigraphy of unit 3 in core 47	90			
26.	Lithostratigraphy of unit 3 in core 48	91			
27.	Lithostratigraphy of unit 3 in core 69	94			
28.	Plot of mean grain size versus arithmetic quartile deviation in samples from core 48	99			
29.	Plot of mean grain size versus arithmetic quartile deviation in samples from core 43	100			
TABLES					
1.	X-ray fluorescence results on laminae of unit 3 in core 43	87			
2.	Total carbon and sulfur concentrations in laminae of unit 3 in cores 43 and 48	89			
3.	X-ray fluorescence results on laminae of unit 3 in core 48	03			

CHAPTER 1

GENERAL INTRODUCTION

During the Late Wisconsinan, the Hudson Bay region was covered by the Laurentide Ice Sheet. Early deglaciation of the bay was marked in the south by the formation of proglacial lakes Agassiz and Ojibway (Vincent and Hardy, 1977). Between 8400 to 8000 BP, the ice retreat allowed the penetration of marine waters through Hudson Strait, and the development of the Tyrrell Sea (Dyke and Prest, 1987). Hudson Bay is today a remnant of the Tyrrell Sea.

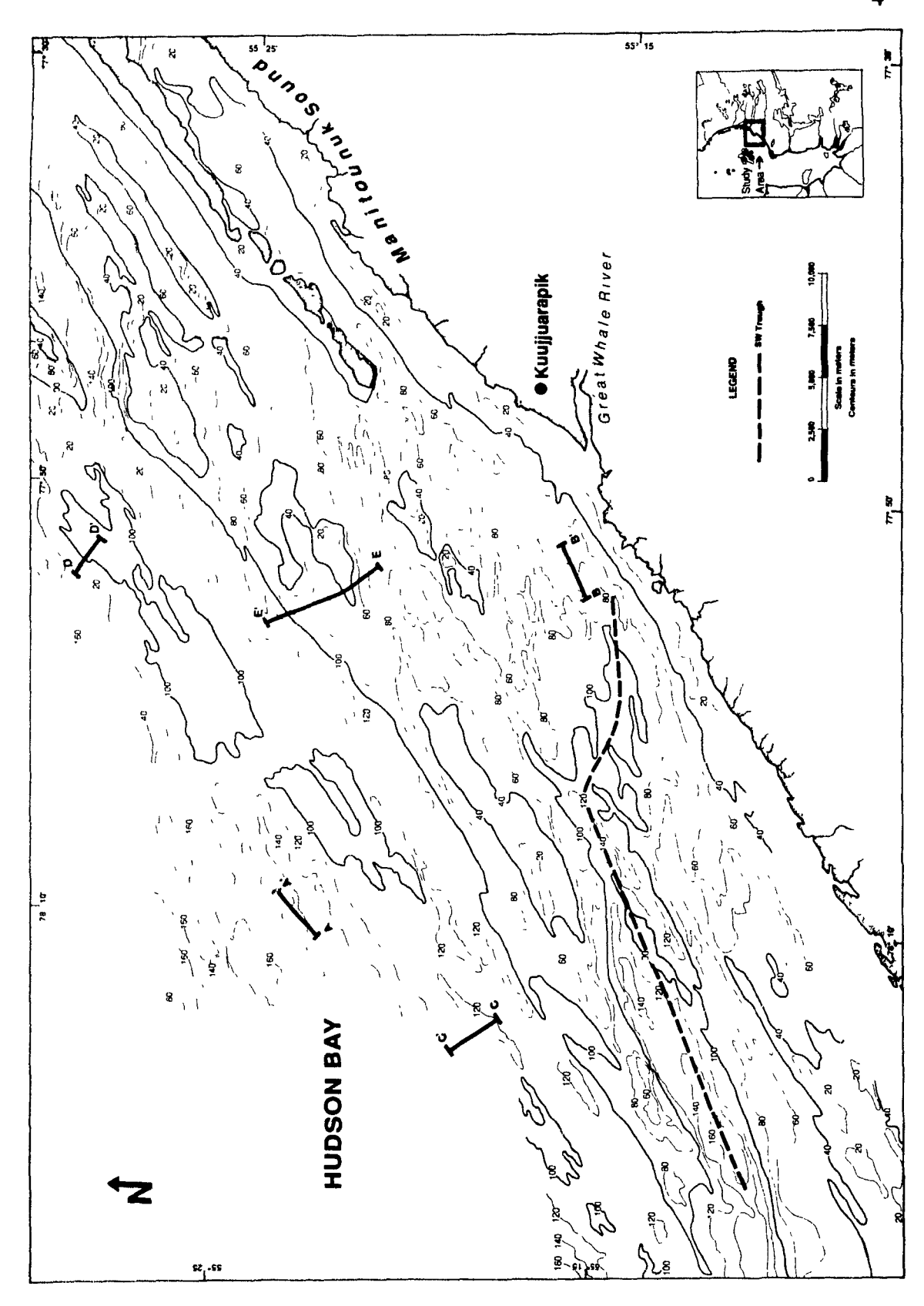
The present study discusses the stratigraphy, the distribution, and the facies of Holocene sediments in southeastern Hudson Bay, off the Great Whale River entrance, between 55°10' and 55°30' North latitude, and 78°20' and 77°30' West longitude, (Figure 1). This offshore stratigraphy is correlated with the sequence established along the Great Whale River banks by Hillaire-Marcel (1976).

REGIONAL DESCRIPTION

Hudson Bay is a large (637,000 km²), shallow (<230 m) epicontinental basin situated in the central part of the Precambrian Canadian Shield (Josenhans and Zevenhuizen, 1990). Its basement consists of Paleozoic carbonate rocks, except for the southeastern part of the bay in which Proterozoic metavolcanic and metasedimentary formations are exposed (Figure 2). Archean metamorphosed crystalline bedrock crop out along the bay coastline except in the southwest where the Paleozoic carbonate rocks are exposed (Figure 2) (Pelletier, 1986; Shilts, 1986). The basement in the bay is overlain by a generally thin (<5m) layer of Holocene glacial and post-glacial sediments, which Josenhans *et al.* (1988) have divided into three acoustic stratigraphic units: glacial till (unit 3), glaciomarine stratified sediments (unit 4), and postglacial basinal muds (unit 5). Their units 1 and 2 respectively refer to the Archean and to the Proterozoic bedrock.

The physiography of the study area (Figure 1) is dominated by parallel ridges and troughs running northeast-southwest with a maximum relief of around 120 m. The ridges form discontinuous rises, of which six have elevations less than 20 m below MSL within 14 km of the shoreline. These appear to be similar to the NE-SW oriented Proterozoic cuestas of the Manitounuk Islands located northeast of the Great Whale River (Figure 1). The cuestas consist of westward-dipping strata of dolomitic carbonates, quartzose sandstones, and basaltic rocks (Kranck, 1951; Biron, 1972; Allard and Tremblay, 1983), and form the western boundary of the Manitounuk Sound (Figure 1) which has an average width of 1.5 km and an

Figure 1. Location map, showing generalized bathymetry of the area fronting the Great Whale River. Heavy dark lines indicate the positions of seismic sections referenced in the text and shown in Figures 7-10 and 15.



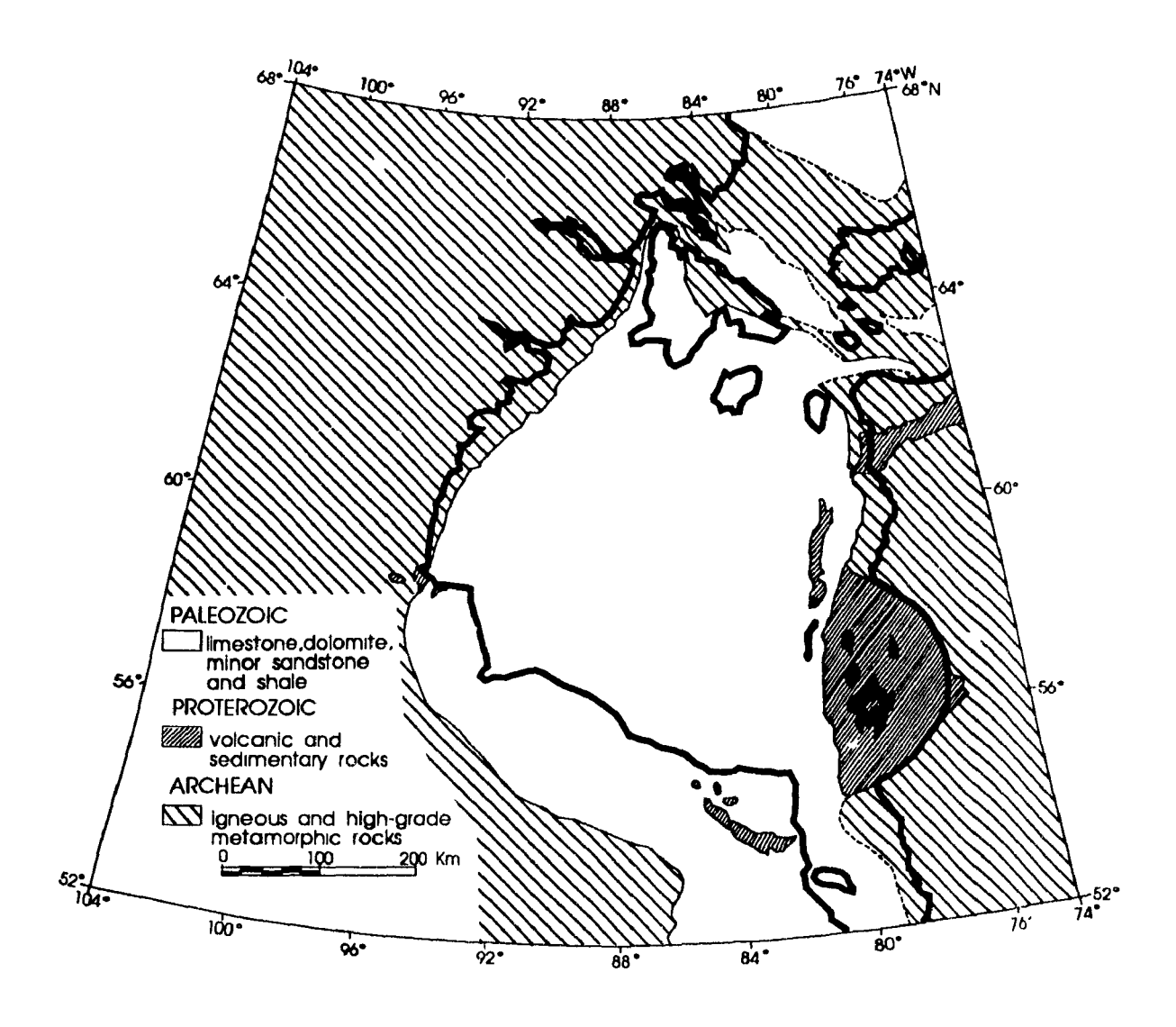


Figure 2. Generalized map of the bedrock geology of the Hudson Bay region (moclified from Henderson, 1989).

approximate length of 58 km (Allard and Tremblay, 1983). In the southwestern part of the study area, the general trend of the ridges is cut by a west-southwest oriented trough, which is generally aligned with the axis of the Great Whale River channel (Figure 1). The morphology of the area apparently reflects pre-glacial erosion controlled by bedrock composition and structural trends (Pelletier, 1986). The regional geology and physiography of the area are discussed at more length in Chapter 2.

Surface circulation of Hudson Bay is wind-driven and cyclonic during the The circulation below the surface layer follows the same general summer. directions but is influenced by bottom topography (Prisenberg 1986a). Arctic water flows into the northern and western parts of the bay through Foxe Channel and Roes Welcome Sound, while Hudson Bay water flows out through Hudson Strait into the Labrador Sea (Figure 3). The summer surface waters of the bay display large spatial variability in temperature and salinity because of the influx of cold and saline waters from the north and the freshwater runoff from the south (Prisenberg, 1986b). In the northern and western regions, temperatures are ≤ 6°C, with salinities reaching 30%, while in the central and southeastern regions, temperatures may exceed 8°C and salinities may be as low as 24‰ (Prisenberg, 1986b). Winter is also marked by latudinal gradients in temperature and salinity under an ice cover that begins to form in November in the north of the bay and in December in the south, and that breaks up around June in both areas (Markham, 1986). In late summer, the water column becomes stratified; the surface layer

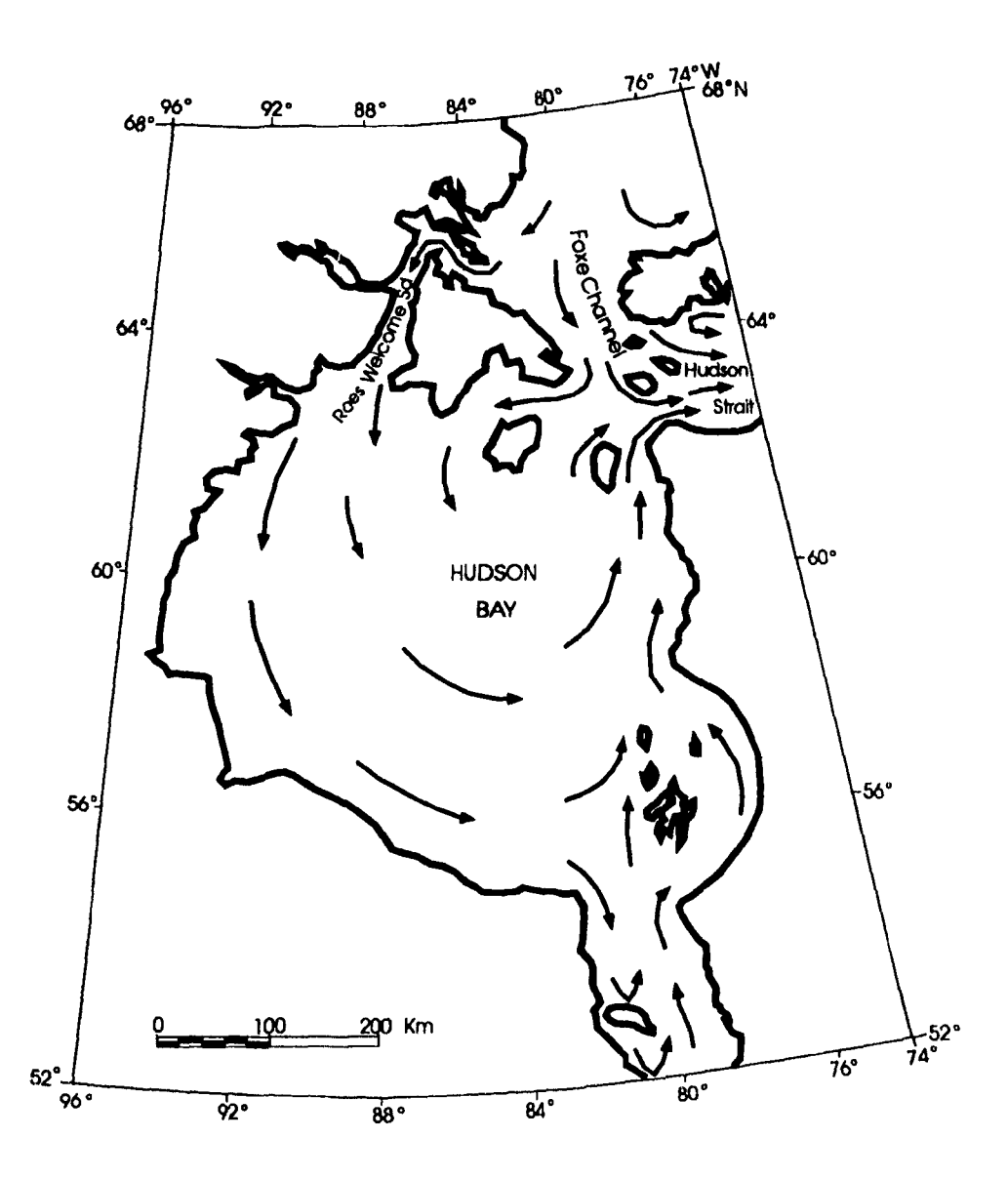


Figure 3. Map showing present surface water circulation in Hudson Bay. (Modified from Prinsenberg, 1986a).

overlies a relatively homogenous bottom layer (32% and -1.5°C) that originates in Foxe Basin (Leslie, 1964; Prisenberg, 1986a).

With a 42,700 km² watershed, the Great Whale River is one of the major rivers entering Hudson Bay (Thibault, 1989). It flows westward over a distance of 726 km (Thibault, 1989) from headwaters located at an elevation of 400 m at Lake Bienville. It has a mean annual freshwater discharge of approximately 700 m³/s, with a maximum of 1300 m³/s in June and a minimum of 200 m³/s in March (Ingram, 1981). Due to relatively weak tidal currents (<10 cm/s) and the large mean freshwater discharge velocity, the river forms an extensive freshwater plume all year round (Ingram and Larouche, 1987). Its suspended load discharge is estimated to be in the order of 0.5 x 10⁶ t.yr⁻¹, with offshore sedimentation rates of 2 to 3 mm.yr¹ (d'Anglejan and Biksham, 1988). Low water depths of 1 m to 1.5 m are recorded at the river mouth due to the presence of a sandbar, while upstream depths do not exceed 7 m in the center of the channel downstream of the first rapids, about 12 km east of the entrance (Ingram, 1981). Seaward of the sandbar, depth increases rapidly to over 60 m within 3 km of the shore (Ingram, 1981). The village of Kuujjuarapik is situated on a prograding sand barrier on the north shore at the river mouth (Figure 1). As explained in Chapter 2, longshore processes have favored the seaward progradation and southward expansion of the sand barrier resulting in a southward migration of the river channel (Figure 23, chapter 2).

The Great Whale River region is characterized by a subarctic climate, with

a mean yearly temperature of -4.3°C. The minimum is reached in January (mean of -22.5°C) and the maximum in July (mean of +10.5°C). The yearly average precipitation is about 63.7 cm of which 38% falls as snow (Thibault, 1989). The vegetation in the first 25 km from the coast consists of a forest tundra where the forest cover is patchy and located only in favorable protected sites (Filion and Morisset, 1984). East of that coastal strip, the remainder of the river watershed is characterized by an open boreal forest cover, mainly of black spruce, over more than 50% of the surface, with a thick ground cover of lichen (Filion and Morisset, 1984).

PREVIOUS WORK

Only limited investigations have been made to date of the marine geology and geophysics of Hudson Bay. In 1961, the Marine Science Branch (Dept. Mines Tech. Surv.), in collaboration with the Geological Survey of Canada, undertook the first reconnaissance survey of the entire bay. It was followed in 1965 by a more intensive program (Leslie, 1964; Leslie and Pelletier, 1965; Pelletier 1966). These studies provided a general background knowledge on the geology, geophysics and oceanography of Hudson Bay. The results are presented in Pelletier *et al.* (1968) and Pelletier (1986).

In 1971, Aquitaine Company of Canada Limited, in collaboration with the Geological Survey of Canada, conducted more detailed acoustic studies of the bay

(Lewis and Sanford, 1972). More recently, a multi-year geophysical and geological program was initiated by the Atlantic Geoscience Centre of the Geological Survey of Canada. Its purpose was to map the regional stratigraphy and the distribution of the Quaternary sediments (Josenhans *et al.*, 1988; Zevenhuizen and Josenhans, 1988; Josenhans and Zevenhuizen, 1990; Josenhans *et al.*, 1991) as well as the underlying bedrock (Grant and Sanford; 1988, Sanford and Grant, 1990).

Previous sedimentological studies in the Great Whale River region were confined to sediments exposed along the river banks. Cailleux and Hamelin (1970) first provided an overview of the geomorphology of the region by describing the Archean bedrock (with glacial striae and crag-and-tails indicating a westward ice flow), the Proterozoic cuestas, the 30 to 40 m high sandy to silty terraces at the river mouth, and the sand dunes. They later made an attempt to trace the positions of the coastline at different times during the last 6000 years (Hamelin and Cailleux, 1972). Portmann (1971) also described the regional geomorphology, and Portmann (1970 and 1972) interpreted the general stratigraphy along the lower river banks as consisting of basal marine clays, overlain by a glacial complex (clayey moraine upstream and banded clays downstream), with deltaic sands on top.

Hillaire-Marcel and de Boutray (1975) modified the above stratigraphy.

They established that ice contact deposits (composed of sandy gravel) associated with proglacial sands were at the base of the sequence, and were covered by

lacustrine sediments (varves). Marine clays and deltaic sands complete the sequence. The ice contact deposits were later attributed to the northern extension of the Sakami Moraine, a "re-equilibration" feature linked to ice recession (Hillaire-Marcel et al., 1981). As the ice receded, emergence due to isostatic uplift raised former marine limits to elevations above present sea level which reached a maximum of 315 m between Little Whale and Great Whale rivers (Figure 4) (Vincent et al., 1987; Hillaire-Marcel, 1976). An emergence curve was established from a sequence of raised beach terraces situated at the entrance to Richmond Gulf which is located between approximately 56°00' to 56°30' North latitude and 75°00' to 75°30' West longitude (Figure 4). The rate of land emergence was found to have fallen from about 6 cm/y for the first 4700 years to about 1.1 cm/y at around 2800 BP (Hillaire-Marcel and Fairbridge, 1978; Hillaire-Marcel, 1980). The present emergence rate is still at the latter value (Hillaire-Marcel, 1976; Hillaire-Marcel and Fairbridge, 1978; Hillaire-Marcel, 1980). Similar conclusions are presented by Hillaire-Marcel and Vincent (1980) and by Vincent et al. (1987)

Recently, Bilodeau *et al.* (1991) made detailed microfaunal and palynological analyses of Quaternary sediments exposed along the Great Whale River lower bank as well as of piston core 69 collected in the study area (Figure 5) at a depth of 165 m (EMR CSS-HUDSON 87-028/87-031 Data Report). They concluded that the varves of Lake Ojibway extend offshore, and that the sand layer that overlay them along the river banks is the result of a major slump rather than recording the drainage of Glacial Lake Ojibway, as previously reported by

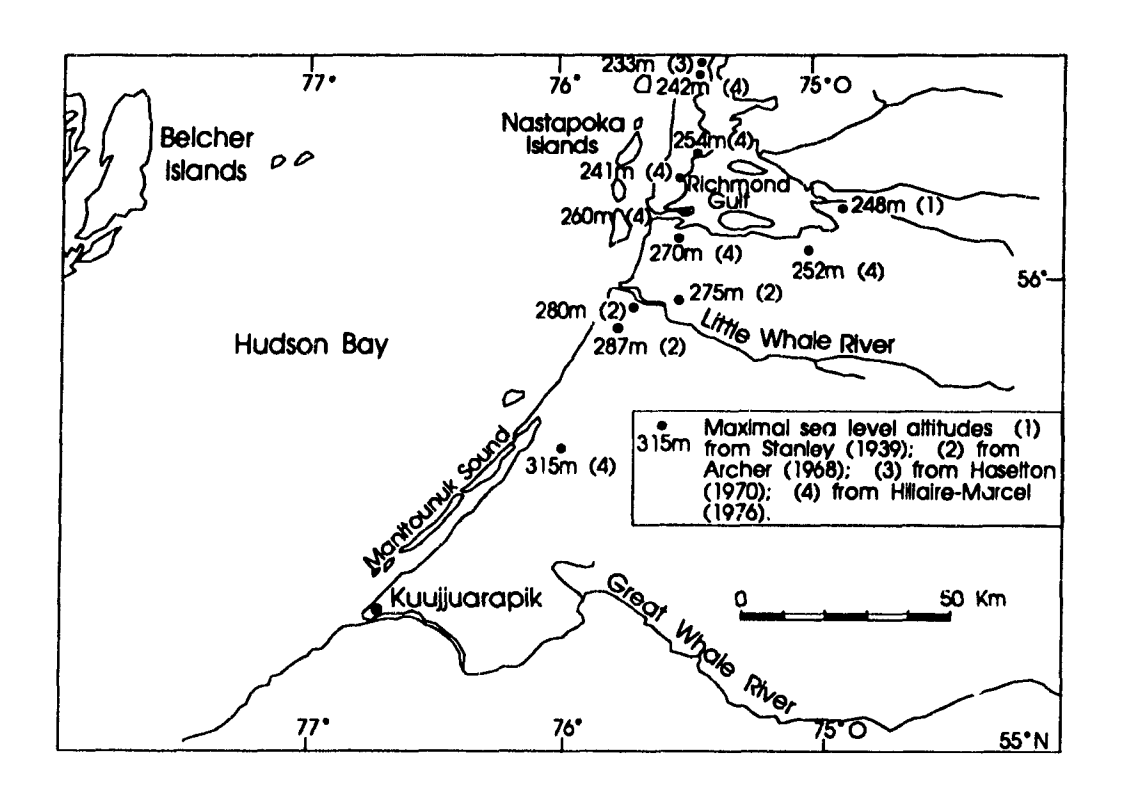
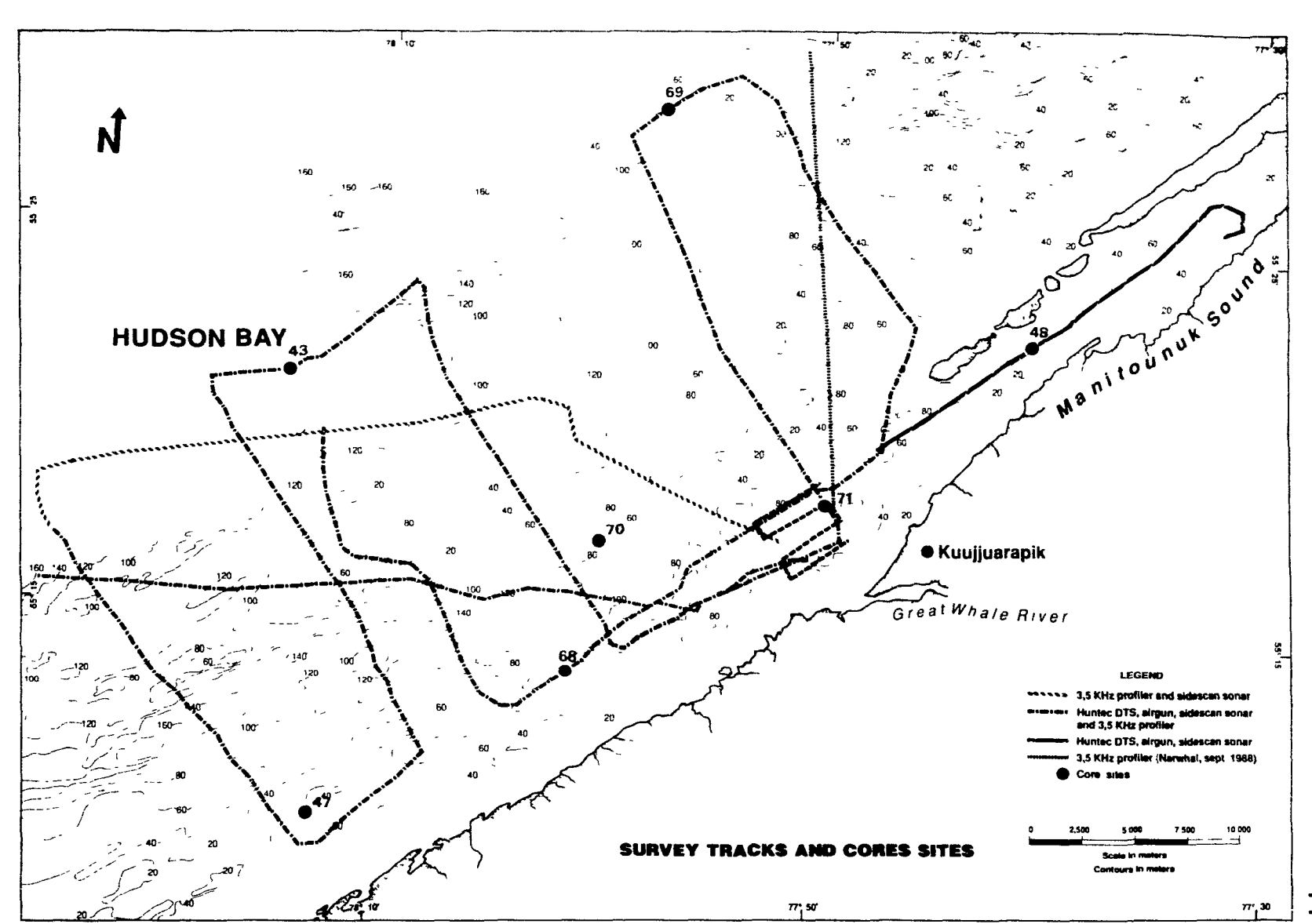


Figure 4. Altitude of Tyrrell Sea marine limit in the region north of the Great Whale River (Modified from Hillaire-Marcel, 1976).

Figure 5. Seismic reflection tracks and core sites.



OBJECTIVES

The general purpose of this study is to provide additional information to better interpret the Holocene deglaciation history of southeastern Hudson Bay coastline. To achieve it, the following objectives were set:

- 1) Examine the regional stratigraphy and distribution of the Holocene sediments offshore of the Great Whale River entrance using reflection seismic profiles and piston cores (Figure 5).
- 2) Identify each facies present on the basis of their acoustic signature, and of their textural properties and composition.
- Determine the depositional processes and environments of each facies, particularly in regard to the rhythmic sediments (unit 3) which are presumed to be lacustrine.
- 4) Correlate the offshore stratigraphic sequence with that established onshore by previous authors.

CHAPTER 2 SEISMO-STRATIGRAPHY AND SEDIMENTOLOGY OF HOLOCENE SEDIMENTS OFF THE GREAT WHALE RIVER (SOUTHEASTERN HUDSON

INTRODUCTION

BAY)

In recent years, sedimentological studies in southeastern Hudson Bay have provided a major insight into the deglaciation history of North America. Precise rates of relative sea level changes, of the ice margin retreat and of post-glacial uplift were obtained from the geometry and age relationships of raised beach terraces near Richmond Gulf (Hillaire-Marcel, 1976). In the Great Whale River basin, early work on regional morphology by Cailleux and Hamelin (1970) and by Portmann (1970, 1971, 1972) were followed by a stratigraphic interpretation of the postglacial sediments exposed along the lower river banks (Hillaire-Marcel and de

Boutray, 1975; Hillaire-Marcel, 1976; Hillaire-Marcel and Vincent, 1980). There, lacustrine varved sediments attributed to glacial Lake Ojibway are lying above ice contact deposits shown to be the northern extension of the Sakami Moraine, a "reequilibration" feature linked to ice recession (Hillaire-Marcel *et al.*, 1981). The lacustrine varved sediments are overlain by Tyrrell Sea marine clays, which in turn are overlain by thick proglacial deltaic sands that record a phase of active erosion and sediment transport through the Great Whale River channel during land emergence.

Offshore of the Great Whale River, little information was available until recently. A detailed bathymetric survey by the Canadian Hydrographic Office (Thompson et al., 1985a; 1985b; 1985c) has now provided us with new insight on the sea-floor morphology in southeastern Hudson Bay. Following earlier reconnaissance work by Leslie (1964), Leslie and Pelletier (1965), and Pelletier (1966), the Atlantic Geoscience Centre of the Geological Survey of Canada initiated in 1987 a multiyear geophysical and geological program in Hudson Bay, with the purpose of mapping the regional stratigraphy and the distribution of Quaternary sediments (Josenhans et al., 1988; Josenhans and Zevenhuisen, 1990, Bilodeau et al., 1990), and of developing a general deglaciation model.

As an outcome of this program, this paper discusses the distribution and seismostratigraphy of the late glacial and post-glacial Quaternary sediments in the region fronting the Great Whale River entrance, including part of the Manitounuk Sound, between 55°10' and 55°30' north latitude, and between 78°20' and 77°30'

east longitude (Figure 1). The conclusions are based on interpretation of reflection seismic profiles and on stratigraphic control provided by piston cores. The objectives are to examine the processes of ice retreat and of post-glacial sedimentation in the light of the offshore stratigraphy and to relate that stratigraphy to the onshore one.

REGIONAL GEOLOGY AND PHYSIOGRAPHY

Hudson Bay is a large (637,000 km²), shallow (<230 m) saucer-shaped basin (Josenhans and Zevenhuizen, 1990). The bedrock consists of Paleozoic carbonate rocks throughout most of the Bay except in its southeastern part where Proterozoic metavolcanic and metasedimentary formations occur. They lie unconformably on an Archean metamorphosed crystalline terrain that forms much of the Hudson Bay coastline (Figure 2) (Pelletier, 1986; Shilts, 1986). The Manitounuk Islands located northeast of the Great Whale River (Figure 1) are NE-SW oriented cuestas formed by erosion of the westward-dipping Proterozoic rocks, which consist of dolomitic carbonates, quartzose sandstones, and basaltic flows (Kranck, 1951; Biron, 1972; Allard and Tremblay, 1983). The bedrock in Hudson Bay is overlain by unconsolidated glacial and post-glacial sediments that were deposited predominantly during and after the Wisconsinan glaciation (Josenhans *et al.*, 1988).

Figure 1 shows the bathymetry of the study area based on recent surveys

by the Canadian Hydrographic Service (Thompson *et al.*, 1985a, 1985b, 1985c) for the bay, and by Hydro-Québec (Service des relevés techniques) for the Manitounuk Sound. The general physiography, which consists of a succession of ridges and troughs running in a NE-SW direction with a maximum relief of approximately 120 m, is generally similar to that of the Proterozoic cuestas of the Manitounuk Islands. The ridges form discontinuous rises, six of which have elevations to within less than 20 m below MSL within 14 km of the shoreline.

The state of the s

THE REPORT OF THE PROPERTY OF

To the southwest, the Great Whale River channel extends underwater into a narrow depression, reaching depths of over 160 m, oriented west-southwest, which cuts across the general trend of the ridges (Figure 1). In the remainder of the text, it will be referred to as the SW Trough. The average gradient through the length of the SW Trough is 3m/km. The regional morphology apparently reflects pre-glacial erosion controlled by bedrock composition and structural trends (Pelletier, 1986).

The reconstruction by Dyke and Prest (1987) of the retreat of the Laurentide Ice Sheet demonstrates that deglaciation of the bay started around 8400 BP. At that time the ice sheet consisted of three large interconnected ice domes: the Labrador, the Hudson, and the Keewatin. Most of the bay was cleared of ice within 400 years (Josenhans and Zevenhuizen, 1990; Dyke and Prest, 1987) The lower basin of the Great Whale River was ice-covered as late as 8100 BP (Hillaire-Marcel, 1976). Sea water which had penetrated Hudson Strait prior to 10000 BP invaded northern Hudson Bay near 8000 BP forming the Tyrrell Sea (Hillaire-

Marcel and Fairbridge, 1978).

The Hudson Ice Dome was rimmed by proglacial Lakes Agassiz to the southwest and Ojibway to the southeast. The latter, which covered the James Bay and Hudson Bay Lowlands, extended eastward as far as the Sakami Moraine (Hardy, 1976) and northward as far as Great Whale River (Hillaire-Marcel, 1976). Between 8100 BP and 8000 BP, the collapse of the ice-barrier between Lake Ojibway and the Tyrrell Sea brought about the catastrophic drainage of the lake northward, followed by marine invasion of southeastern Hudson Bay (Hillaire-Marcel, 1976). At approximately the same time, the sea reached glacial Lake Agassiz along a suture between the Keewatin and Hudson Ice domes, invading the southwestern Hudson Bay Lowlands (Dredge and Cowan, 1989).

As the ice receded, emergence due to isostatic uplift raised former marine limits to elevations above present sea level which range from 198 m south of James Bay (Hardy, 1976) to a maximum of 315 m between Little Whale and Great Whale rivers (Vincent et al., 1987; Hillaire-Marcel, 1976). North of Richmond Gulf, the marine limit east of Povungnituk decreases to elevations not exceeding 105 m above present sea level (Gray and Lauriol, 1985). The rate of land emergence fell from about 10m/100y at 8000 BP to about 1m/100y at around 2800 BP. It has remained approximately constant since then (Vincent et al., 1987). For a general synthesis of the Late Wisconsinan history of the Canadian Shield in Quebec-Labrador, see Vincent (1989).

INSTRUMENTS AND METHODS

The interpretation of the regional seismo-stratigraphy presented here is based on high-resolution reflection seismic profiling and on piston coring. The main source of data is a multi-parameter grid of reflection seismic lines totalling more than 60 km (Figure 5) collected during a cruise of CSS HUDSON in August 1987 (EMR CSS_HUDSON 87-028/87-031 Data Report). The following seismic equipment was operated simultaneously: a) a Huntec® DTS (Deep Tow System) containing a boomer and two single channel hydrophones, one internal for maximum resolution and one external for maximum penetration, b) an airgun with a 653 cm³ chamber fired at a 3 s rate, coupled with analog hydrophones, for intermediate penetration; c) an ORE® 3.5 kHz subbottom profiler; d) Klein® 100 kHz and BIO 73 kHz sidescan sonar systems; and e) a 12 KHz echosounder. The Huntec® DTS and 3.5 kHz records were the principal data used in establishing our seismo-stratigraphic units and their distribution.

Eight piston cores of 10 cm diameter, averaging 3.5 meters in length (maximum of 7.53 m), provided stratigraphic control. The selection of the core sites (Figure 5) was made on the basis of the acoustic data in areas of condensed sections so as to improve the chances of the corer penetrating a maximum number of stratigraphic units. The cores were split, X-rayed and subsampled for laboratory analyses to determine geotechnical (Marsters, 1988) and physical properties (Henderson, 1989). In addition, microfaunal and palynological analyses were made on core 69 (Figure 5 for location) by Bilodeau *et al* (1990). A

combination of global positioning and satellite navigation provided a positioning accuracy generally within 20 meters.

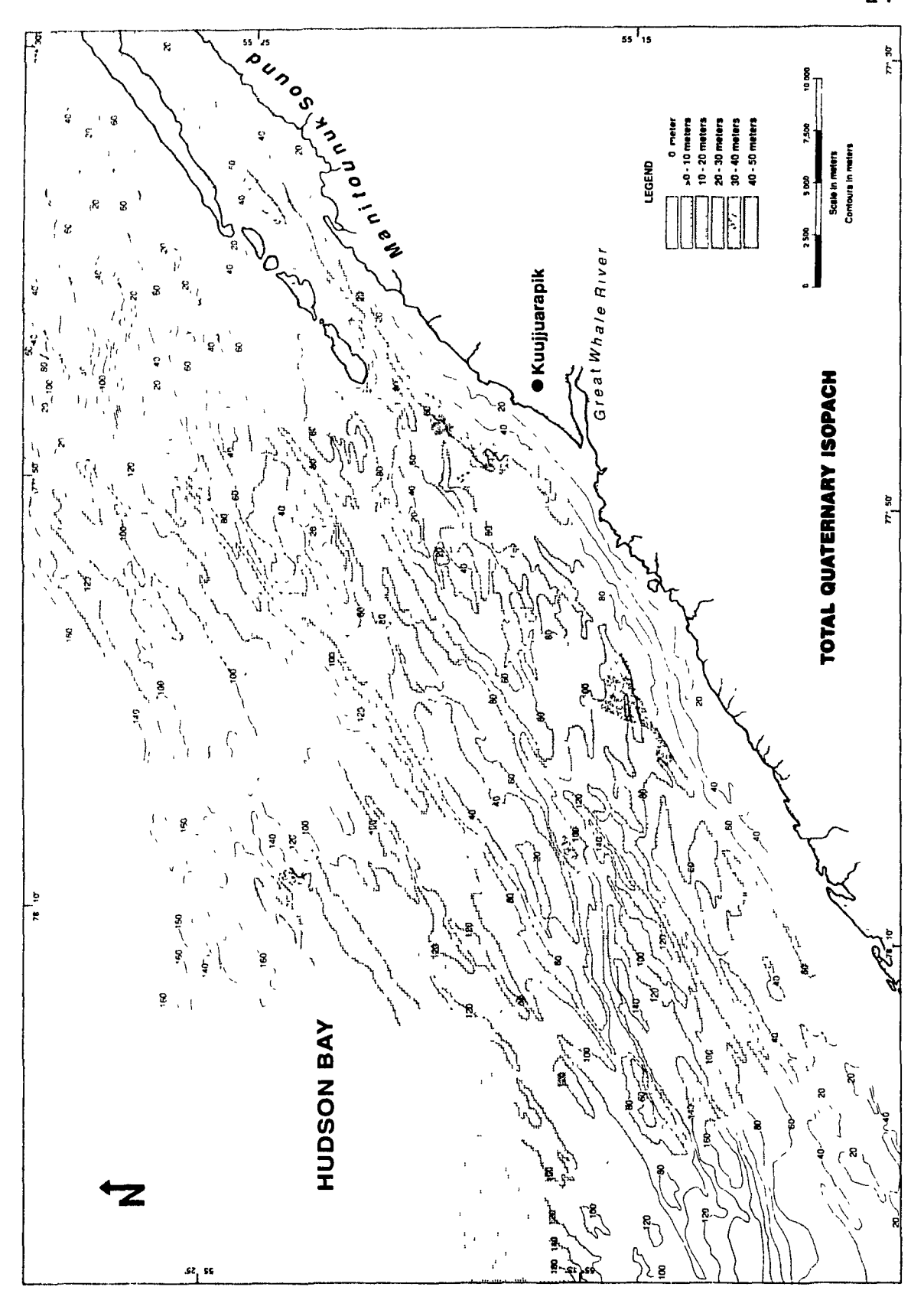
Additional seismic records were collected on a Canadian Hydrographic Service cruise aboard the CCGS NARWHAL (Zevenhuizen and Josenhans, 1988), one line of which falls within the study area (Figure 5). The data along this line, taken by a 3.5 kHz subbottom profiler, were incorporated into our study.

ACOUSTIC STRATIGRAPHIC UNITS

This section deals exclusively with the stratigraphic analysis and interpretation of the reflection seismic records, which led to the identification of several seismo-stratigraphic units. These units were subdivided on the basis of their acoustic character as defined by the high resolution Huntec DTS and 3.5 kHz systems. Units were established at one or several well-defined sections, and then traced laterally to establish a regional stratigraphy. During this process, variations in definition of the acoustic attributes, geometry, or bedding style of the different units were often encountered, making interpretation necessary.

Isopach maps of the total Quaternary sequence and of each of the individual acoustic units were made based on the acoustic coverage shown in Figure 5. The isopach map of the total Quaternary sequence (Figure 6) shows that the sediment cover is generally thick nearshore (10 to 42 m), and that two distinct lenses are present, one on each side of the Great Whale River entrance.

Figure 6. Total Quaternary sediment isopach map.



Farther offshore the sediment cover thins out over the ridge-and-trough topography, generally to less than 10 m, and increases to 10-30 m on the offshore slope beyond the 100 m contour. These observations are supported by underwater pictures, obtained with a bottom camera system of the Bedford Institute of Oceanography, showing smoothed out topography in the troughs and partly exposed bedrock on the ridges. Within the surveyed outer region of the Manitounuk Sound, sediment thicknesses vary between 0.5 m and 38 m. Regional variations in thickness of the total Quaternary sequence reflect the changing styles of sedimentation across the study area.

Examination of the seimic profiles led to the recognition of four distinct units overlying the Proterozoic bedrock (unit 1). They were chosen on the basis of their similarity to established units from other similar surveyed areas; i.e. Hudson Bay (Josenhans *et al.*, 1988; Josenhans and Zevehuisen, 1990), Labrador Shelf (Josenhans *et al.*, 1986), Scotian and mid-Norwegian Shelves (King *et al.*, 1991), and Gulf of St-Lawrence (Syvitski and Praeg, 1989). These are designated as: ice contact sediments (unit 2), ice proximal sediments (unit 3), ice distal sediments (unit 4) and, distal fluvio-deltaic sediments (unit 5). Each unit represents a particular stage in the deglaciation of the coastal region. As discussed later, these interpretations are supported by the piston core stratigraphy.

UNIT 1: BEDROCK

The bedrock surface is identified by a relatively well-defined reflector

characterized by variable relief and lack of penetration (Figure 7 and 8). It can be traced across most of the record, except in some areas where it is hidden by the first multiple or where resolution is poor. Outcrops of bedrock in the study area are limited because of the presence of a thin sediment cover on many ridge tops.

The topography of the bedrock surface is generally rough (Figures 7, 8, 9). Cuesta ridges, dipping to the NW, characteristic of the Proterozoic terrain, can be observed at some sites (Figure 9).

UNIT 2: ICE CONTACT SEDIMENTS

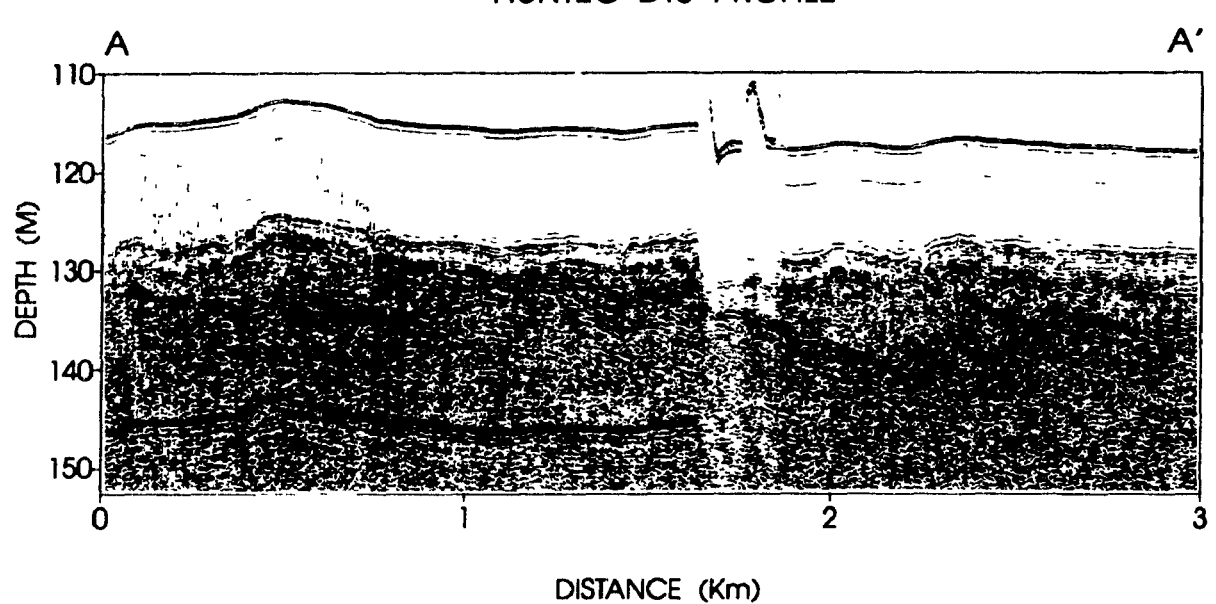
Unit 2 is the lowermost unconsolidated layer. It is characterized by a uniformly dark grey tone, lack of coherent reflectors and an undulating upper surface (Figure 7 and 8). It discontinuously overlies the bedrock and commonly occurs as fill in topographic depressions (Figure 7 and 8) or locally forms mounds or ridges (Figure 10). The upper contact is always sharp. However, the lower contact with the bedrock is sometimes hard to define as the acoustic impedance of the two units is similar.

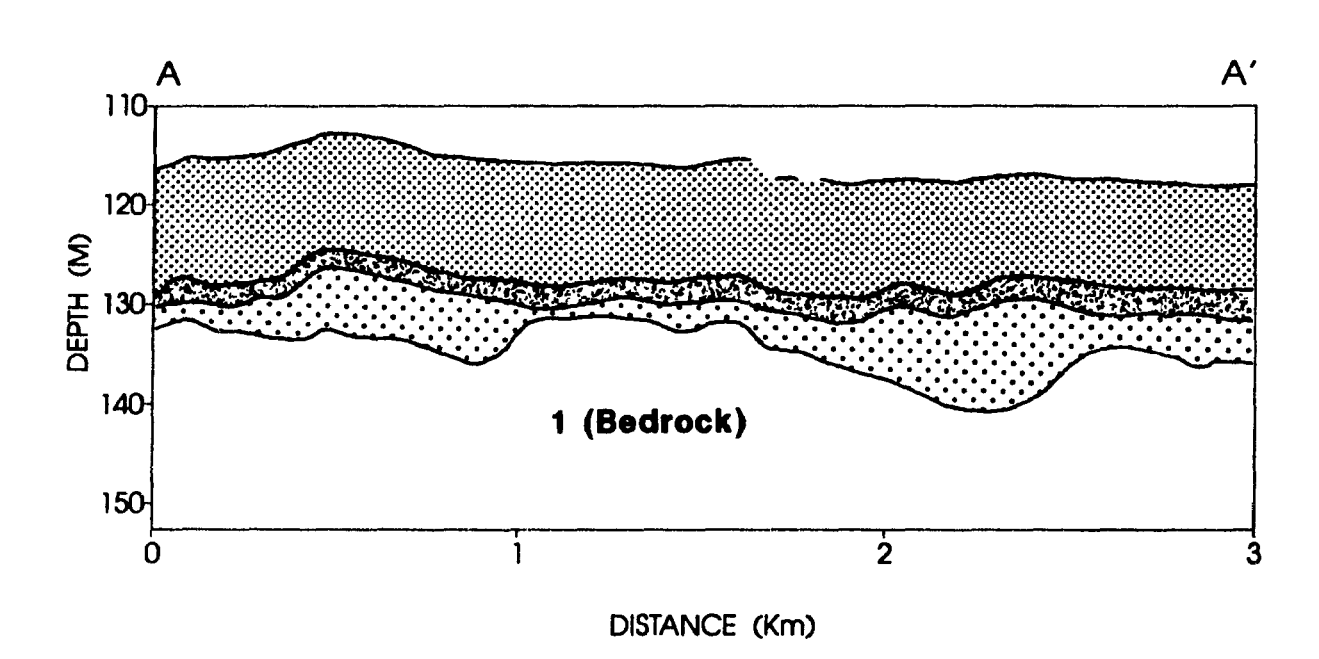
The isopach map of this unit (Figure 11) indicates that it is generally thin (average: 5 m) and is missing locally. Thicker patches reaching a maximum thickness of 30 m are found scattered throughout the area.

The acoustic character (uniform tone with no internal reflectors, undulating surface, and strong surface reflector), of this unit are characteristic of glacial till (King et al, 1991; Josenhans et al, 1988; Josenhans et al, 1986). This

Figure 7. Seismic profile A-A', showing acoustic character of units 1, 2, 3, and 4. See Figure 1 for position of profile. Legend applies to Figures 7-10 and 15.







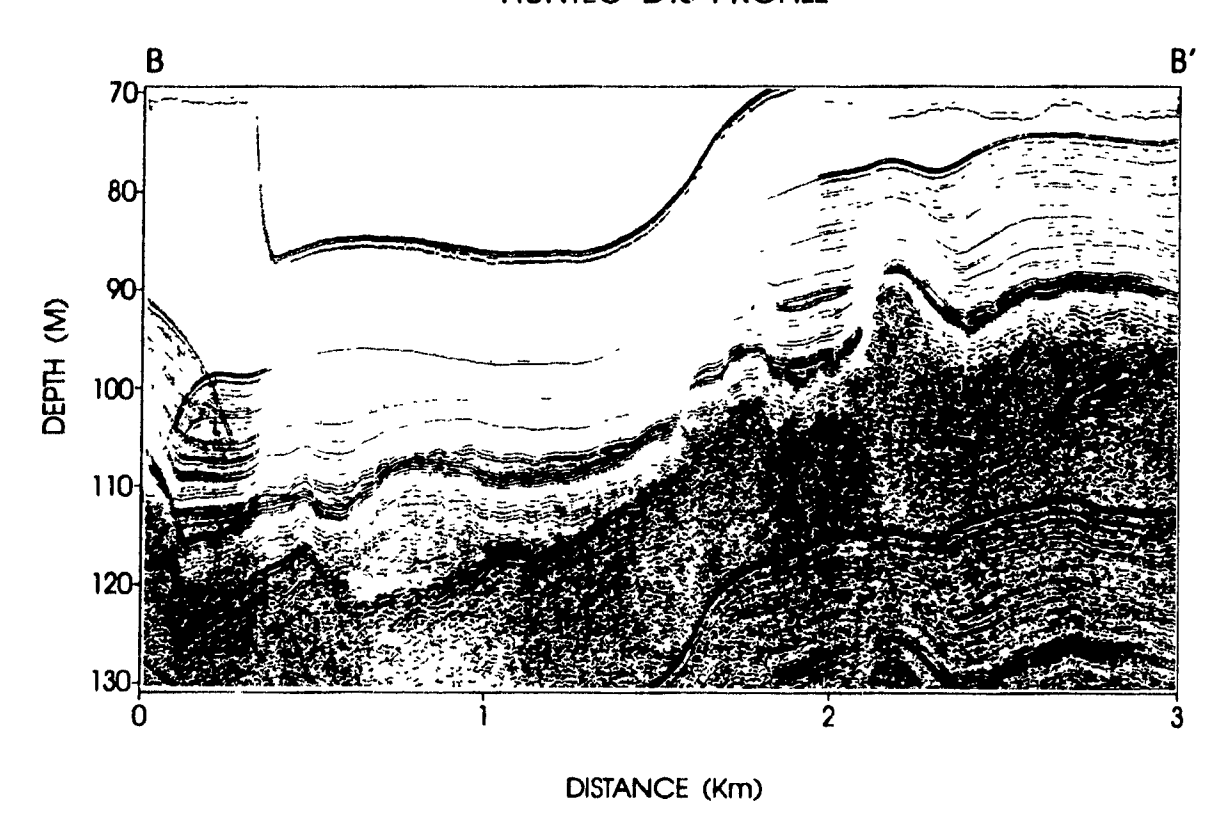
Unit 2 : Ice-contact sediments

Unit 4 : Ice distal sediments

Unit 3 : Ice proximal sediments

Unit 5: Distal fluviodeltaic sediments Figure 8. Seismic profile B-B', showing acoustic character of units 1, 2, 3,

4, and 5. See Figure 1 for position of profile. See Figure 7 for legend.



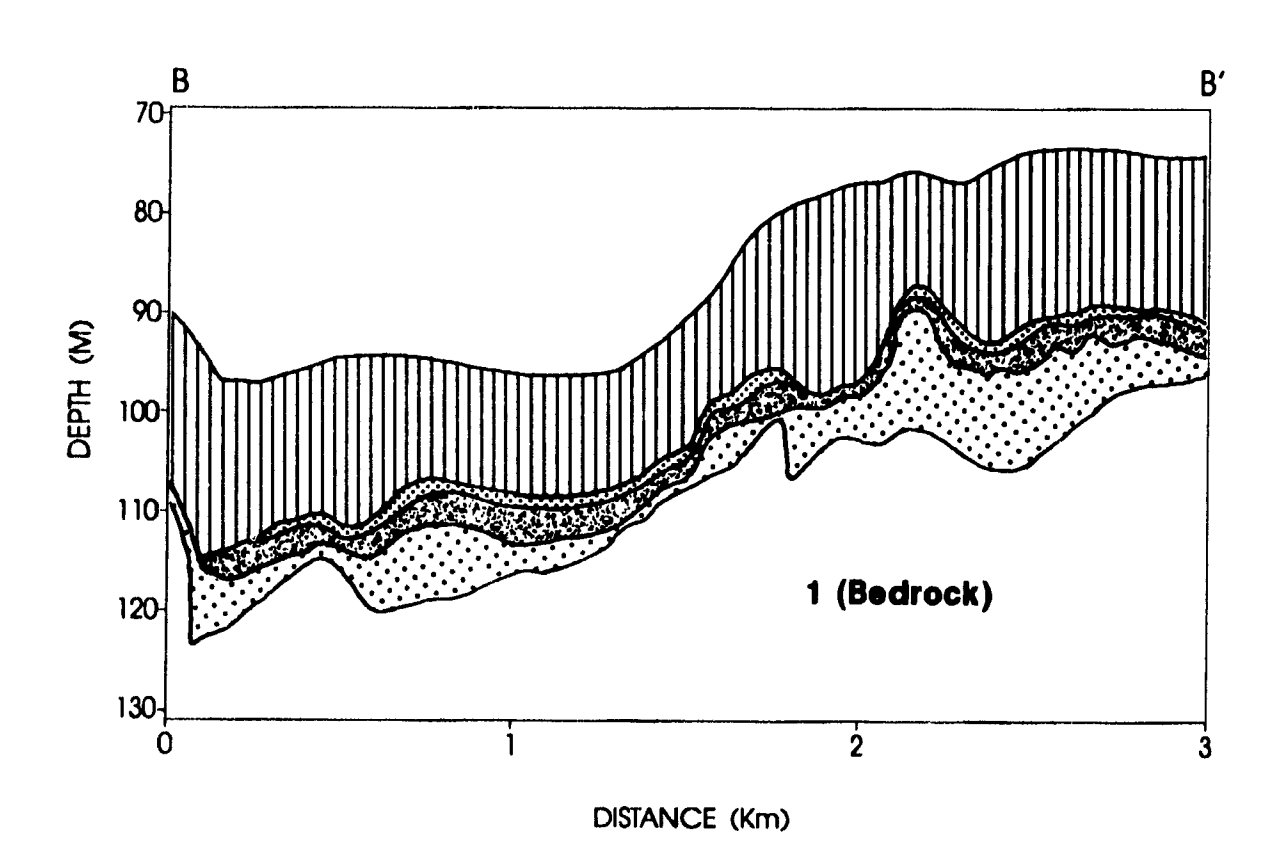
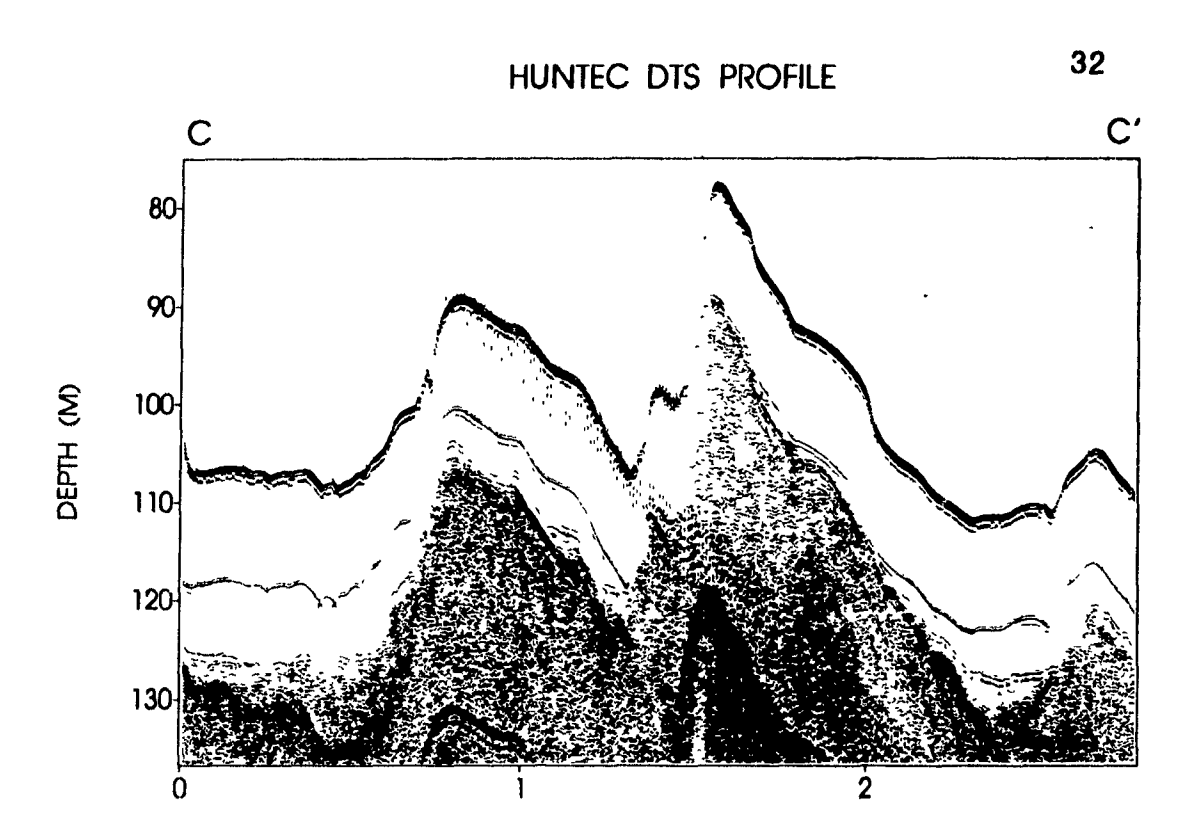


Figure 9. Seismic profile C-C', showing the cuesta-shaped topography of the bedrock. See Figure 1 for position of profile. See Figure 7 for legend.



DISTANCE (Km)

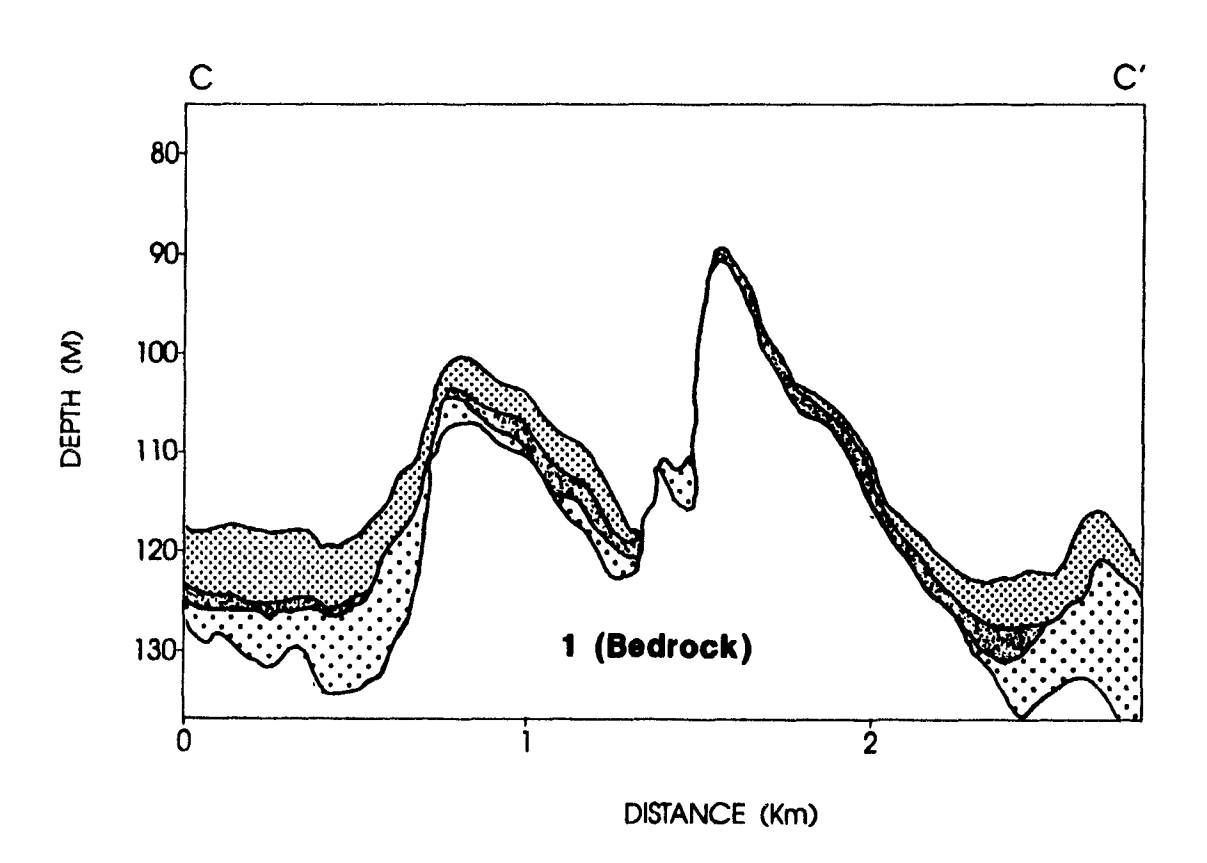
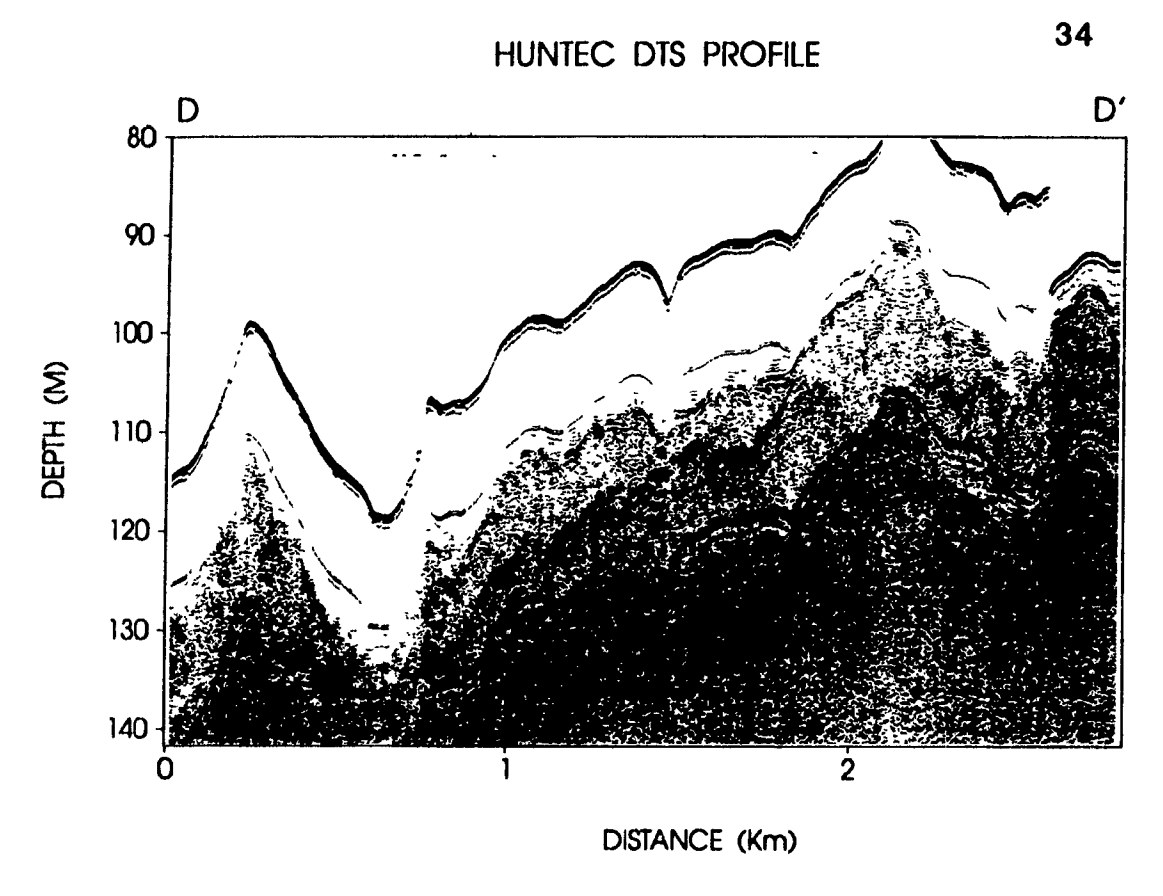


Figure 10. Seismic profile D-D', showing mounds formed by unit 2. Unit 3 onlaps each side of the ridges and is absent on their crests. See Figure 1 for position of profile. See Figure 7 for legend.



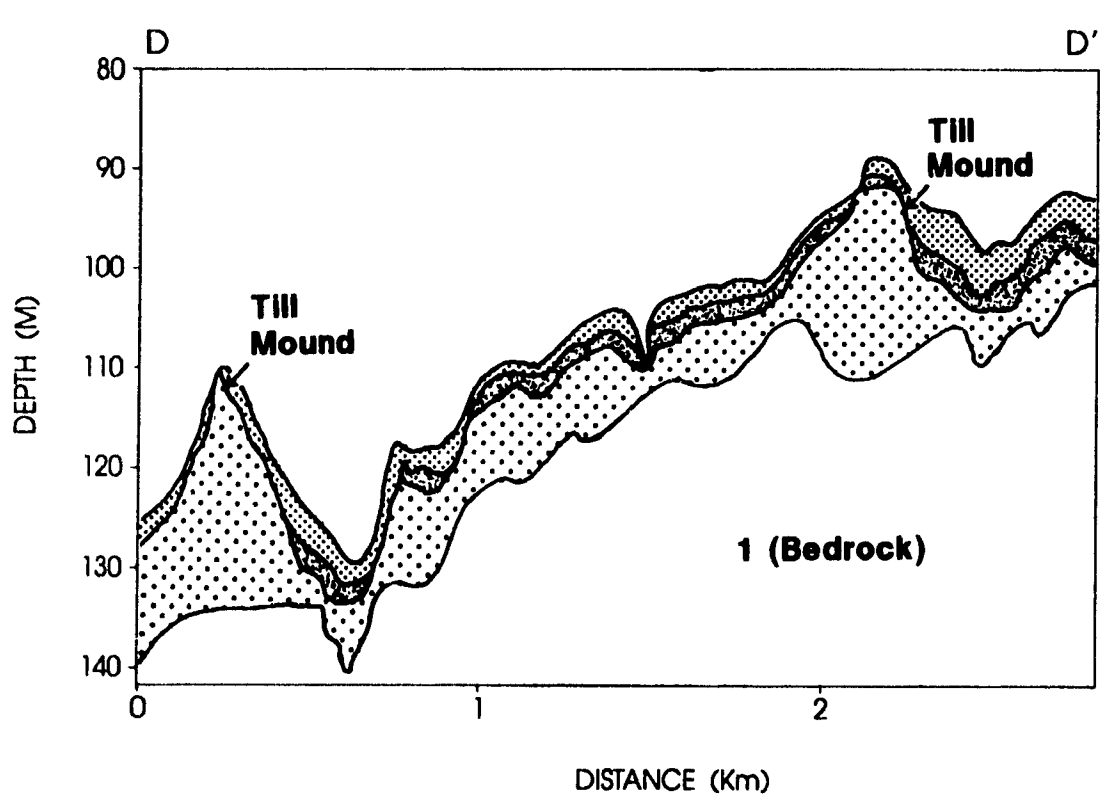
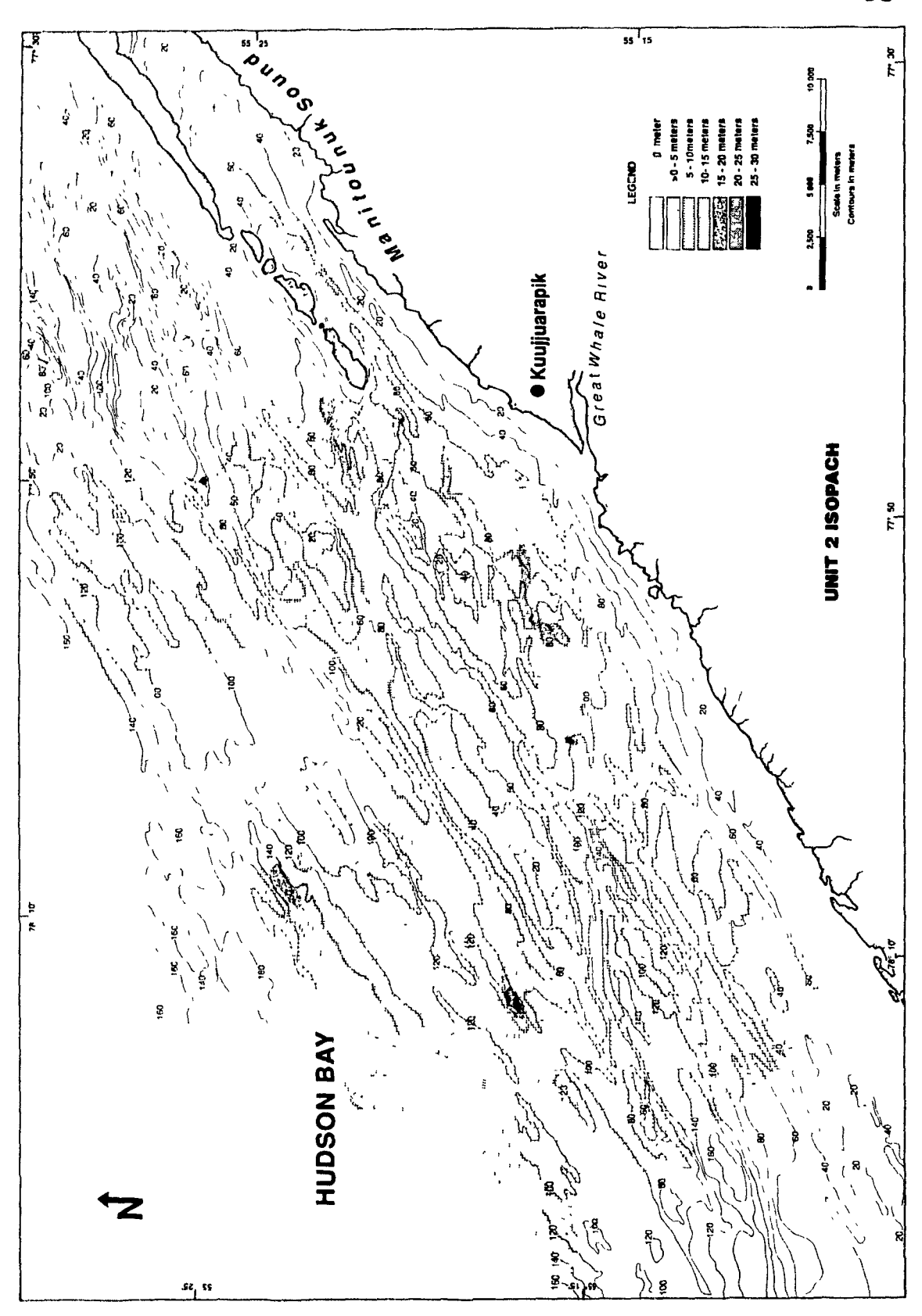


Figure 11. Isopach map of unit 2 (ice-contact sediments).





interpretation is confirmed by the piston core analysis as explained below. The occurrence of these deposits as a fill in topographic depressions suggests that they have been formed by processes of abrasion and accumulation similar to those operating under a land-based glacier flowing over rough surfaces as described by Boulton (1975).

UNIT 3: ICE PROXIMAL SEDIMENTS

Unit 3 occurs within the seismic section as an acoustically well-stratified unit, with strong and closely spaced reflectors. It is uniform but relatively thin, with an average thickness of 2 m and a maximum of 5 m. It occurs as a conformable deposit draped over the bedrock substrate, or the ice contact sediments (unit 2) where present (Figure 7 and 8). Occasionally, where unit 2 (till) forms a ridge, unit 3 onlaps each side of the slope, but is missing on top (Figure 10).

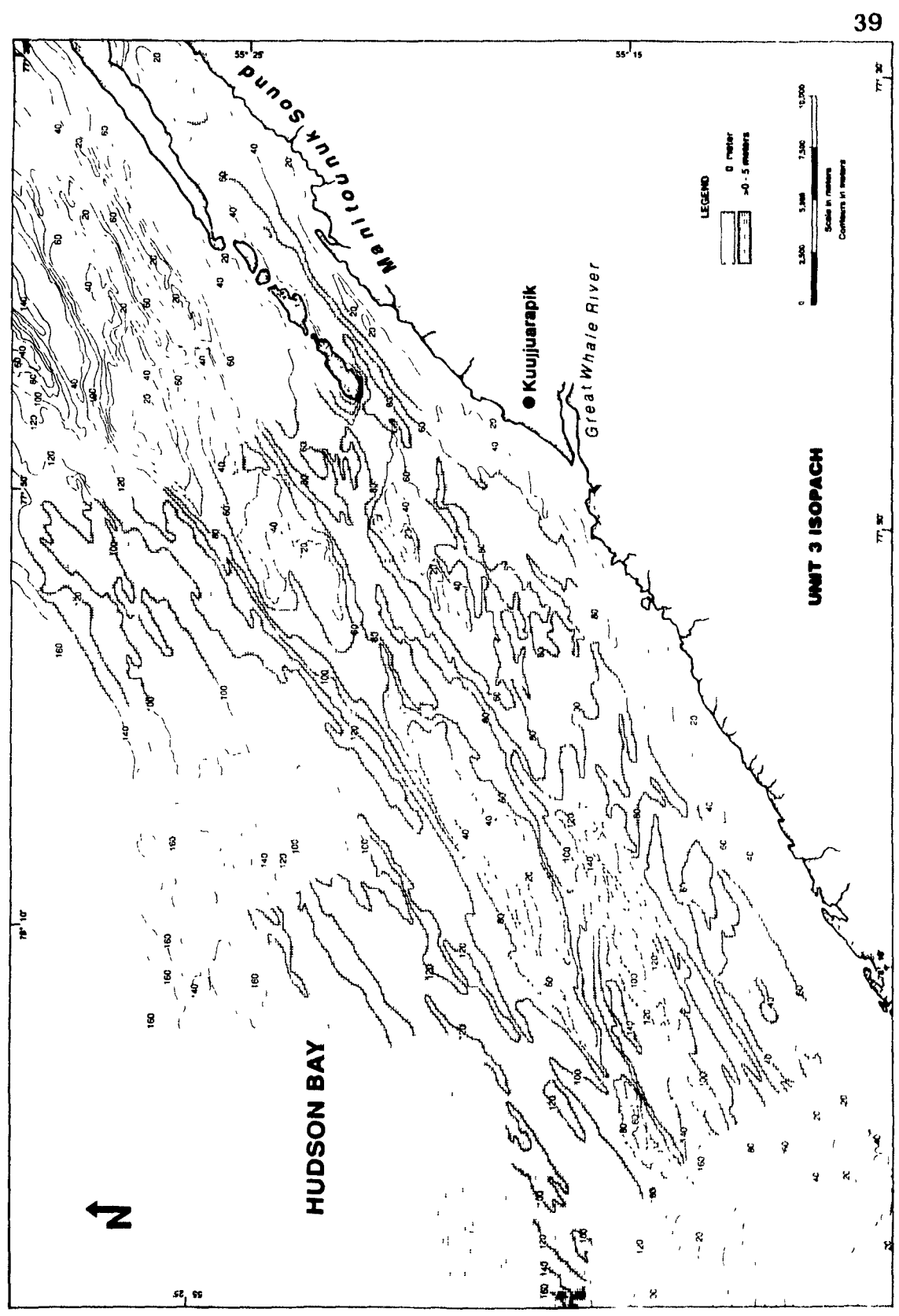
It is distributed throughout the entire study area except on topographic highs and in the SW Trough (Figure 12). It is acoustically similar to the ice proximal glaciomarine sediments described by King *et al* (1991), Josenhans *et al* (1988) and Josenhans *et al* (1986). However, the core analysis suggests that the sediments were deposited in a glaciolacustrine rather than a glaciomarine environment as discussed below.

UNIT 4: ICE DISTAL SEDIMENTS

This facies is characterized by very low tone and weak stratification (Figure



Figure 12. Isopach map of unit 3 (ice proximal sediments).



7 and 8). It occurs as a conformable deposit over the ice proximal sediments (unit 3) or sometimes over the ice contact sediments (unit 2) or the bedrock (unit 1). Within 12.5 km of the shoreline, it is overlain by unit 5, but it grades into recent marine muds farther offshore. The recent muds cannot be differentiated acoustically from unit 4 because the environment of deposition has not changed substantially.

The isopach map of unit 4 (Figure 13) indicates thicknesses not exceeding 5 m nearshore and ranging between 5 to 16 m on the outer slope at depths below 120 m, with an average value of about 3 m. As with unit 3, this unit is missing on top of some topographic highs and in the SW Trough. Its acoustic characters are similar to those of the ice-distal glaciomarine sediments described by King *et al.* (1991). This is confirmed by the analysis of piston cores which indicates that those sediments consist of fine marine muds (see below).

UNIT 5: DISTAL FLUVIO-DELTAIC SEDIMENTS

The isopach map (Figure 14) indicates that unit 5 is present only nearshore and in the Manitounuk Sound. It is characterized by strong and dense acoustic stratifications with a sharp reflector at its base, and has a slightly undulating upper surface (Figure 8). Where present, unit 5 conformably overlies unit 4. However, at some sites, it was found to lie directly on either the ice proximal sediments, the ice contact sediments, or the bedrock. Near its top, the unit grades into recent sediments which cannot be resolved seismically from unit 5 because of lack of

Figure 13. Isopach map of unit 4 (ice distal sediments).

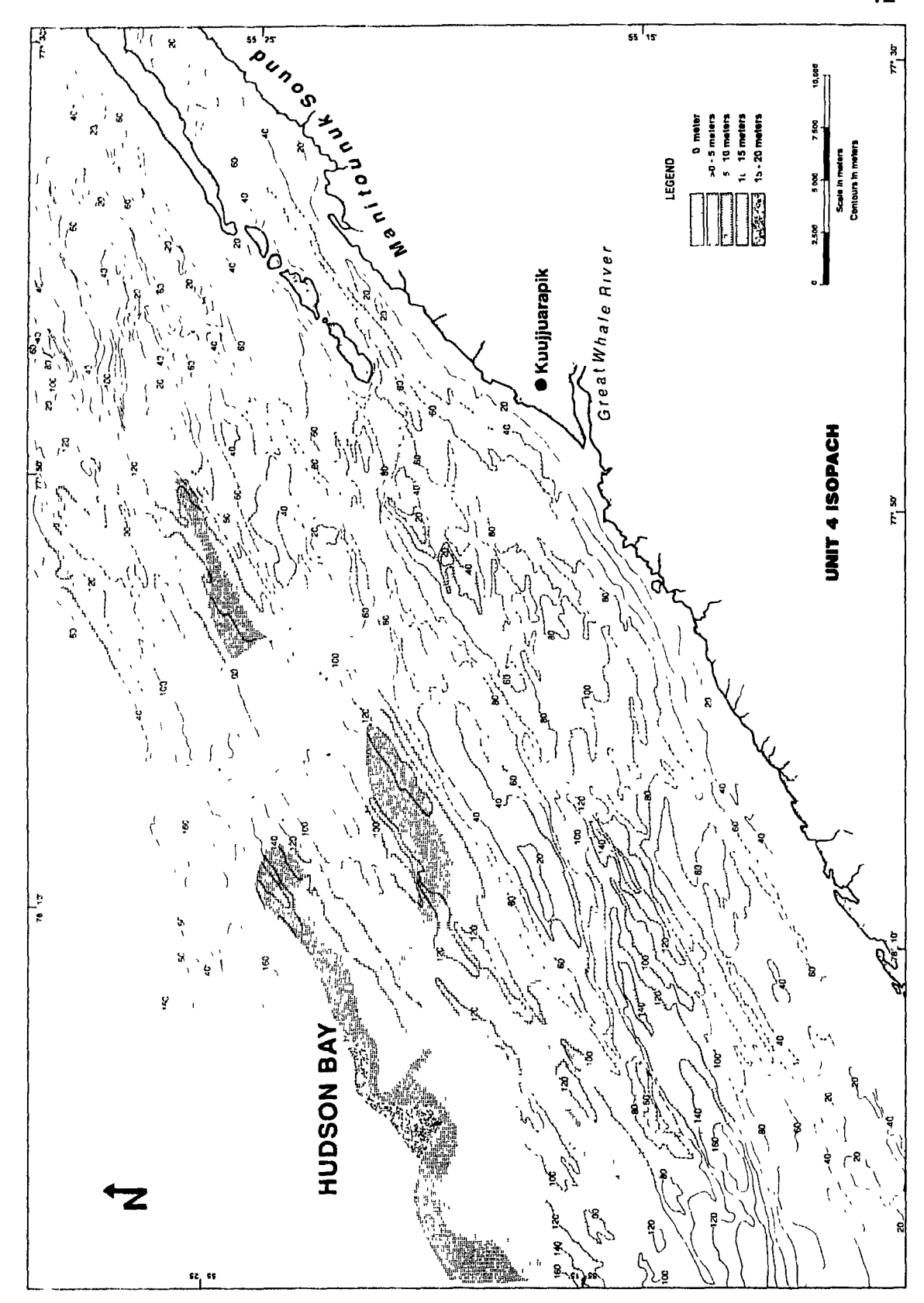
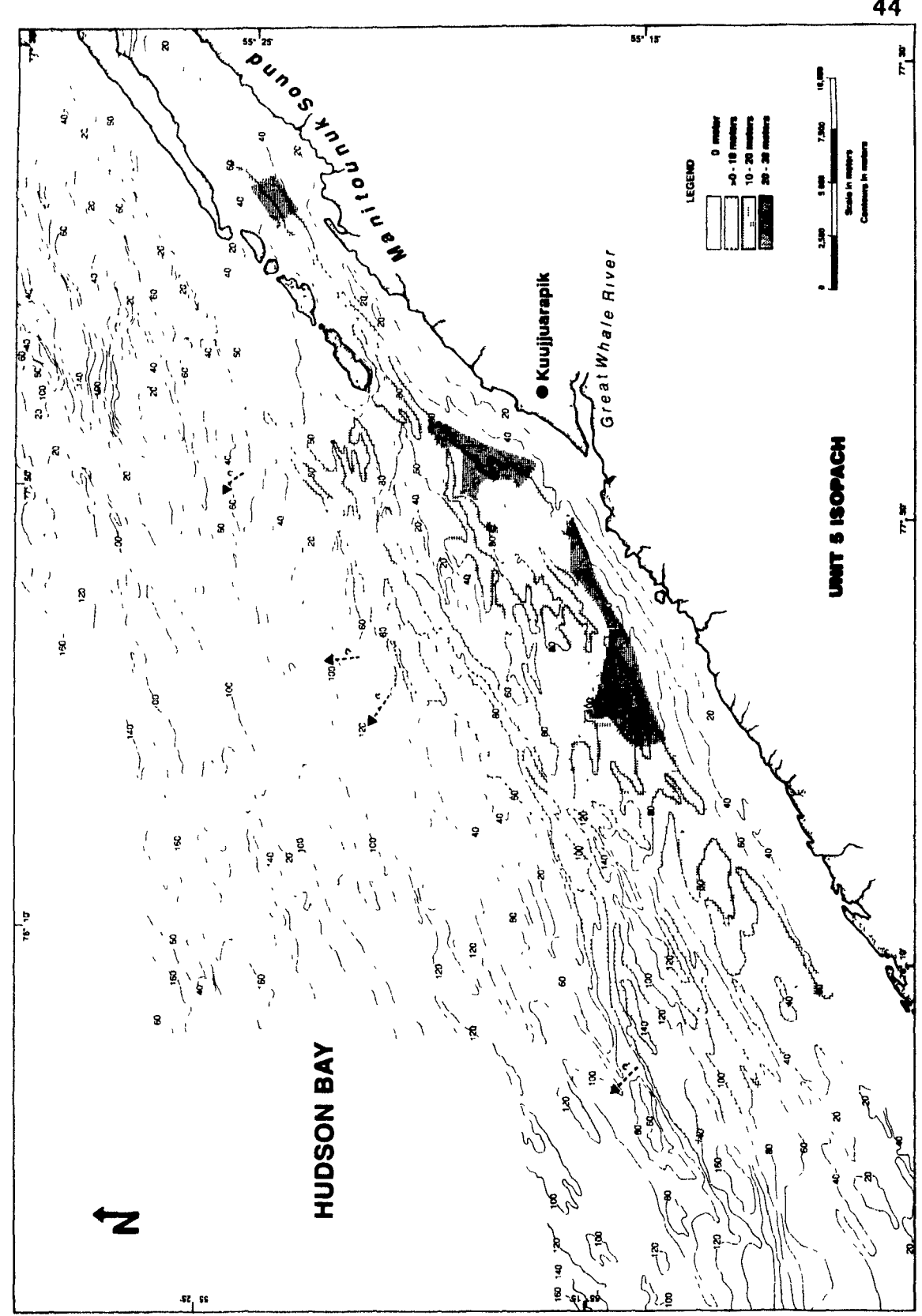


Figure 14. Isopach map of unit 5 (distal fluvio-deltaic sediments).



contrast.

А,

Unit 5 is acoustically similar to the paraglacial deltaic unit described by Syvitski and Praeg (1989), but is of different origin as it postdates the retreat and disappearance of the ice sheet (see below). It occurs as a constructional deltaic wedge built outward from the mouth of the Great Whale River Immediately offshore of the river mouth, the unit thins out to less than 10 m in the axis of the river channel, whereas north and south of the axis, 10 to 30 meter-thick sediment lobes are present (Figure 14). Seaward, beyond 5 km from the shore, thicknesses remain below 10 m, except for scattered patches which may reach 20 m (Figure 14). The sediments of unit 5 cover approximately 400 km². With an average thickness of 15 m, this unit represents approximately 6 x 109 m³ of sediments. It is missing on two topographic highs northwest of the Great Whale River mouth, and also over the deeper parts (>120 m) of the SW Trough (Figure 14).

Because of increasing faintness of the reflectors away from the river entrance the exact offshore limit of the unit is difficult to determine. However, from the analysis of the seismic records, it seems that these sediments are not observed northwest of the bedrock ridge located approximately 11 km from the shoreline (Figure 14). Figure 15 explains how that limit was established. On the left end of the figure, southeast of the ridge, the upper unit is interpreted as unit 5 on the basis of faint acoustic stratifications as well as a thin and weak basal reflector. On the other side of the ridge, to the northwest, the upper unit shows weak stratifications but no basal reflector and is comformable with the underlying

Figure 15. Seismic profile E-E', showing an example of the disappearance of the distal fluvio-deltaic unit (unit 5) to the northwest. See Figure 1 for position of profile. See Figure 7 for legend. Note that this figure is at half the scale of Figures 7-10.

units. These features are more characteristic of unit 4, and so this acoustic interval is interpreted to represent that unit. Hence unit 5 does not occur northwest of the ridge.

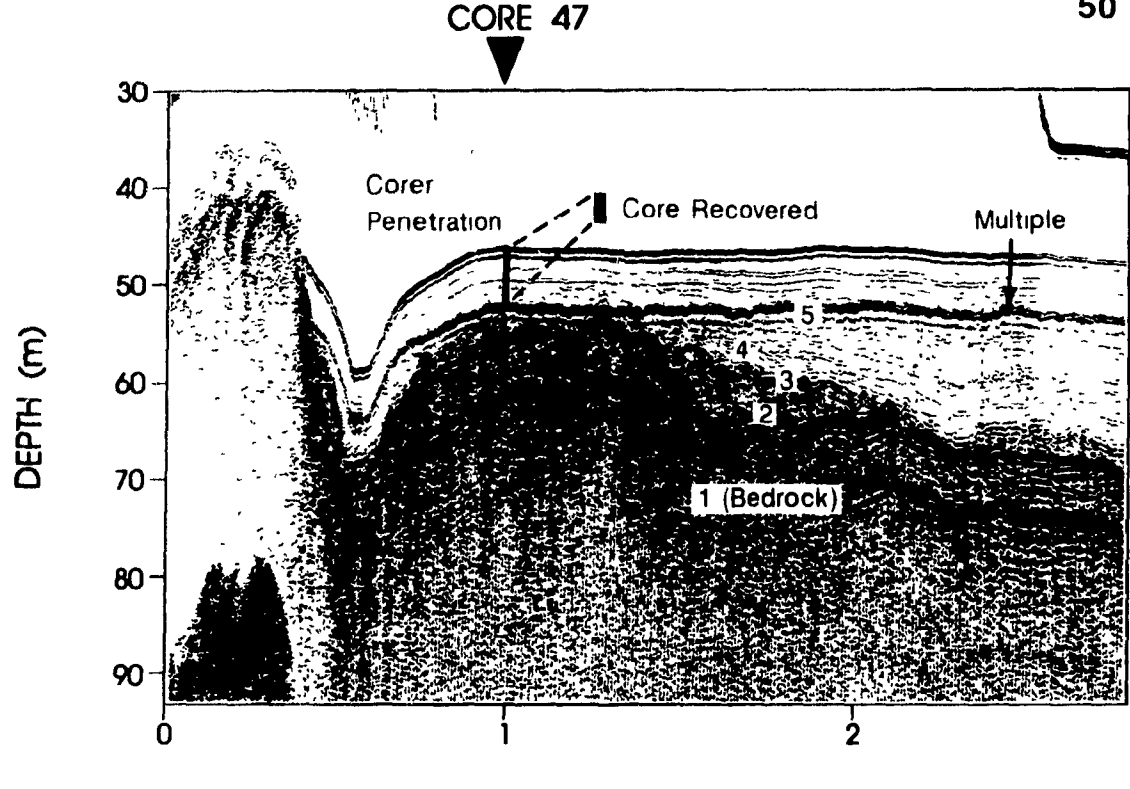
LITHOSTRATIGRAPHIC CHARACTERISTICS OF THE UNITS

Coring of the Quaternary sequence along the seismic profiles provides an opportunity for first-hand observations and direct sampling of the units. Of the eight cores collected, four intersect more than one unit. Core 47 (Figure 5 for core location) is the only one showing the complete nearshore stratigraphic sequence, which consists of a sandy diamicton (unit 2) at the base, overlain by rhythmically banded sediments (unit 3), followed by a short section (14 cm) of dark grey silty clay sediments (unit 4), and finally on top by an olive grey silty clay sediment (unit 5). A more detailed description is given on Figure 16. In core 48 (Figure 17) the sequence starts with the rhythmically banded sediments (unit 3). The unit is interrupted by an erosional surface over which lies unit 5 directly; the contact there is sharp. Core 69 (Figure 18) may show the complete stratigraphic sequence farther offshore, which consists of till (unit 2) overlain by rhythmites (unit 3) and by marine silty clays (unit 4). Core 43 (Figure 19) intersects only units 3 and 4.

The four remaining cores (50, 68, 70, 71) intersect the upper part of a single unit (unit 5), without reaching its base. The physical characteristics of each unit, based on the core descriptions, are presented below.

Figure 16. Lithostratigraphy of core 47 and its approximate position and penetration relative to the seismic section. Core description is from Henderson (1989). See Figure 5 for core locality. TWC = trigger weight core. PC = piston core.





DISTANCE (Km)

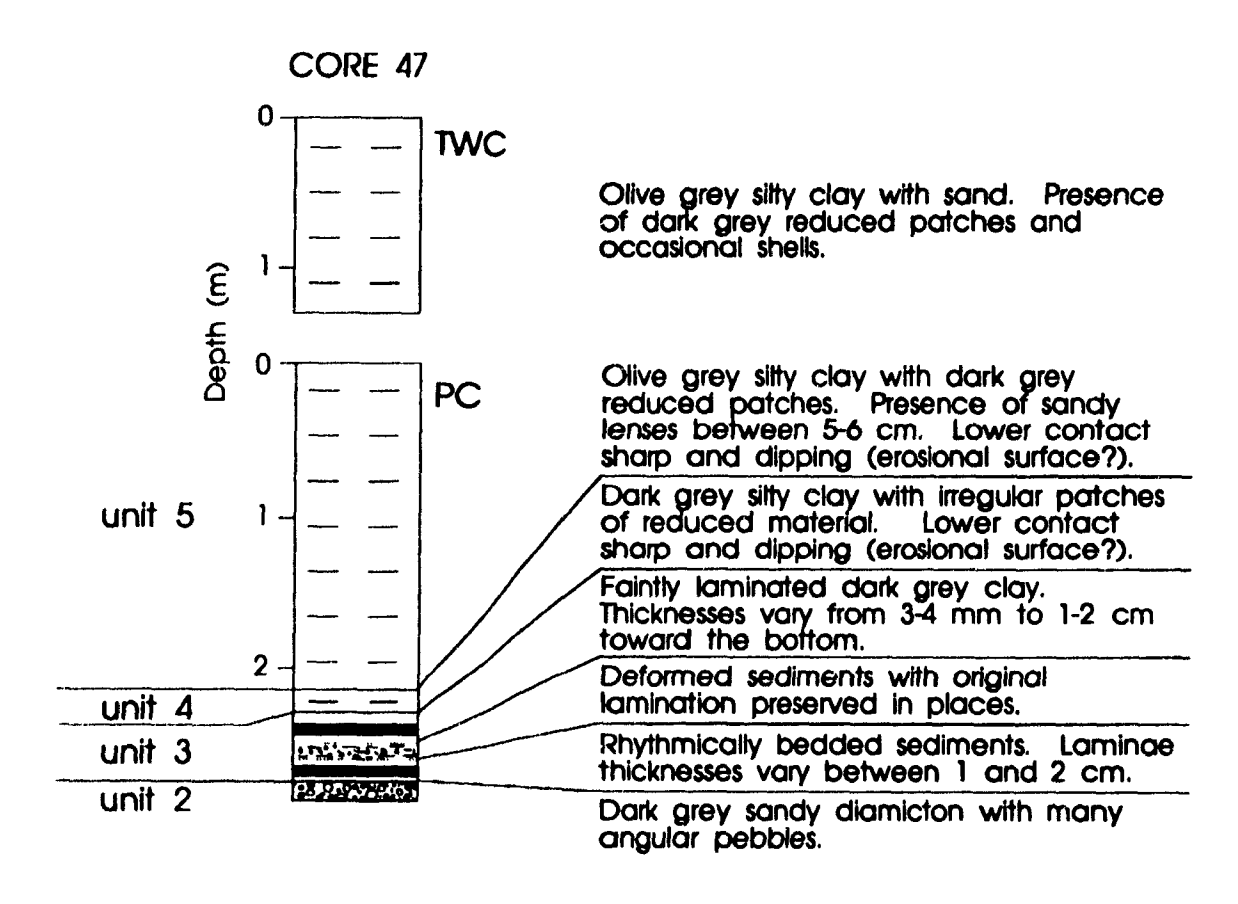
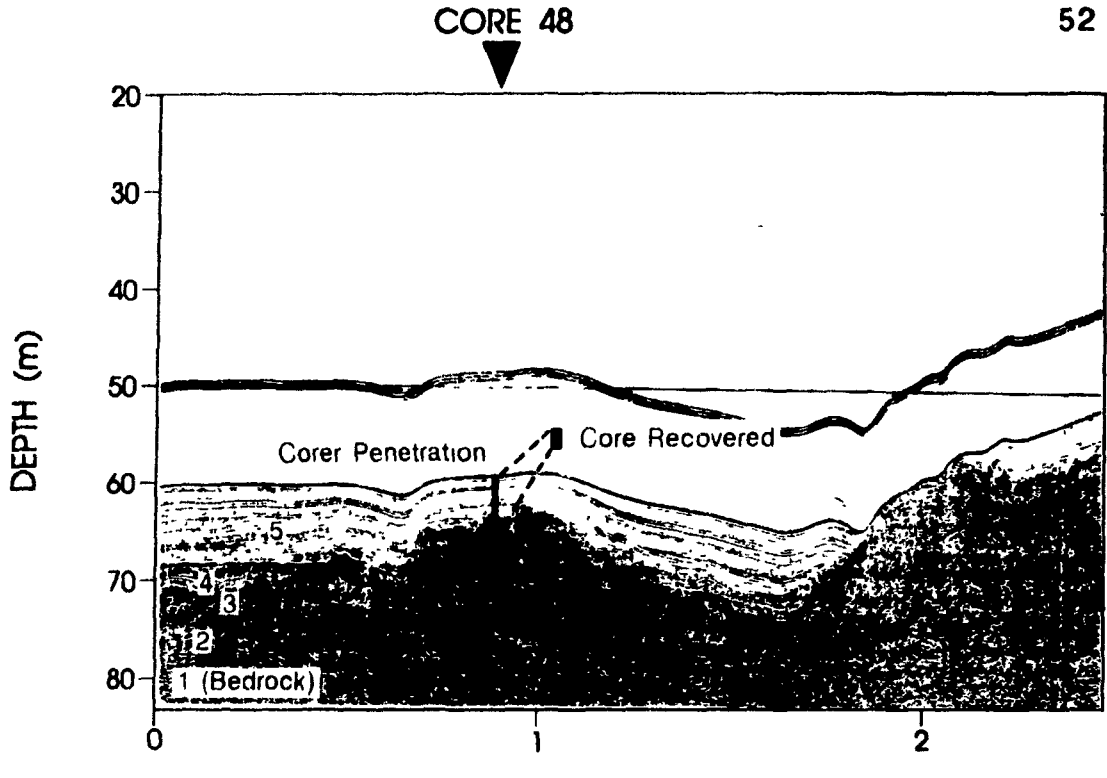


Figure 17. Lithostratigraphy of core 48 and its position and penetration on the seismic section. Core description is from Henderson (1989). See Figure 5 for core locality. TWC = trigger weight core. PC = piston core.





DISTANCE (Km)

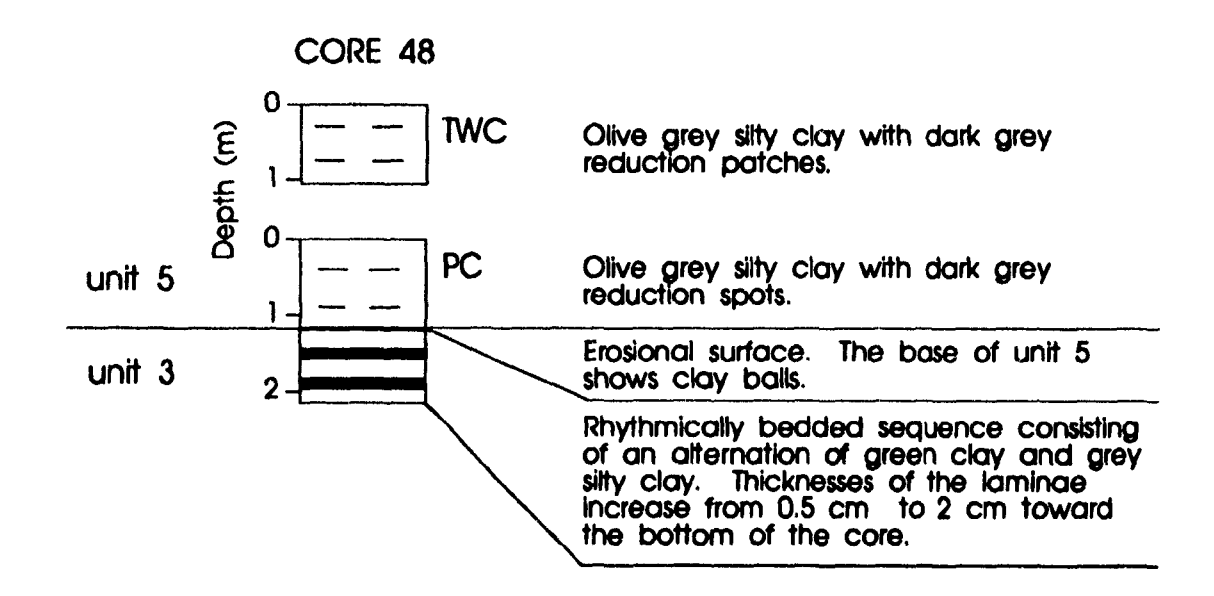
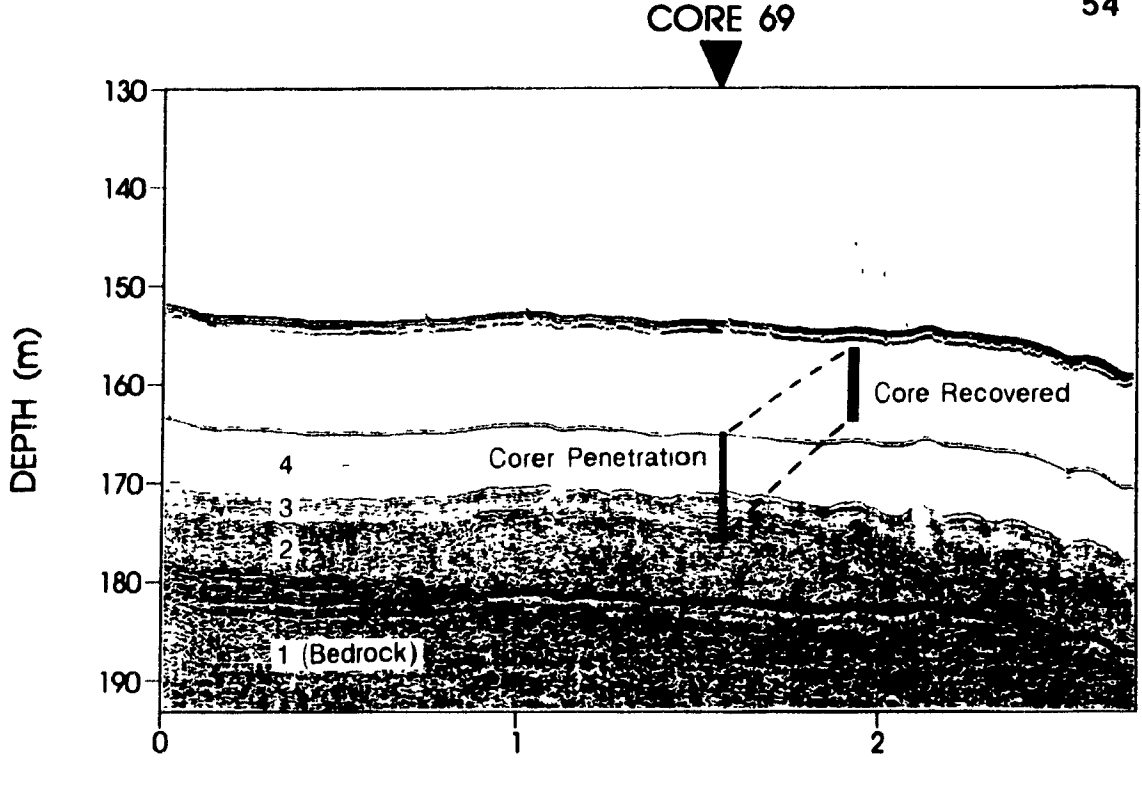


Figure 18. Lithostratigraphy of core 69 and its position and penetration on the seismic section. Core description is from Henderson (1989). See Figure 5 for core locality. TWC = trigger weight core. PC = piston core.





DISTANCE (Km)

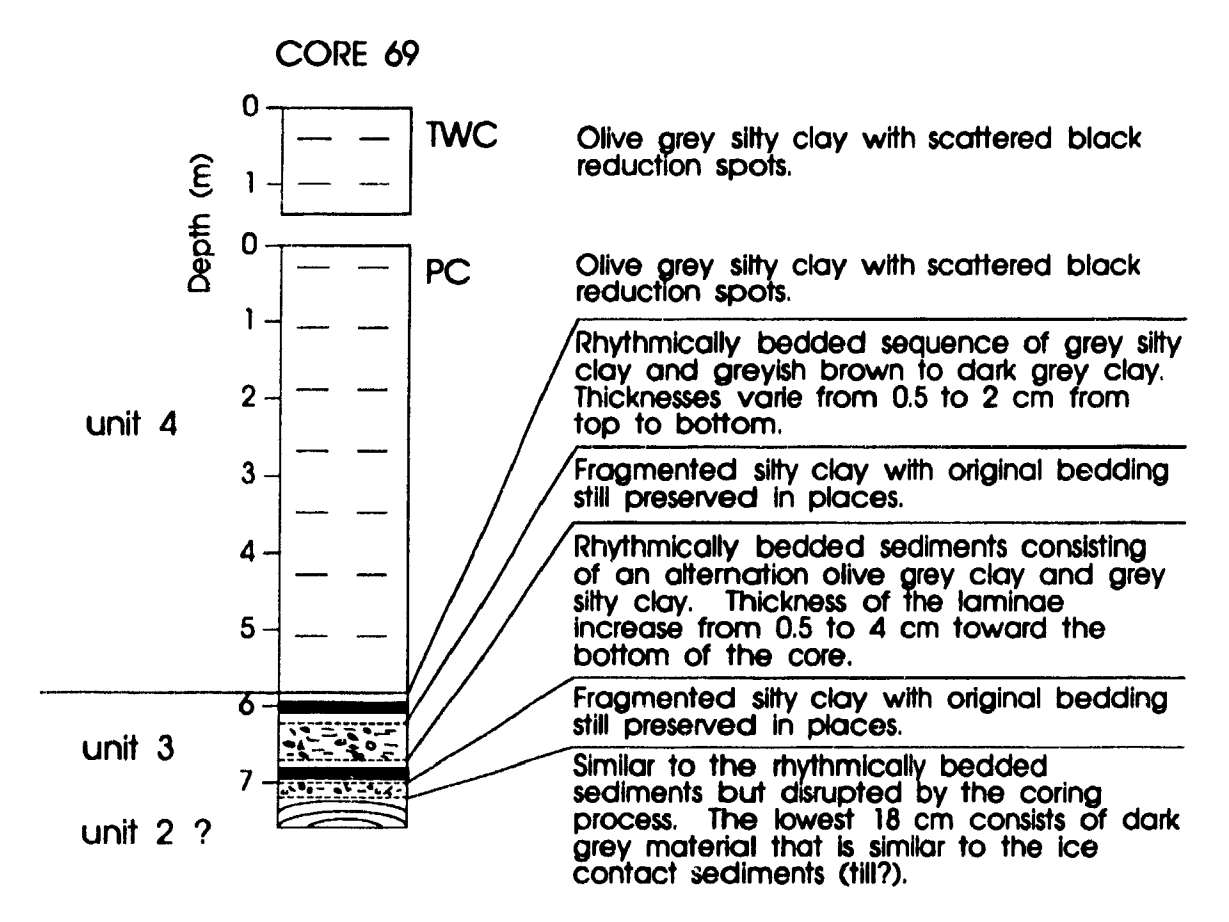
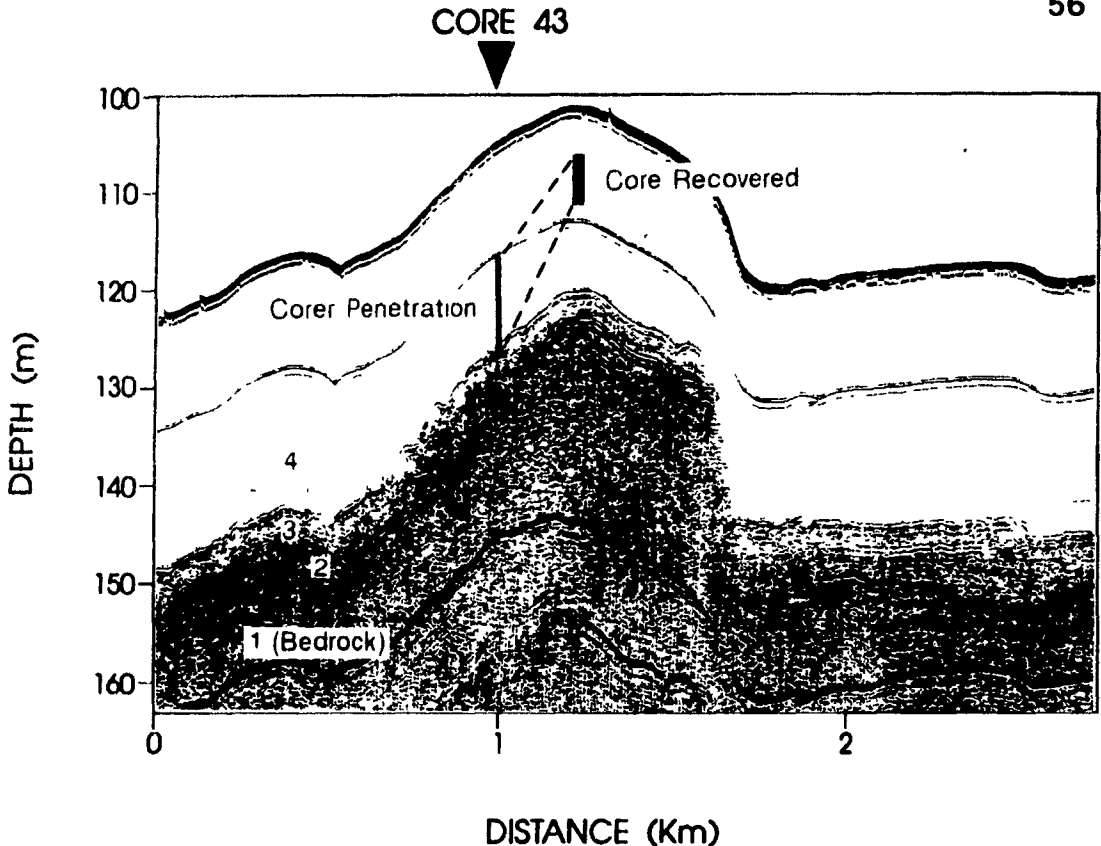
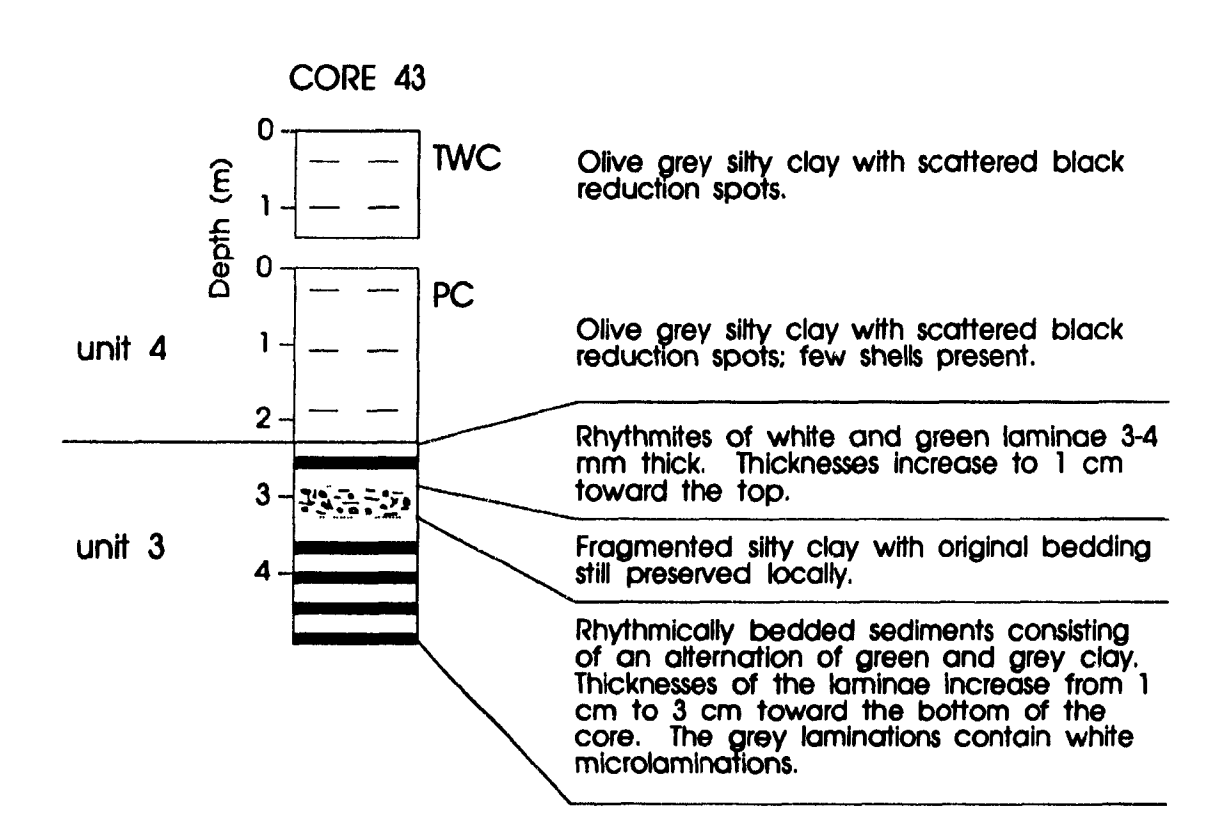


Figure 19. Lithostratigraphy of core 43 and its position and penetration on the seismic section. Core description is from Henderson (1989). See Figure 5 for core locality. TWC = trigger weight core. PC = piston core.





UNIT 2: ICE CONTACT SEDIMENTS

Unit 2 is penetrated best by core 47 (Figure 16). Cores 69 and 48, and possibly core 43, probably bottomed out on the upper surface of unit 2. The base of core 69 (Figure 18) has been partially disrupted during the coring process but the dark grey mud observed within the last 18 cm of that section is similar to the till/ice contact sediments observed in core 47. It is therefore possible that the lower 18 centimeters of core 69 are composed of till. As for core 48, geotechnical data show a marked near-bottom increase in both sound velocity and bulk density, as well as a sharp drop in water content, characteristics that are commonly observed at the upper contact of unit 2 (Marsters, 1988)

Unit 2 in core 47 consists of an unstratified, dark grey (Munsell colour code 7.5YR 4/0), gravelly mud with sand (Figure 16). The gravel fraction (2-5 6 mm) is composed mainly of crystalline (62 to 64%) and of Proterozoic carbonate rock fragments (31 to 34%) (Henderson, 1989). Because it is unstratified, poorly sorted, contains exotic rock fragments, and forms irregular ridges and mounds, unit 2 is interpreted as a basal till.

UNIT 3: ICE PROXIMAL SEDIMENTS

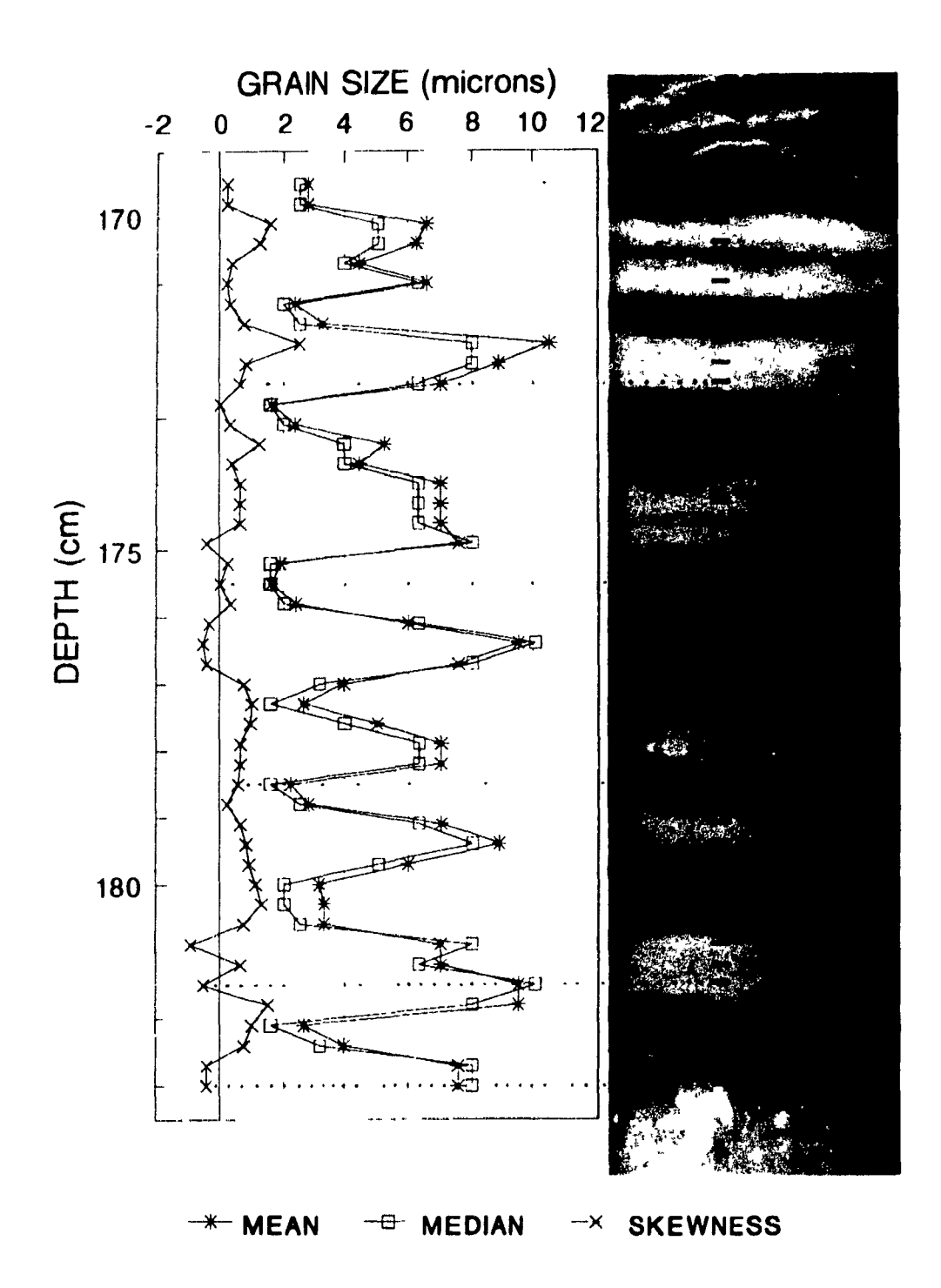
Unit 3 consists of rhythmically bedded clays and silty clays marked by dark and light laminations of varying colour and thickness. It was penetrated by four cores; 47 (thickness: 0,46 m; Figure 16), 48 (thickness: 0,98 m; Figure 17), 69 (thickness: 1,38 m; Figure 18), 43 (thickness: 2,60 m; Figure 19). The lower

contact with unit 2, as seen in core 47, is sharp, which is consistent with the sharp basal seismic reflector in the seismic record.

Couplets of dark and light laminae in the unit generally thin upward. The light laminae (dark grey brown to olive grey; Munsell colors 2.5Y 3/2 to 5Y 4/2) have thicknesses that do not vary appreciably throughout the unit (3mm to 2 cm). However, the dark laminae (dark grey to very dark grey; Munsell colors 5Y 4/1 to 5Y 3/1) get much thicker toward the bottom of the unit, with thicknesses increasing from 3mm at the top to a maximum of 14 cm at the bottom. The thicker laminae often contain white intra-microlaminations. The rhythmites are often interrupted by fractures. Each core, with the exception of core 48, contains an interval (core 69 has two), 12 to 48 cm thick, that appears completely disaggregated, forming balls or lumps, although traces of original bedding remain visible.

Unit 3 is mainly composed of clay (7-96%) and silt (2-61%) usually with little sand and gravel (Henderson, 1989). The variations in grain-size, obtained by Coulter counter measurements (method described in more detailed in Chapter 3) within individual laminations in a section of core 48, are shown in Figure 20; low values in the graph correspond to the fine-grained (1-5 μm) light laminae while peak values correspond to the coarse-grained (6-11 μm) dark laminae in individual couplets. The contact between successive laminations is sharp, as shown by the abrupt changes in grain size across the interface. Geochemical analysis indicates that the coarse dark-colored laminae contain significantly higher amounts of SiO₂, CaO and Cu, and lower amounts of Al₂O₃, Fe₂O₃, Na₂O, K₂O, MgO₁ TiO₂, MnO₁

Figure 20. Graph showing variation of grain size in laminations of the ice proximal unit (unit 3) in core 48, aligned with X-radiographic negative print of the core slab. Note fracture at the top of the print; it is one of many that are observed within that unit and that were probably produced by the freezing of fresh pore water as explained by Bilodeau *et al.* (1990).



というない なななない

Zn, Ni, and Co than the fine light-colored laminae (Chapter 3).

Geotechnically, the unit shows a general trend toward an increase in bulk density and a decrease in water content downward, indicating a normally consolidating sequence (Marsters, 1988). The bulk density varies from 1 52 to 2.07 g/cm³, and water content ranges from 99 6 to 25 5% of dry weight (Marsters, 1988). Shear strength values are between 4 4 and 15.0 kPa (Marsters, 1988).

Micropaleontological examination of the unit in core 69 indicates a very sparse microfauna consisting only of badly preserved ostracods possibly of lacustrine origin (Bilodeau *et al.*, 1990). Sparse assemblages of pollen characteristic of open tundra vegetation in the early Holocene (≥8000 BP) are also found (Bilodeau *et al.*, 1990).

UNIT 4: ICE DISTAL SEDIMENTS

This unit, observed in core 47 (thickness 0,14 m; Figure 16), core 69 (thickness: 6,71 m; Figure 18), and core 43 (thickness: 3,69 m; Figure 19), is a bioturbated olive grey silty mud (Munsell colour code 5Y 4/2) with black sulphide mottling. In all cores, the lower contact is sharp. The unit consists mainly of clay-size material, ranging between 60% and 73% by weight. Scattered patches, higher in gravel or sand content, have clay-size fractions ranging from 38% to 49%. Silt forms most of the remainder (20-38%), with little sand (0-23%) and gravel (0-20%) (Henderson, 1989). Geotechnically, the unit shows a general trend toward an increase in bulk density and a decrease in water content downward,

indicating a normally consolidating sequence (Masters, 1988). It has a shear strength of approximately 3-14 kPa, a water content of 79-104 % of dry weight, and a bulk density of 1 50-1 70 g/cm³ (Marsters, 1988).

Unit 4 contains a diverse microfauna dominated by tests of foraminifera indicative of cold water and near normal seawater salinities (Bilodeau *et al.*, 1990). Pollen and spore assemblages, also abundant, indicate a change from early post-glacial vegetation (ca. 8000-6500 BP) to regionally widespread open spruce woodland vegetation (<6500 BP) (Bilodeau *et al.*, 1990).

UNIT 5: DISTAL FLUVIO-DELTAIC SEDIMENTS

This unit is an olive grey silty clay (Munsell colour code 5Y 4/1) with numerous dark grey reduction spots that were formed by the decomposition of buried organic matter. It shows more silt (37-55%) and less clay (38-58%) than unit 4, as well as little sand (1-12%) and gravel (0-6%) (Henderson, 1989). The unit has been sampled by cores 47 (3,47 m; Figure 16), 48 (2,23 m; Figure 17), 50 (0,89 m), 68 (7,45 m), 70 (2,42 m), and 71 (4,70 m). The lower contact with unit 4, observed only in core 47, is sharp. In core 48, unit 5 lies abruptly on an erosional surface at the top of unit 3.

Geotechnical analyses show a bulk density of 1.56-1.87 g/cc, a water content of approximately 39.9 to 87 3 % of dry weight, and a shear strength of 3.3-15.4 KPa. However, a trend toward an increase in bulk density and a decrease in water content downward indicative of normal consolidation is not observed. This

suggests underconsolidation, possibly as a consequence of high sedimentation rates (Marsters, 1988).

DISCUSSION

DEPOSITIONAL SETTING AND PROVENANCE

The physical and acoustical characteristics of unit 2, as well as its irregular thickness over the area, suggest a basal till. The presence of gravel composed of crystalline and of Proterozoic carbonate rock fragments derived from the coastal uplands (Figure 2) to the east indicates that the material was transported westward by the ice sheet. The well compacted diamicton, not easily penetrated by the corer, would have been deposited under grounded ice

In contrast, the fine-grained texture of unit 3, which is draped over and comformable to the upper surface of unit 2 or rests directly over the bedrock, suggests deposition in a quiescent deep environment. As palynostratigraphy at the base of unit 4 gives an age of around 8000 BP (Bilodeau *et al.*, 1990), unit 3 would have been deposited earlier, that is prior to the Tyrrell Sea invasion, which began around 8000 BP, and during the time when Lake Ojibway is reported to have extended over the lower Great Whale River estuary (Hillaire-Marcel, 1979).

A paleontological analysis made only on core 69 indicates that microorganisms in unit 3 are very sparse, consisting only of badly preserved ostracods interpreted to possibly indicate a lacustrine environment by Bilodeau *et al* (1990).

Furthermore, the regularity as well as the systematic difference in grain-size between dark and light laminae noted in the rhythmites brings up the possibility that these are glaciolacustrine varves (Chapter 3). Varved sediments consist of annually-produced couplets, with a sharp contact between the two laminae (Smith and Ashley, 1985). The fine-grained laminae show normal grading, whereas the coarser grained ones may or may not show any grain size trend. characteristics of varves in general are observed in the rhythmites of unit 3. Sharp interfaces between the light (fine) and dark (coarse) laminae, and fining upward in the fine-grained laminae, are disclosed by the grain size analysis of core 48 (Figure 20). Also an overall trend in all cores toward thinner couplets upward may be related to eastward retreat of the ice front and of the sediment sources. The fracturing (Figure 20) and fragmentation of sediments observed in segments of unit 3 within cores 43, 47, 48 and 69 are interpreted to be due to post-depositional freezing of the interstitial freshwater of lake sediments suddenly exposed to temperatures below 0°C during invasion of the area by marine waters (Bilodeau et al., 1990). Such a process is discussed by Chamberlain et al. (1979) All features noted above (comformable draped attitude, palynostratigraphy, micropaleontology, textural variations, thinning of the laminae upward, fracture and fragmentation of the sediments) are in agreement with deep water deposition in glacial Lake Ojibway.

These observations add further support to the conclusion of Hillaire-Marcel (1979), based on the river bank sections, that glacial Lake Ojibway in its late

phase extended to the latitude of Great Whale River. Because in the river bank sections the lake deposits are abutting against the Sakami moraine, continuation of the moraine 18 km farther north into Manitounuk Sound, as postulated by Hardy (1980), could signify a further northward extension of the lake basin. In support of this, core 48, collected 5 km into the sound, contains 0.98 meters of varve-type deposits belonging to unit 3, interpreted as lacustrine. Also, unit 3 is identified on the seismic profile which extends 15 km into the sound (Figure 5).

Contrasts in textural and chemical compositions between layers can be used to interpret the depositional processes of the varves and are discussed in more detail in Chapter 3. Because of coarser texture and thicker layering, as well as the presence of microsublaminations within some of the layers, which are suggestive of pulsating flow conditions, the dark laminae point to more dynamic conditions of transportation than do the light ones The dark laminae are presumed to have been deposited by a combination of underflows and of overflowinterflows during the open water season (Chapter 3). A combination of these two types of flows tends to form thicker accumulations in the bathymetric lows than in the highs because underflows are constrained by the bottom relief (Smith and In contrast, the fine-grained light laminae would have been Ashley, 1985). deposited quietly by widely spreading overflow-interflows, possibly under a full seasonal lake ice cover, thus forming a uniform deposit over the entire area (Chapter 3). As a result of this combination of processes, thinner deposits would have formed on the ridge crests and thicker ones in the troughs. However, Figure

12 shows that no sediments are present on ridge crests. Therefore, it is probable that the thin ridge crest deposits may have been eroded by shallow water processes after isostatic uplift brought up the deposits above wave base.

The alternation of dark "summer" laminae and lighter "winter" laminae, which is inverse to the color banding commonly observed within varved sediments (Eyles and Miall, 1984), is explained, on the basis of geochemical data, by the conditions of deposition in glacial Lake Ojibway (Chapter 3). The dark coloration of coarse "summer" laminae possibly results from the formation of black authigenic iron monosulfides within a suboxic pore water environment. Deposition of the light laminae probably occurred in oxic conditions in the surface sediments, and did not allow such precipitation (Chapter 3).

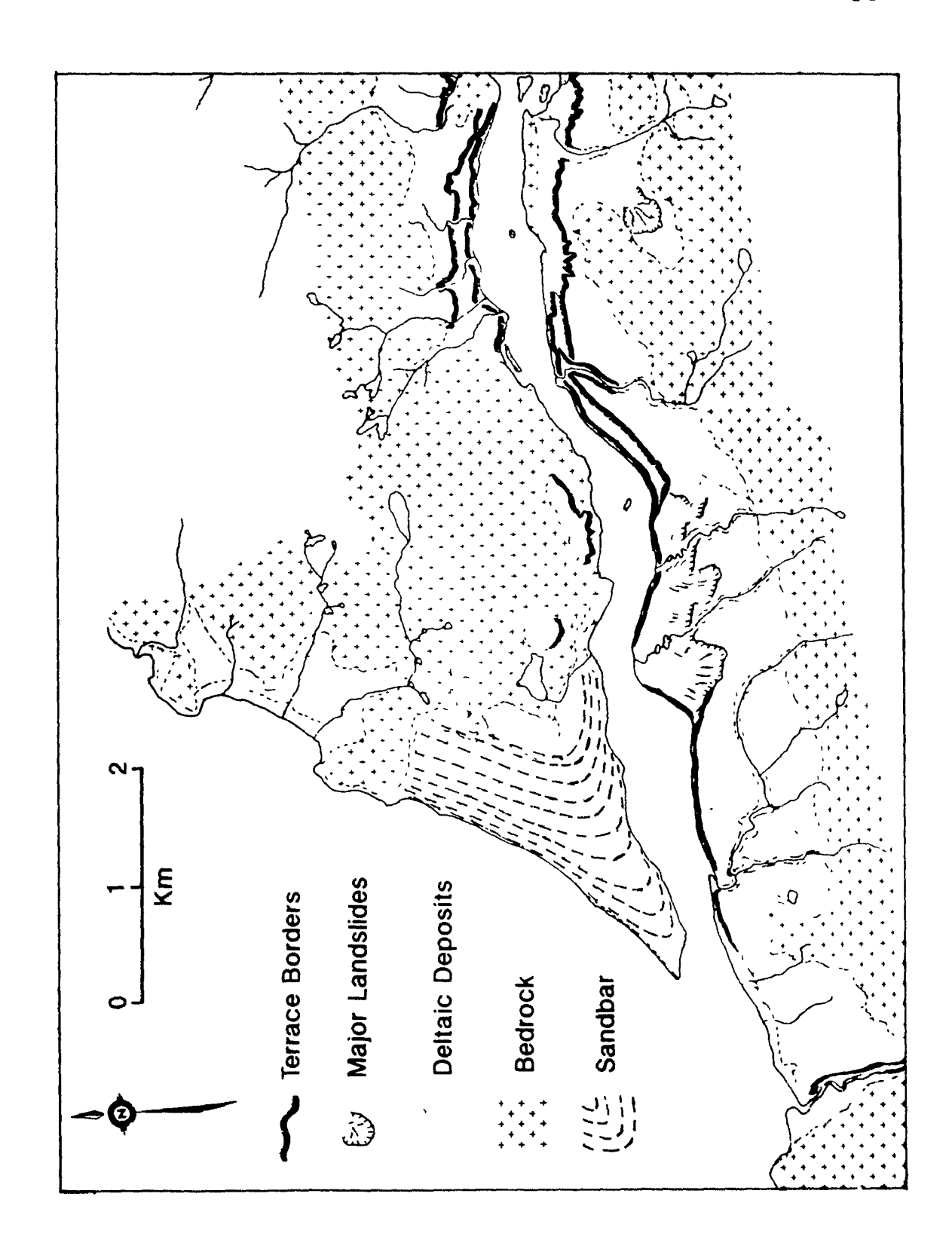
The absence of unit 3, as well as of units 4 and 5, in those parts of the SW Trough that are deeper than 120 m may result from a combination of two processes. First, slumping of the entire sedimentary sequence toward the southwest and out of the surveyed area of the trough, in spite of the moderate slope gradient (3m/km), might have resulted from the weight of unit 5, thick and underconsolidated, lying on the quick clays of units 3 and 4. This is supported by the presence of large slumping on the delta front off Little Whale River, which has produced sediment flows that extend up to 7.5 km seaward of the delta (Josenhans *et al.*, 1991). Large slumps were also observed along the Great Whale River banks where they affected the entire stratigraphic sequence from lacustrine muds to deltaic sands (Bégin and Filion, 1987). Second, sedimentary

furrows have been observed by sidescan sonar at the bottom of the SW Trough (Josenhans et~al., 1991). Furrows are indicative of recurring, directionally stable, strong (\pm 50 cm/sec) bottom currents (Flood, 1983). The southwest orientation of the furrows parallel to the trough axis (Josenhans et~al., 1991) suggests nondeposition or erosion due to bottom currents at present. Thus slumping of the entire sedimentary sequence and subsequent non deposition of segiments due to strong bottom current would explain the absence of sediments in the SW Trough

Because of its fine texture and its draping over the substratum, unit 4 also appears to have been deposited in a deep quiescent environment at some distance from the ice margin. It is again absent from ridge tops, presumably because of erosion during and following uplift, and from the SW Trough for reasons given above. The microfauna indicates a marine origin, and the palynological assemblage gives an age of post 8000 BP (Bilodeau *et al.*, 1990) corresponding to that of the Tyrrell Sea. Unit 4 would, therefore, represent hemipelagic post-glacial marine muds of that period

Unit 5 sediments consist of thick postglacial accumulations of silts and clays and are interpreted to be detrital sediments transported out of the watershed as the strandline prograded westward. They are most probably the distal equivalents of the onshore alluvial deltaic sands, described by Hillaire-Marcel and de Boutray (1975) which form raised terraces that reach 40 m of altitude on the south side of the channel upstream of the river exit (Figure 21). These sands deposited on top of the Tyrrell Sea clays during marine regression vary in grain-size from fine to

Figure 21. Deltaic sand distribution along the banks of the Great Whale River lower estuary (modified from Hillaire-Marcel and de Boutray, 1975).



coarse, and contain lenses of gravel or pebbles (Bilodeau *et al.*, in press). They represent deposition of material derived from remobilization of the Sakami moraine and proglacial sands farther upstream during the terminal phase of emergence (Hillaire-Marcel and de Boutray, 1975). The finer particles, which originated either from winnowing of the moraine or from the lacustrine and marine clay horizons above it, were transported offshore and formed unit 5. Because nearshore areas shallower than 40 meters could not be surveyed by the CSS HUDSON, information is missing from within 3 km of the river mouth, a region where the transition between the topset deltaic sands to sandy silts onshore and the bottom set clayey silts offshore is expected to occur.

In recent times, the seaward progradation and southward expansion of the sand barrier by longshore processes has favored the southward migration of the river channel, undercutting the raised deltaic sand terraces along the left bank of Great Whale River (Figure 21) and causing cliff recession. Most of the sediments from these terraces have settled near the river mouth as suggested by the presence of a shallow (depth of 1 to 1.5 m) sandbar (Ingram, 1981).

The time interval covering the deposition of unit 5 can be indirectly estimated by reference to the known regional emergence rates, assuming that these rates are the main control on the river solid discharge. Based on the regional topography, C¹⁴ dating, and Andrews' (1968) emergence curve, Hamelin and Cailleux (1972) postulated the migration of the coastline through time. If the paleo-shores are interpreted using the emergence curve of Hillaire-Marcel and

Vincent (1980), they would show that the present river channel came into existence at around 4000 BP, which suggests an upper limit to the age of unit 5. However, an age of 3810 ± 50 BP was obtained in a river bank section by Bilodeau *et al.* (in press) at one meter below the boundary between the deltaic sands and the Tyrrell Sea sediments, which suggests that deltaic sediments began to be deposited around 3500 BP.

Near that time the fluctuating regional emergence rate could have temporarily reached values as high as 4.5 cm yr⁻¹ with a mean value of 2.9 cm.yr⁻¹ (Hillaire-Marcel and Fairbridge, 1978). At these rates, peak periods of channel downcutting, river sediment transport, and unit 5 buildup are expected. The current emergence rate of 1.1 cm.yr⁻¹ was reached around 2800 BP (Vincent *et al.*, 1987), an age which most likely marked the termination of deposition of unit 5. At the present rate, the sediment discharge is in the order of only 0.5 x 10⁶ t yr⁻¹, with offshore sedimentation rates of 2 to 3 mm.yr⁻¹ (d'Anglejan and Biksham, 1988). Expected rate of sedimentation is on the order of 2.1 cm.yr⁻¹ during unit 5 deposition.

Distribution of the deltaic sediments, as observed on Figure 14, was mainly controlled by bottom topography. The sediments accumulated preferentially in basins and troughs with thinner deposits over bedrock ridges. Thus two lobes of thick sediments present north and south of the river channel axis (Figure 14) indicate the presence of two topographic lows in the bedrock, while in the axis of the river, thinner accumulations occurred on a rise.

Where it underlies unit 5, unit 4 occurs only as a thin (>5 m) layer (Figures 13 and 14). Based on sedimentation rates estimated at 75 to 100 cm.10⁻³yrs in the Tyrrell Sea (Bilodeau *et al.*, 1990), and assuming 4500 years of deposition following the marine invasion at 8000 years BP, the Tyrrell Sea sediment (unit 4) thickness nearshore should be approximately 3.4 to 4.5 m. This is consistent with observed thicknesses nearshore of about 1 to 5 m for unit 4 where it underlies unit 5. Unit 5 sediments nearshore are in lateral continuity with the upper marine muds of unit 4 offshore and therefore contemporaneous with them.

It is likely that during the period of high discharge which produced unit 5, the river's finest suspension load was dispersed seaward to the deeper parts of the basin along general directions imposed by the bottom topography, which are shown by arrows on Figure 14. Deposition of these suspended sediments may have contributed to unit 4 offshore, increasing its thickness, as observed in the deeper troughs there (Figure 13).

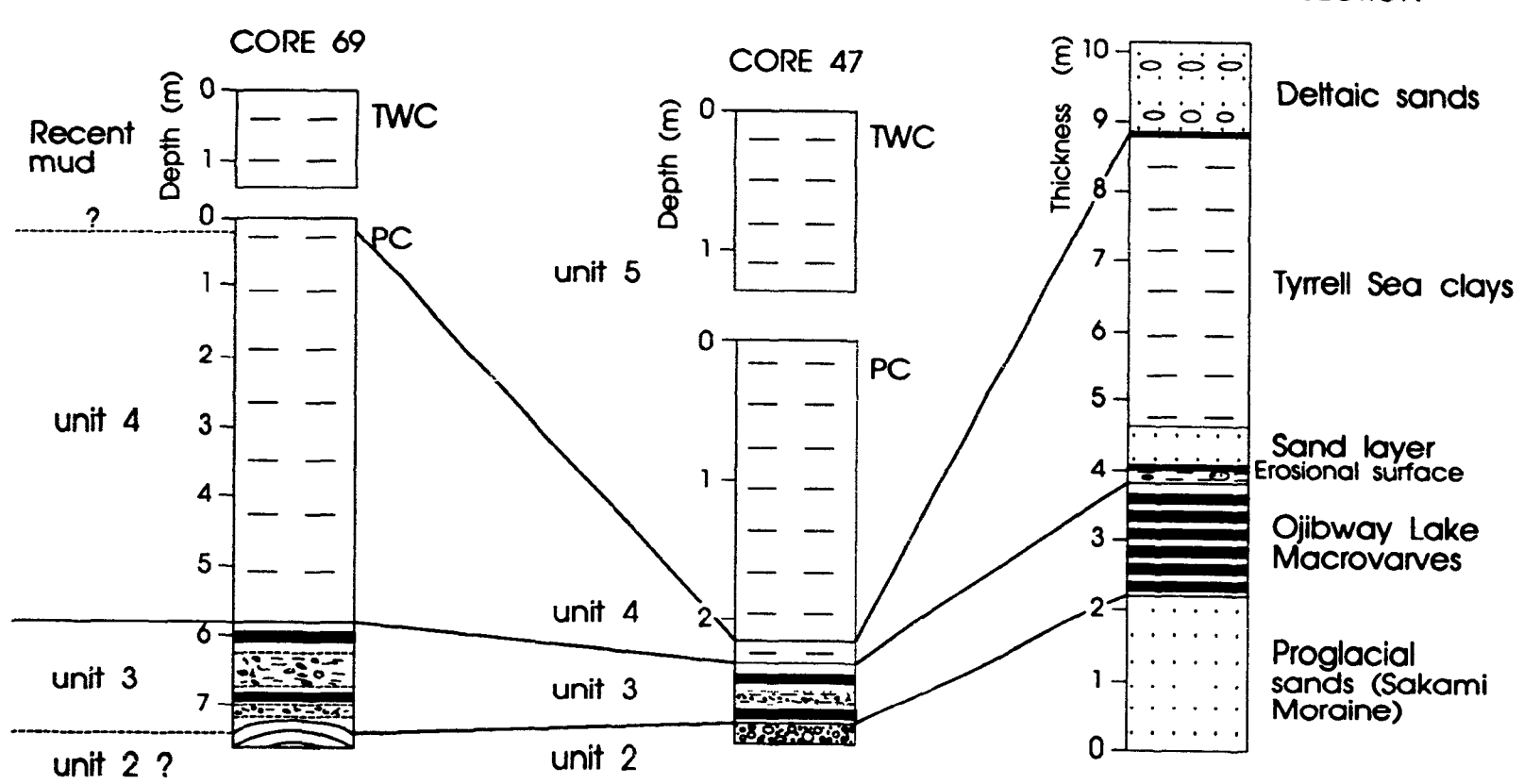
RELATIONSHIP TO ONSHORE STRATIGRAPHY

A biostratigraphic correlation based on micropaleontology and palynology was made between an onshore section along the Great Whale River and core 69 (Figure 5) by Bilodeau *et al.* (in press). Core 47, taken closer to shore, provides additional lithostratigraphic details as it includes unit 5.

Figure 22 shows that the proglacial sands observed onshore lateraly correspond to a basal till offshore. This unit is observed best in core 47, and

Figure 22. Correlation between onshore and offshore stratigraphic sequences. See Figures 16 and 18 for lithologic descriptions of cores 47 and 69. See Figure 5 for core localities.

GREAT WHALE RIVER SECTION



possibly in core 69, as explained above. Figure 22 thus correlates unit 2 in core 47 with the base of core 69.

The overlying unit (unit 3) consists of rhythmites thought to have been deposited in glacial Lake Ojibway. It is traced continuously from onshore to offshore, suggesting that the lake extended across the entire region. Offshore, the Tyrrell Sea clays (unit 4) directly overlie unit 3, whereas onshore a 60 cm sand layer separates them. This layer was first interpreted by Hillaire-Marcel and Vincent (1980) as a by-product of the rapid drainage of glacial Lake Ojibway into the Tyrrell Sea (around 8000 BP). However, Bilodeau $et\ al\$ (in press) established that it is more recent (5190 \pm 60 BP), and suggested that it might record strong subaquatic currents set by a major landslide upstream. This is in better agreement with the lack of a sand layer noted offshore

The upper unit of deltaic sand noted onshore correlates with the nearshore silty clays of unit 5. As mentioned earlier, unit 5 is absent farther offshore and is the time equivalent of the upper Tyrrell Sea muds (unit 4). Onshore, because of land emergence the deltaic sands are at the top of the sequence (Hillaire-Marcel and de Boutray, 1975). Offshore, recent sediment overlies both unit 5 of core 47 and unit 4 of core 69. Recent sediments cannot be distinguished from unit 4 neither acoustically nor physically because the environment of deposition has not changed substantially; the present Hudson Bay is merely a remnant of the Tyrrell Sea. Nor can the layer of recent sediments be distinguished on the top of unit 5 because it is too thin for acoustic resolution and lacks textural contrast in cores.

SUMMARY AND CONCLUSIONS

Medium- and high-resolution seismic profiles and piston cores were used to interpret four acoustic stratigraphic units and to map their lateral distributions in front of the Great Whale River. These interpretations are supported by the lithostratigraphy provided by eight piston cores, as well as textural, geotechnical, paleontological, and palynological information available on four of these. This study agrees largely with the interpretations of Hillaire-Marcel and Vincent (1980) and of Bilodeau et al (in press) concerning the Holocene stratigraphy and deglaciation processes, but it encompasses a larger data base and covers a much greater area, and thus significantly expands and refines our understanding of the sedimentation and deglaciation processes that have occurred in the area since the Laurentide Ice Sheet withdrawal. The additional details and refinements include the following.

- Unit 2, which is interpreted as a basal till, is present as a generally thin, irregular deposit over the entire surveyed portion of the inner shelf. It was transported by a westward-flowing ice sheet and it was deposited under grounded ice.
- 2) The conformably draped attitude of unit 3 over the substratum and its textural characteristics support the interpretation of Bilodeau *et al.* (1990) that this unit was deposited in a lacustrine environment, probably glacial

Lake Ojibway. The varves became thinner upward as the ice sheet retreated. The absence of unit 3 sediments on the tops of the ridge crests may have resulted from a combination of processes that favored accumulation within depressions and reduced deposition on the crests, with subsequent erosion during uplift. Also, the absence of unit 3, 4, and 5 in those parts of the SW Trough that are deeper than 120 m probably resulted from slumping of the entire sedimentary sequence and subsequent nondeposition of sediments due to strong bottom currents

- 3) Unit 4 consists of hemipelagic postglacial marine muds deposited in the Tyrrell Sea and it occurs as a comformable layer throughout the area. Its absence from ridge crests also suggests erosion subsequent to uplift.
- A distal deltaic unit (unit 5) formed in front of the Great Whale River mouth between approximately 3500 BP and 2800 BP. The sediments forming this unit originated from the excavation of the river channel through the morainic deposits and the glaciolacustrine and marine muds exposed presently along the Great Whale River banks. The approximate volume of this unit is 6 x 10⁹ m³, and the expected rate of sedimentation was on the order of 2.1 cm.yr¹ during deposition of the unit. Evidence suggests that unit 5 sediments are contemporaneous with and distal to the deltaic sands exposed along the Great Whale River banks, implying that the deltaic



sequence grades from sands onshore to clayey silts offshore. Unit 5 correlates with the upper part of the Tyrrell Sea sediment sequence (unit 4) farther offshore.

CHAPTER 3

THE ICE PROXIMAL SEDIMENTS OF UNIT 3

INTRODUCTION

During the last deglaciation, the retreat of the Laurentide ice sheet led to the formation of proglacial Lake Ojibway southeast of Hudson Bay. Lake water flooded the lowlands east of James Bay as far east as the Sakami Moraine (Hardy, 1976) and as far north as the Great Whale River (Hillaire-Marcel et Vincent, 1980). The areal extent and duration of the lake is recorded by well-preserved varves. Study of the varves has yielded a time interval of 2110 years for the lake existence, from the time of deposition of the first varve southwest of Lake. Temiskaming until the drainage of Lake Ojibway (Vincent et al., 1987; Vincent, 1989). The northern limit of the lake migrated northward and northeast with time, resulting in a thinner varve sequence in these directions, which indicates a shorter

duration of lacustrine conditions there. Between 8300 and 8025 B.P., three ice surges (Cochrane I, Rupert, and Cochrane II) originating from the Hudson Glacier reached the lake causing an increase in the grain size, thickness, and carbonate content of the varves (Vincent *et al*, 1987; Vincent, 1989).

Based on reflection seismic profiling and on coring, the stratigraphy of the post-glacial deposits off the Great Whale River consists of four different units (see Chapter 2). One of them (unit 3) is a layer of ice-proximal, rhythmically color banded sediments which are presumed to have been deposited within the northern extension of glacial Lake Ojibway (Bilodeau *et al*, 1990). The color bands form couplets which generally thin upward from a maximum of 22 cm in the lower part of the unit to 3-4 mm in the upper part. The rhythmites often show fracturing, as well as an interval of disaggregated sediments with the original laminations still discernable. The unit is mainly composed of clay (7-96%) and silt (2-61%), with little sand and gravel (Henderson, 1989)

This chapter attempts to provide a better understanding of the depositional environment and processes of these sediments by examining the physical characteristics of unit 3 in the four piston cores (43, 47, 48, 69) that intersected it (Figure 5), and the results of detailed textural and geochemical analysis performed on individual laminae of core 43 and 48. These two cores were selected because the rhythmites are well defined in both, and also because one is located nearshore (48) while the other (43) is farther offshore.

METHODS

Slabs of sediment 25 cm long and 1 cm thick were taken from cores 43, 48, and 69 following the method described by Mosher and Asprey (1986). They were X-radiographed in a Picker (Mini-shot II) X-Ray machine at the McGill Department of Geological Sciences, using Kodak Industrex AA ready pack films. The sample to source distance was 53cm and the exposure varied from 50 to 60 kV at 3mA for a period of 50 seconds. The prints of the X-radiograph can be found in Appendix 1.

Two of the slabs, one from each of core 43 and 48, were then subsampled for various analyses. Grain-size analysis was performed with a Coulter counter model TA, on small samples collected every 3 mm along the slabs. These were suspended in an isotonic solution, and dispersed in an ultrasonic bath for 15 to 20 seconds. The suspensions were then passed through a 70 μ m aperture tube, which can determine particle size between 1 μ m and 32 μ m

Samples of individual dark and light laminae from the same two slabs were also taken and oven-dried. A fraction was ground and analyzed by X-ray fluorescence on a Philips PW 1400 unit to determine the following major and trace elements: SiO_2 , TiO_2 , Al_2O_3 , Fe_2O_3 , MnO, MgO, CaO, Na₂O, K₂O, P₂O₅, Co, Cr₂O₃, Cu, Ni, and Zn. All analyses were done on fused beads prepared from ignited samples. Measurement precisions are of less than \pm 1% for SiO_2 , less than \pm 5% for Na₂O and MgO, less than \pm 2% for the other major elements, and less than \pm 5% for the trace elements. Another fraction was used to determined carbon and

sulphur concentrations in a LECO induction furnace with a gravimetric absorption bulb for the CO₂ analysis and an Alpha sulphur titrator for the SO₃ analysis. The precision of the analyses are 0.01% for C and 0.2% for S. Finally, an aliquot of three samples from core 48, suspended in distilled water and mounted on a glass slide (Gibbs, 1965), was analyzed by X-ray diffraction on a Siemens unit # D500 in the geochemical laboratory of the McGill Department of Geological Sciences. CuKa radiation was used with the following setting: 40 KV; 20 mA; chart speed 2° 20/min; at 1000 cps

PHYSICAL CHARACTERISTICS OF UNIT 3

Slight differences are found in the appearance of unit 3 in each core, as follows:

CORE 43

In this core, unit 3 is 2.60 m thick (Figure 23). The top 11 cm of the unit (core interval 230-241 cm; Figure 23) consists of alternating greyish brown (2.5Y 5/2) clay and grey (5Y 4/1) silty clay laminae 3 to 4 mm thick. The next 123 cm section (core interval 241-364 cm; Figure 23), shows thicker (0.5 to 1 cm) laminae of olive grey (5Y 4/2) clay and very dark grey (5Y 3/1) silty clay. Of that section, a sublayer 48 cm thick (core interval 280 to 328 cm; Figure 23) is fragmented, although the original bedding is still apparent in places. In the next section, 86 cm

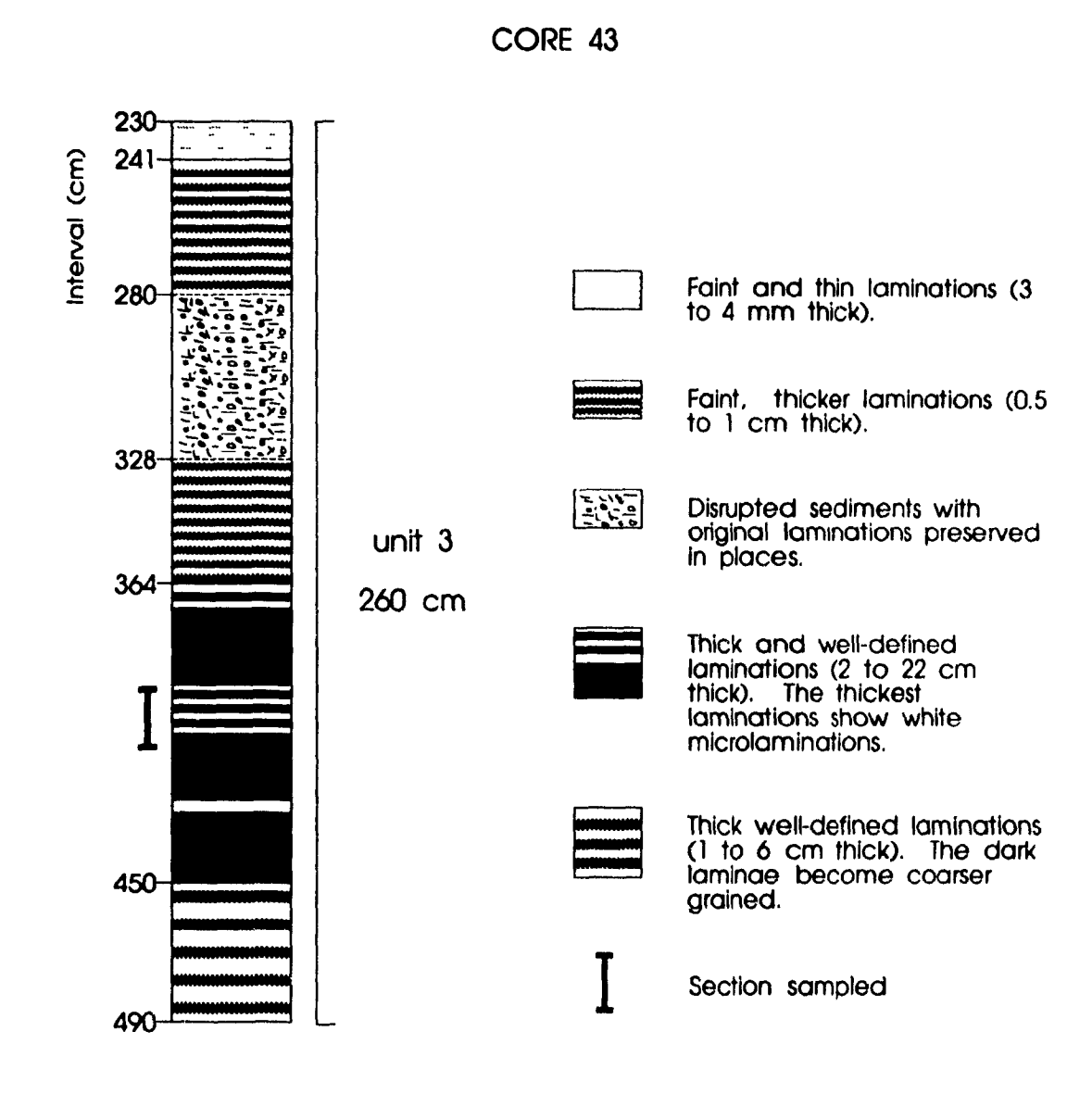


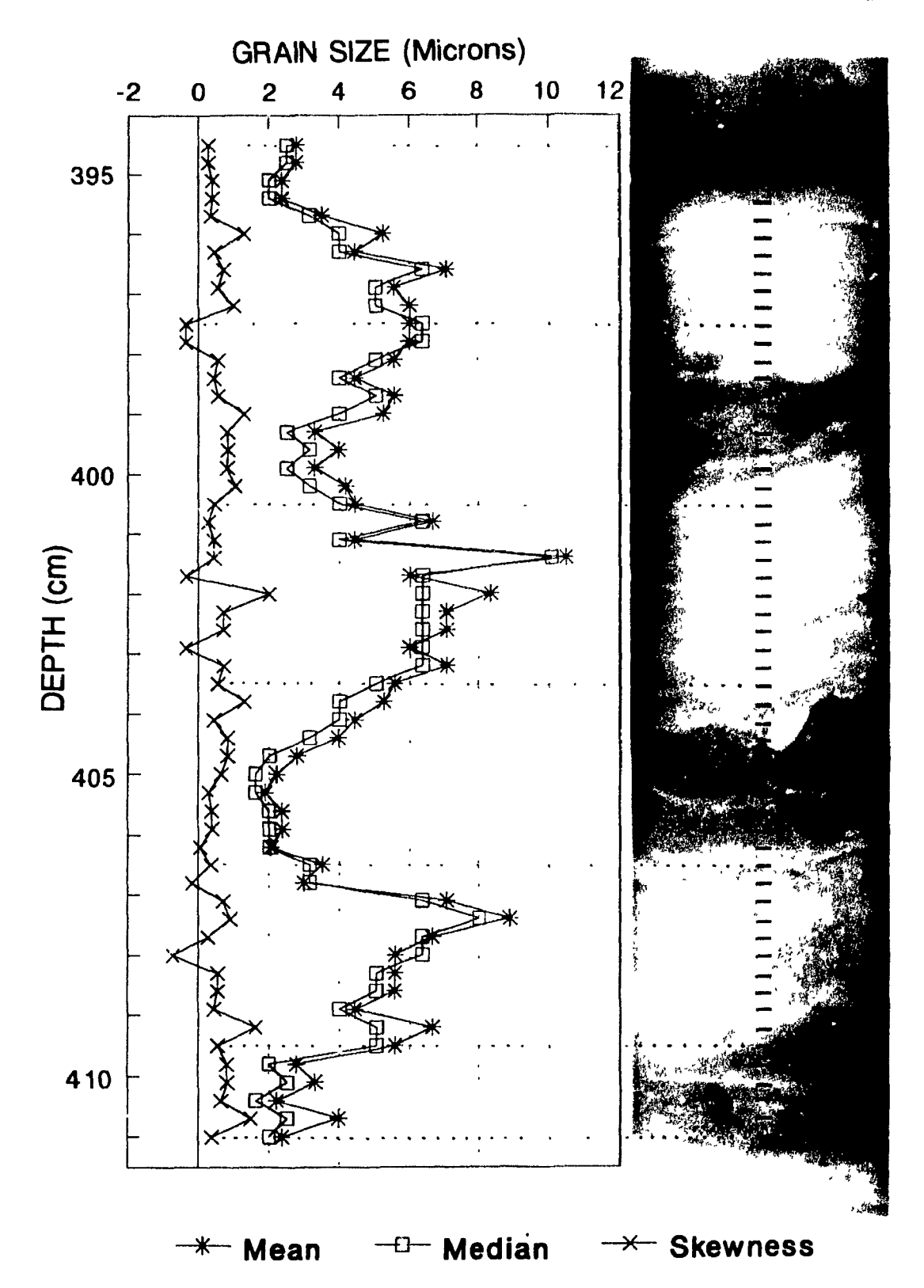
Figure 23. Lithostratigraphy of unit 3 in core 43. Section sampled corresponds to the interval sampled for grain-size analysis as shown in Figure 24.

downward (core interval 364-450 cm; Figure 23), the very dark grey coarser-grained laminae, increase in thickness to between 2 and 22 cm. They contain interspersed white microlaminations, scattered clay clasts, sand grains, and small pebbles. The olive grey clay layers remain 1 to 2 cm thick. In the lower 40 cm of the core (core interval 450-490 cm; Figure 23), laminations become more diffuse and the grey silty clay layers tend to become coarser grained with an average thickness of 3 cm, whereas the clay laminae become light grey and are 3 to 4 cm thick.

Grain size analysis of material from each alternating lamina was performed on a section taken between 3 94 m and 4.11 m from the top of the core 43 (Figure 23). The results indicate that within each couplet, the light layer is mainly composed of clay-size to very fine silt material, with particle sizes between 2 μ m and 6 μ m, whereas the dark layer contains, as its main component, very fine to fine silt-size particles 3 μ m to 10 μ m in size (Figure 24). Contacts between successive layers are fairly sharp and no apparent grading is observed within the light fine-grained laminae. However, a reversed grading is noticed in the dark coarser-grained ones.

X-ray fluorescence analysis indicates that the coarse dark-colored laminae contain significantly higher amounts of SiO₂, CaO and Cu, and lower amounts of Al₂O₃, Fe₂O₃, Na₂O, K₂O, MgO, TiO₂, MnO, Zn, Ni, and Co (on a LOI free basis), than the fine light-colored laminae (Table 1). Concentrations of total carbon expressed as %CO₂ by weight are higher in the coarse dark layers than in the fine

Figure 24. Graph showing variation of grain size in laminations of the ice proximal unit (unit 3) in core 43, aligned with X-radiographic negative print of the core slab.



		,	, 		,
Sample no color texture	43-00 dark coarse	43-01 light fine	43-02 dark coarse	43-03 light fine	43-04 dark coarse
S ₁ O ₂ (%)	69.60	61.25	68.78	61.05	70.11
TiO ₂ (%)	0.48	0.60	0 47	0.58	0.44
Al ₂ O ₃ (%)	13.56	16.75	13.38	16.43	13.26
Fe ₂ O ₃ (%)	4.25	6.47	4.75	7.78	4.08
MnO (%)	0 05	0.09	0.06	0.08	0.05
MgO (%)	1.73	3.52	1.92	3.21	1.72
CaO (%)	3.03	2.71	3.40	2.63	3.17
Na ₂ O (%)	3.83	4.48	3.74	4.16	3.74
K ₂ O (%)	3 25	3.89	3.26	3.82	3.22
P ₂ O ₅ (%)	0.20	0 22	0.22	0.24	0.20
Co (ppm)	<10	11	<10	27	<10
Cr ₂ O ₃ (ppm)	70	135	100	61	<15
Cu (ppm)	76	44	87	53	91
Ni (ppm)	16	42	<10	27	<10
Zn (ppm)	21	60	25	58	23

Table 1. X-ray fluorescence results on individual laminae of unit 3 in core 43. Sample positions are indicated in Appendix 1.

light layers (Table 2). This seems to be caused by differences in inorganic C, which is more abundant in the dark laminae than in the light ones (Table 2). Total sulphur values (as %SO₃) are equivocal (Table 2).

CORE 47

In core 47, the rhythmite unit is 46 cm thick (Figure 25). It has faint and thin (3-4 mm) laminae in the top 13 cm (core interval 229-242 cm, Figure 25). In the lowest 33 cm (core interval 242-275 cm; Figure 25), the laminae, although faint, get thicker. The coarse-grained darker layers reach thicknesses of about 1 to 2 cm, whereas the lighter fine-grained layers remain between 0 5 and 1 cm thick. The section also contains a fragmented sublayer, 12 cm thick (core interval 250-262 cm; Figure 25), in which laminae are discernable on X-ray photographs

CORE 48

Unit 3 is 98 cm thick in core 48 (Figure 26). Throughout the top 52 cm (core interval 117-169 cm; Figure 26), it consists of faint 1 cm thick laminations. The next 29 cm (core interval 169-198 cm; Figure 26) contains dark grey brown (2.5Y 3/2) grading to olive grey (5Y 4/2) clay and dark grey (5Y 4/1) grading to very dark grey (5Y 3/1) silty clay, both layers maintaining thicknesses around 0.5 to 1 cm. Although the lower 17 cm interval of unit 3 has been disturbed during coring (core interval 198-215; Figure 26), the coarser layers can be identified and appear to be thicker (around 2 cm) over the bottom 12 cm, with more sand and

Sample no. color/texture	Total carbon (CO ₂ %)	Inorganic carbon (ppm)	Organic carbon (ppm)	SO ₃ (%)
43-00 dark/coarse	0.67	7254	<250	5.25
43-01 light/fine	0.48	2042	2708	Insufficient sample
43-02 dark/coarse	1.63	1.05%	5742	3.46
43-03 light/fine	0. £0	2509	6493	Insufficient sample
43-04 dark/coarse	1.57	6252	9482	4.00
48-00 light/fine	0.62	4995	1253	<0.20
48-01 dark/coarse	0.40	501	3504	0.69
48-02 light/fine	0.68	250	6507	0.69
48-03 dark/coarse	0.44	251	4242	0.69
48-04 light/fine	0.52	251	4999	4.61
48-05 dark/coarse	0.48	1999	2752	2.30
48-06 light/fine	0.63	502	5760	3.29
48-07 dark/coarse	0.38	1506	2245	0.69
48-08 light/fine	0.48	1252	3503	4.36
48-09 dark/coarse	0.46	251	4258	1.15

Table 2. Total carbon and sulfur concentrations in individual laminae of unit 3 in core 43 (samples labelled 43-00 to 43-04) and in core 48 (samples labelled 48-00 to 48-09). Sample positions are indicated in Appendix 1.

CORE 47

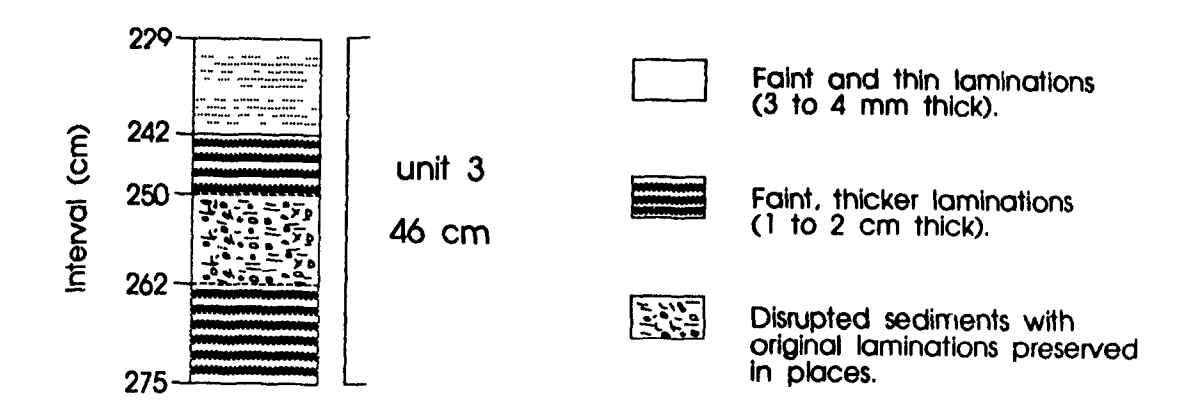


Figure 25. Lithostratigraphy of unit 3 in core 47.

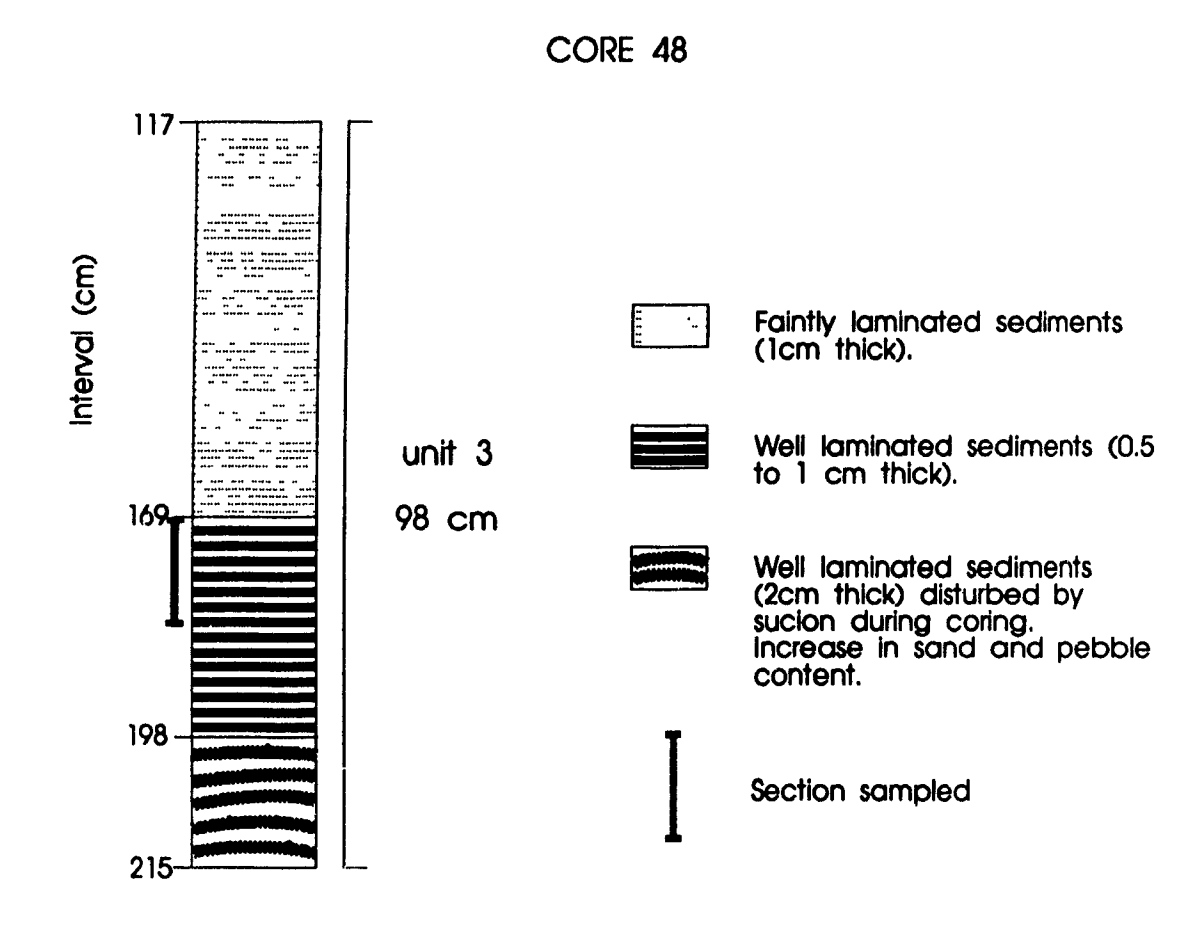


Figure 26. Lithostratigraphy of unit 3 in core 48. Section sampled corresponds to the interval sampled for grain-size analysis as shown in Figure 20.

pebbles.

Laminae between 1.69 m and 1.83 m down the core were analyzed for grain-size (Figure 26). The results are shown in Figure 20 (Chapter 2). Clay-size to very-fine-silt (1-5 μ m) layers alternate with fine silt (6-11 μ m) laminations. The contacts are somewhat sharper and better defined than in core 043. Also, fining upward of the fine-grained laminae is observed.

The results of the X-ray fluorescence analyses on individual layers (Table 3) indicate the same differences in chemical composition between light (finer) and dark (coarser) layers as noted in core 43 (Table 1). Comparison of X-ray diffractograms indicates that the finer laminae contain relatively more clay minerals (chlorite and illite), and less quartz and feldspar than the coarse laminae (Appendix 2). In contrast to core 43, core 48 total carbon content tends to be higher in the light laminae than in the dark ones, the differences being well above the analytical error. However, there are no trends in the distributions of inorganic C, organic C and total sulfur (Table 2).

CORE 69

Unit 3 is 1.58 m thick (Figure 27) The uppermost 22 cm (core interval 582-604 cm; Figure 27) shows thin (0.5 to 1 cm) laminae of greyish brown (2.5Y 5/2) clay and grey (10YR 5/1) silty clay. The next 66 cm section (core interval 604-670; Figure 27) shows thicker laminae (1 to 2 cm) of dark grey clay (5Y 4/1) and grey (10YR 5/1) silty clay. It contains also two sublayers, respectively 16 cm

Sample no. color texture	48-06 light fine	48-07 dark coarse	48-08 light fine	48-09 dark coarse
SiO ₂ (%)	63.09	68.51	62.59	69.88
TiO ₂ (%)	0.56	0.49	0.58	0.46
Al ₂ O ₃ (%)	16.23	14.24	16.30	13.85
Fe ₂ O ₃ (%)	6.01	4.60	5.83	4.39
MnO (%)	0.07	0.04	0.07	0.04
MgO (%)	2.79	1.60	2.95	1.18
CaO (%)	2.57	2.70	2.57	2.77
Na ₂ O (%)	4.72	4.35	4.97	4.10
K ₂ O (%)	3.70	3.21	3.89	3.07
P ₂ O ₅ (%)	0.23	0.24	0.23	0.24
Co (ppm)	16	<10	10	<10
Cr ₂ O ₃ (ppm)	119	111	118	50
Cu (ppm)	55	65	52	50
Ni (ppm)	30	30	35	20
Zn (ppm)	40	25	36	18

Table 3. X-ray fluorescence results on individual laminae of unit 3 in core 48. Sample positions are indicated in Appendix 1.

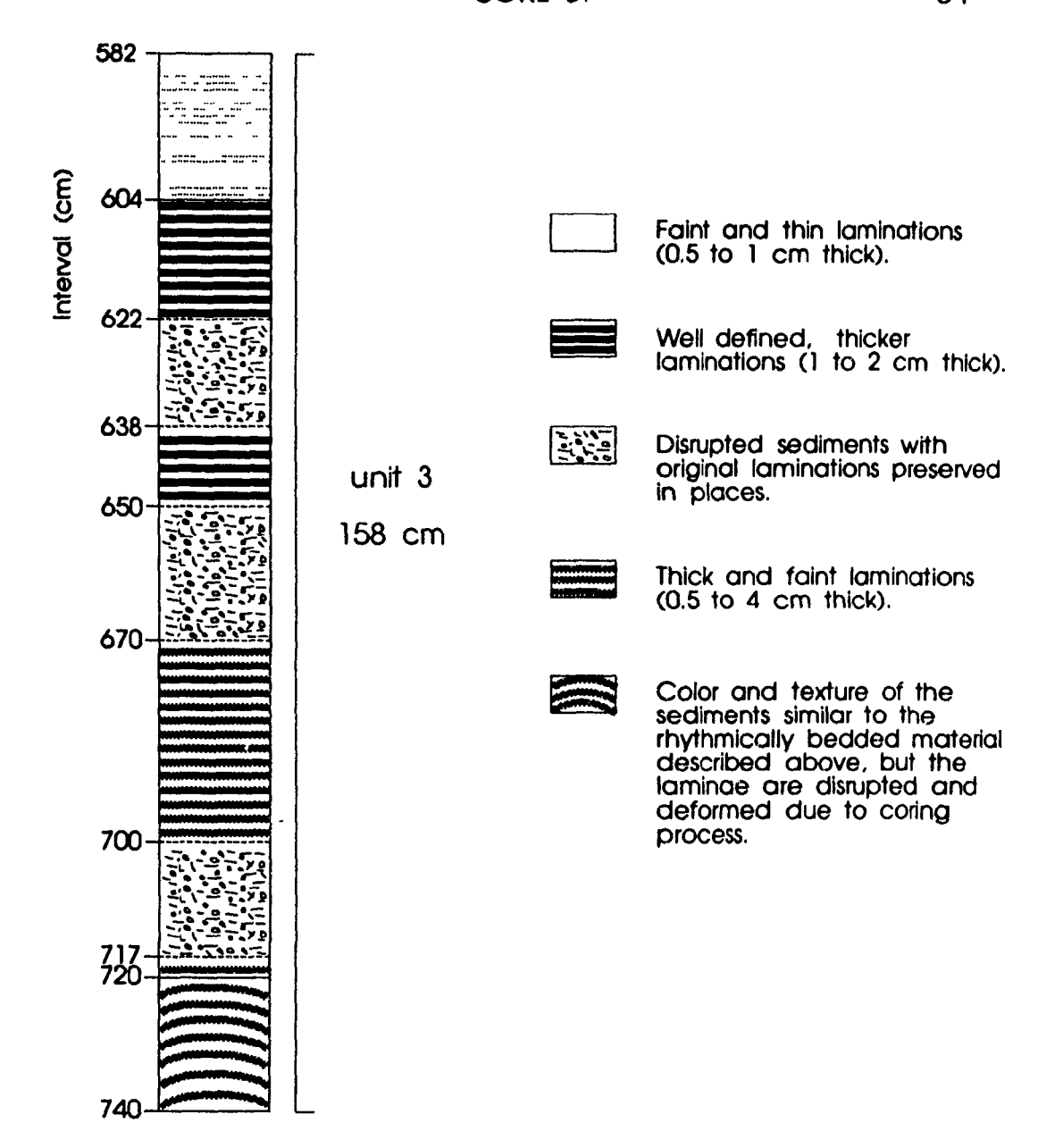


Figure 27. Lithostratigraphy of unit 3 in core 69.

(core interval 622-638 cm; Figure 27) and 20cm (core interval 650-670 cm; Figure 27) thick, of disrupted and deformed laminae, the original bedding being preserved in places. The following downward 50 cm section (core interval 670-720 cm; Figure 27) shows thin (around 0.5 cm), dark silty clay laminations while the light clay laminae may be as much as 4 cm, but mostly around 2 cm thick. A 17 cm sublayer (core interval 700-717 cm; Figure 27) shows fragmentation, although the original bedding is preserved in places. In the lower 20 cm (core interval 720-740 cm; Figure 27), the couplets are similar to those of the section described above but have been deformed during coring.

DISCUSSION

DEPOSITIONAL ENVIRONMENT

The evidence presented in Chapter 2 suggests that the sediments of unit 3 are glaciolacustrine varves. It is well established that the Tyrrell Sea did not invade the southeastern Hudson Bay area before 8000 BP (Hillaire-Marcel, 1976; Dredge and Cowan, 1989; Vincent, 1989). Based on C¹⁴ dates obtained on calcareous concretions, the fossil free rhythmites found onshore west of the Sakami Moraine were deposited prior to 8000 BP and were interpreted to be glacial Lake Ojibway varves (Hillaire-Marcel, 1979). This interpretation is based on age as well as on the fact that a few km upstream, east of the Sakami Moraine.

marine rhythmites younger than 8000 B.P. are found containing abundant macro and micro-fossils (Hillaire-Marcel and Vincent, 1980, Bilodeau *et al*, in press)

The rhythmite deposits found offshore in the study area contain only a few badly preserved ostracods, possibly of lacustrine origin, and no macro fossils (Bilodeau *et al*, 1990). Also, the palynological content indicates that the sediments are older than 8000 B.P. (Bilodeau *et al*, 1990). Both observations suggest that unit 3 was deposited in glacial Lake Olibway.

The percentages of sulphur (as SO3, Table 2) recorded in the individual layers reach high values that are not characteristic of a lacustrine environment Berner and Raiswell (1984) indicated that dissolved sulfate concentrations in fresh water is much lower, averaging less than 1% of that found in the oceans possible also to distinguish brackish water concentrations from fresh water ones. but only at salinities higher than 18% for which the percentages of sulfate are higher than 1%. However, at salinities over 18% brackish and marine waters cannot be distinguished (Berner and Raiswell, 1984) Table 2 shows that sulfur concentrations (calculated as SO₃) are over 1% in all the coarse laminae of core 43, and in half of all the laminae of core 48. This can be explained by one of the two following processes. 1) fresh water of the lake was contaminated by sea water from northeastern Hudson Bay seeping under the Hudson Ice Sheet barner, and became brackish, or 2) the water of the lake was fresh during deposition of the sediment but the interstitial pore waters were contaminated by downward diffusion of sea water sometime between the time of the Tyrrell Sea invasion and the

present, hence increasing the sulphur content within the sediments.

The second hypothesis is more plausible for three reasons. First, the pore waters have salinity values of 30 to 34‰ (Marsters, 1988), which are consistent with values for Tyrrell Sea and modern Hudson Bay waters, suggesting the possibility of marine contamination of pore waters. Secondly, as mentioned in Chapter 2, the sediment fracturing (Figure 20) and fragmentation observed within sections of unit 3 are interpreted as resulting from the freezing of lake sediments exposed to marine waters cooler than 0°C when the Tyrrell Sea invaded the area (Bilodeau *et al.* 1990). Finally, the isotopic ratios of Li⁶/Li⁷ in sediments of unit 3 have concentrations that are similar to those observed in modern lakes (A. Mucci, pers. comm., 1991), thus suggesting a fresh water environment.

As lacustrine deposits, the rhythmites of unit 3 are probably varves. Varves are annually-produced couplets that usually contain a light-colored silt layer deposited during the active melting period of ablation (summer), and a dark-colored clay layer deposited during the closed lake ice cover period (winter) (Eyles and Miall, 1984). According to Smith and Ashley (1985), varves occur as couplets with sharp contacts between the two layers. Within the fine layer, grain size commonly fines upward, whereas the coarser layer may or may not show any grading. The coarse layer thicknesses vary, but the finer layers maintain a consistent thickness throughout the basin. In addition, multilaminations are commonly present in proximal coarse layers, reflecting short-term fluctuations in source intensity. The rhythmites of unit 3 have all these characteristics, except the

color/grain-size relationship.

Grain size analyses performed on individual layers of cores 43 and 48 (Figure 20 and 24) show mean grain sizes of 1 to 6 μm in the light layer and 3 to 11 µm in the dark layer. A plot of the arithmetic quartile deviation (QDa) (Figure 28), which is indicative of sorting, versus mean grain size of both light and dark laminae of core 48 illustrates the well defined bimodality of the varved sediments. as samples of the light laminae are both finer and better sorted than those of the dark ones. The same is also noted in the varves of core 43 (Figure 29), although the bimodality is not as sharply defined due to the multilaminated nature of the dark coarse layers that incorporate microlaminations of clay within the silt layer This bimodality of the laminae indicates that each couplet is not a uniform graded bed, but consists of two distinct populations of particles deposited by two alternating processes Considering the quantity of sediments involved in the deposition of each couplet over the entire study area, the consistent repetition of two processes responsible for the rhythmicity of unit 3 is better explained by an annual cycle rather than by haphazard processes of sediment supply

Other physical features observed within the rhythmites of unit 3 suggest an annual cyclicity. Contacts between the different layers are sharp, thus recording a switch in depositional process from one layer to the other (Figures 20 and 24). The grain-size analysis results suggest normal grading in the fine-grained layers of core 48 (Figure 20), which is indicative of deposition of suspended material in quiet waters, possibly under an ice cover. On the other hand, the coarse-grained

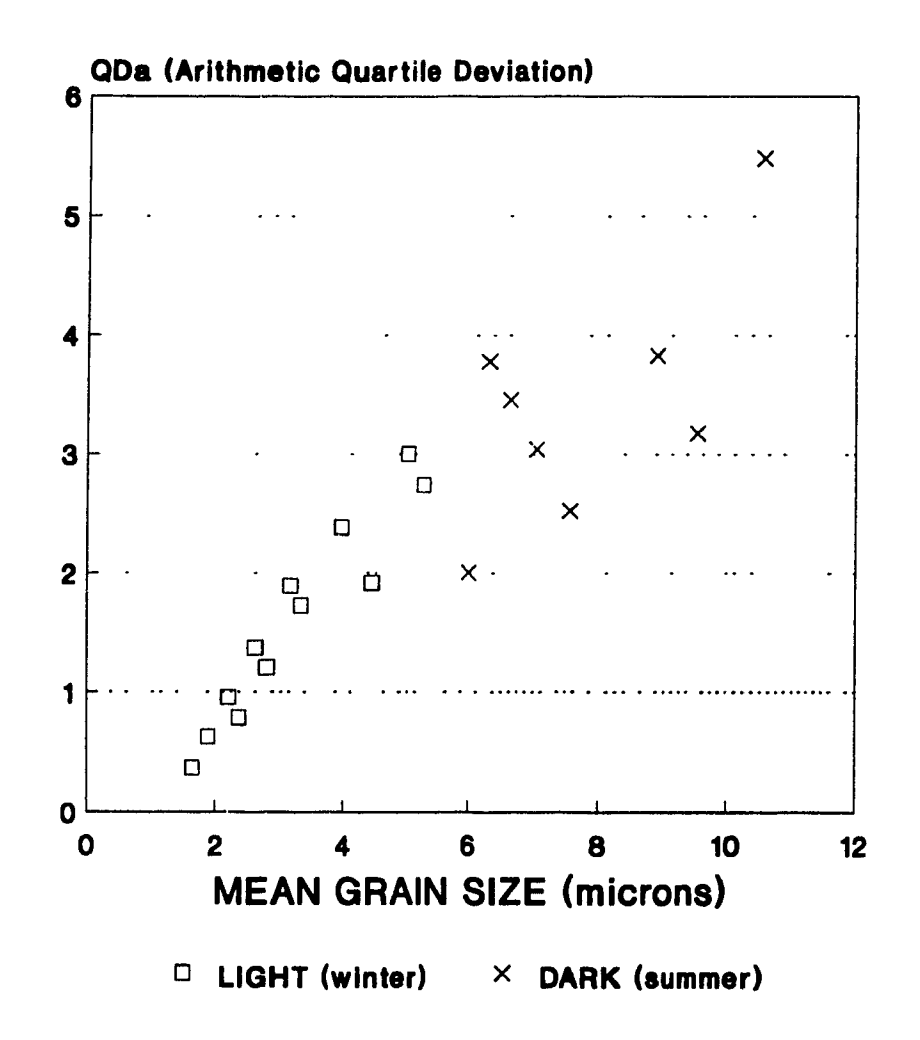


Figure 28. Plot of mean grain size versus arithmetic quartile deviation (QDa) in samples from core 48 as shown in Figure 20. The number of values plotted appears to be fewer than the number of samples indicated in Figure 20 because plots of samples with equal values overlie each other. A low value of QDa indicates better sorting.

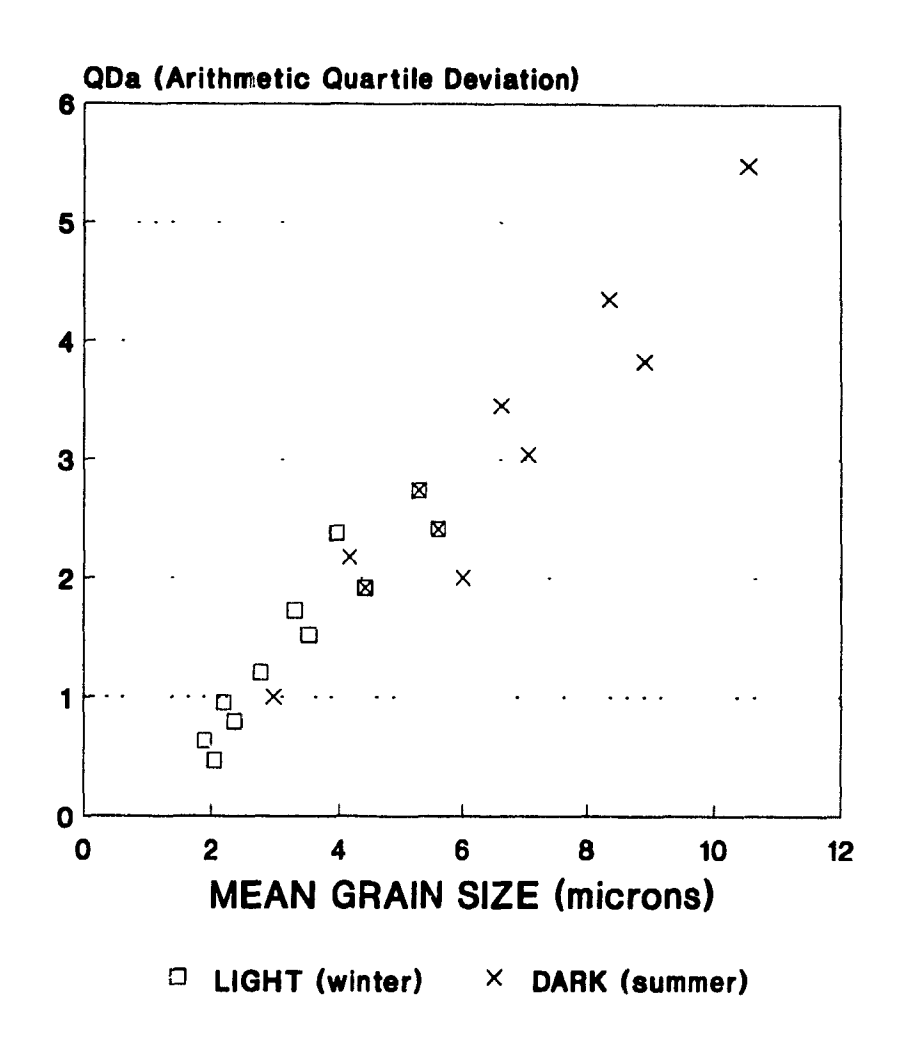


Figure 29. Plot of mean grain size versus arithmetic quartile deviation (QDa) in samples from core 43 as shown in Figure 24. The number of values plotted appears to be fewer than the number of samples indicated in Figure 24 because plots of samples with equal values overlie each other.

layers of core 43 show reversed grading and multiple microlaminations (Figure 24), the latter being suggestive of deposition by several intermittent density flows. Finally, the fine-grained layers display more constant thicknesses (generally from 3 mm to 1 cm with a maximum of 4 cm) than the coarser-grained ones (generally from 3 mm to 2 cm with a maximum of 14 cm) which suggests a more uniform depositional process

However, in contrast to what is normally observed within varved sediments (Eyles and Miall, 1984), dark laminae were found to be coarser-grained than the light ones This could be interpreted as follows. Coarse laminae may represent more active suspension transport and greater terrigenous inputs by seasonal meltwaters. Abundant fragments of tundra-type vegetation have been found in unit 3 of core 69 by Bilodeau et al (1990) Mildly reducing conditions could have developed in the sediments as a result of accumulation of detrital organic debris. With sufficient rates of burial, black disseminated sulfides would have formed, explaining the dark coloration. The lower amounts of oxidized Fe in the dark layers as compared to the light ones (Tables 1 and 3) may mean that some Fe went into solution in the suboxic pore water environment. It is assumed that enough sulfate was available in the lake waters to forms authigenic iron monosulfides which have been found to occur in fresh or brackish water sediments (Berner et al., 1979). In this interpretation the dark laminae could be "summer" layers, which are different from the coarse light summer layers of classical varves (Eyles and Miall, 1984).

In contrast, the better sorted fine-grained layers may indicate quiet winter settling, perhaps under an ice cover, of finer inorganic particles held in suspension in the water column, with little or no addition of new material from the rivers. Higher concentrations of Fe and Mn in the light laminae as compared to the dark coarse layers (Table 1 and 3) suggest lower rates of burial, forming oxic conditions in the surface sediments. The light laminae would then be the "winter" layers.

DEPOSITIONAL PROCESSES

The overall rhythmicity of unit 3 is best explained by a seasonally-controlled alternation in sedimentation between a short glacial-melt season and the rest of the year. As established in Chapter 2, after its initial westward advance, the ice front regressed eastward, remaining parallel to the actual coastline. This is in agreement with the orientation of a till ridge situated 20 km from the coastline (Figure 11; Chapter 2) which is parallel to the coast, and with the general direction of the Sakami Moraine perpendicular to the Great Whale River channel 5 km upstream. In the four cores intersecting unit 3, the thicknesses of the couplets diminish toward the top of the unit as a result of the retreat of the melting ice sheet.

The composition of the fine light-colored laminae, which contain more clay minerals and less coarser detrital particles than in the dark layers, suggests that their deposition resulted from the overflow-interflow dispersal process described by Smith and Ashley (1985). This mode of sediment delivery leads to deposition

of the coarse grains nearer to the ice margin, whereas the finer silt- and clay-size particles are transported throughout the lake by inertia and subsequently settle to the bottom during the winter.

The coarse layer was formed in a more dynamic environment, as the larger detrital grains, mainly quartz and feldspars, demand more energy to be distributed across the lake. The process responsible for these accumulations must then have been dominated by single pulsating or intermittent density underflows with possibly a minor contribution of pelagic material from overflow-interflows. As described by Smith and Ashley (1985) the underflows occur during the glacial melt season when the waters released from the ice sheet, which contains large concentrations of sediments, spread along the bottom of the lake due to its high density. The dominance of the underflow currents as the main depositional process of the coarse layer is supporte by its multilaminated nature and the fact that it is usually thicker than the fine layers, hence indicating a larger sediment contribution. As the ice front regressed eastward, the couplets became much thinner, and the laminae attained similar thicknesses. The underflow dominance therefore diminished in favor of the overflow-interflow processes.

Modern studies show that thermal statifications within ice-distal or ice-contact lakes is common (Smith and Ashley, 1985). As mentioned in the previous chapters, raised former marine limits reach elevations of 315 m between Little Whale and Great Whale rivers (Vincent *et al.*, 1987; Hillaire-Marcel, 1976), implying that before the Tyrrell Sea invasion, the ground was depressed by 300

m relative to the present topography. Therefore, Lake Ojibway was well over 300 m deep. It is likely that such a deep lake was thermally stratified for at least part of the year. The bimodality of unit 3 sediments suggests stratification; it has been argued that bimodality occurs only when discontinuous seasonal influxes of suspended matter coincide with seasonally stratified lake conditions (Sturm, 1978). Otherwise, different sedimentary structures such as chaotic sediments or completely graded beds are expected (Sturm, 1978).

Underflows responsible for the deposition of coarse laminae propagate as density flows along the lake bottom, as a result of the weight of suspended particles. Thermal discontinuities therefore have negligible influence on this type of sediment transport. This is supported by the non-graded or reversed graded character of underflow deposits which contrasts with the normal grading observed in sediments from thermally controlled flows (Sturm, 1978)

On the other hand, in order to efficiently disperse the finer sediment particles throughout the lake by overflows-interflows, thermal stratification is required (Smith and Ashley, 1985) As clay layer thicknesses are relatively uniform throughout the entire study area, it is probable that thermal stratifications developed near the lake surface during winter, following fall overturning.

CONCLUSIONS

Sedimentological and geochemical studies of the rhythmites of unit 3 in four

piston cores support the view that dark and light laminae occur in couplets, reflecting seasonal deposition, hence that they are true varves. These appear to have been deposited in a lacustrine environment, that of glacial Lake Ojibway, which extended farther north than Great Whale River. The alternation of dark "summer" laminae and lighter "winter" laminae, which is inverse to the color banding commonly observed within varved sediments (Eyles and Miall, 1984), is explained on the basis of geochemical data. The dark coloration of coarse "summer" laminae probably results from the formation of black authigenic iron monosulfides within a suboxic pore water environment. As for the light "winter" laminae, oxic conditions would have prevailed in the surface sediments, and would not have allowed such precipitation (Chapter 3)

The grain size variations as well as the mineral and chemical compositions suggest that a "summer" darker layer made up of coarse material was transported by a combination of underflows and overflows-interflows whereas the "winter" lighter-colored layer consisting of very fine particles was transported by overflows-interflows only. The importance of underflows in the lake basin diminished following the eastward ice sheet retreat, which explains the thinning of couplets upward.

The raised former marine limit elevations suggest that glacial Lake Ojibway was well over 300 m deep. Therefore, it was probably thermally stratified for at least part of the year. Underflows responsible for coarse-grained sediment transport are not affected by thermal stratifications, thus no conclusions can be

made as to whether the lake was stratified or not during the "summer" season. The efficiency of the overflows-interflows, which allowed the transportation of the fine-grained particles, is dependent on thermal stratifications. The relatively uniform thickness and distribution of the fine-grained laminae throughout the entire area therefore suggest the presence of thermal stratification during the "winter" season.

CHAPTER 4

GENERAL CONCLUSIONS

Medium- and high-resolution seismic profiles and piston cores were used to define stratigraphic units in front of the Great Whale River and to map their lateral extent. The stratigraphic sequence overlying Proterozoic bedrock (unit 1) consists of a glacial till/ice contact deposit (unit 2), glaciolacustrine stratified muds (unit 3), hemipelagic postglacial marine muds (unit 4), and distal fluvio-deltaic sediments (unit 5). The total Quaternary sequence reaches a maximum of 42 m near the Great Whale river mouth, thins out to less than 10 m over the ridge and trough topography, and increases to 10-30 m on the offshore slope beyond the 100 m contour.

The glacial till (unit 2) forms a thin (5 m) cover over the entire study area, and locally forms irregular ridges and mounds. A lithological provenance analysis

performed on the ice-contact sediments indicates that they were transported by a westward-flowing ice sheet. They were subsequently deposited under grounded ice during ice retreat as indicated by their highly compacted nature.

Unit 3 occurs as a thin (average thickness of 2 m), uniform, and conformably draped deposit throughout the entire study area, except on topographic highs and in the SW Trough where it is missing. Sedimentological and geochemical studies of the rhythmites of unit 3 support the view that these sediments are true varves. Paleontological analysis results, which suggest that the unit was deposited in a lacustrine environment, are available only from core 69 (Bilodeau et al, 1990), but the continuity of the unit as observed on seismic profiles suggests a similar depositional environment throughout the area. Such an environment would have been provided by glacial Lake Olibway, which extended farther north than the present site of the Great Whale River coloration of the laminae from that commonly observed within varved sediments is explained on the basis of geochemical data. The dark coloration of the coarse "summer" laminae probably resulted from the formation of black authigenic iron monosulfides within a suboxic pore water environment, whereas the light "winter" laminae formed under oxic conditions, which did not allow such precipitation

The grain size variations as well as the mineral and chemical compositions suggest that the "summer" coarse-grained laminae were transported by a combination of underflows and overflows-interflows, whereas the "winter" fine-grained laminae were transported by overflows-interflows only. The importance



of underflows in the lake basin diminished as the ice sheet retreated eastward, which explains the thinning of the couplets upward.

Sediment transport by seasonal alternation of underflows and overflows-interflows produced only thin accumulations on the ridge crests because underflows, which spread along the bottom, favored accumulations in depressions. Such thin ridge crest accumulations may have been subsequently eroded by shallow water processes as they were isostaticly uplifted to within wave base, which explains the absence of unit 3 sediments on bathymetric highs. The absence of unit 3 (and of units 4 and 5) in those parts of the SW Trough that are deeper than 120 m probably resulted from slumping of the entire sedimentary sequence and subsequent non deposition of sediments due to strong bottom currents.

The deep and quiescent environments of the Tyrrell Sea favored deposition of the fine sediments of unit 4 as a thin (average of 3m) and comformable deposit over the area. These sediments reached a maximal thickness of 16 meters in marginal troughs. They are, however, absent on ridge crests possibly because of erosion by surface currents after isostatic uplift.

The distal deltaic unit (unit 5) occurs as a constructional deltaic wedge built outward from the mouth of the Great Whale River It occurs preferentially at the river mouth where it forms two thick lobes (up to 42 m thick) localized in topographic depressions. Seaward, beyond 5 km from the shore, thicknesses remain below 10 m, except for scattered patches which may reach 20 m where the

sediments accumulated preferentially in basins. Unit 5 deposits cover approximately 400 km² and have an average thickness of 15 m. A time interval of deposition of 700 years has been estimated, beginning at 3500 BP and ending at 2800 BP after which river discharge attained its current regime. The approximate volume of the unit is 6 x 109 m³, and the expected rate of sedimentation was on the order of 2.1 cm yr¹ during its deposition. Sediments forming this unit originated from excavation of the river channel through the morainic deposits and the glaciolacustrine and marine muds exposed presently along the Great Whale River banks. Unit 5 sediments are shown to be contemporaneous with and distal to the deltaic sands exposed along the Great Whale River banks, implying that the deltaic sequence grades from sands onshore to clayey silts offshore. Unit 5 correlates with the upper part of the Tyrrell Sea sediment sequence (unit 4) farther offshore

REFERENCES CITED

- Allard, M. and Tremblay, G., 1983. La dynamique littorale des îles Manitounuk durant l'Holocène. Zeitschrift für Geomorphologie N.F., Suppl. Bd. 47: 61-95
- Andrews, JT, 1968. Postglacial rebound in Arctic Canada: similarity and prediction of uplift curves. Canadian Journal of Earth Sciences, 5: 39-47.
- Archer, D.R., 1968. The upper marine limit in the Little Whale River area, New Quebec. Arctic, 21, 153-160.
- Bégin, C and Filion, L, 1987. Morphologie et interprétation des glissements de terrain de la région de Poste-de-la-Baleine, Québec subarctique. Géographie physique et Quaternaire, 41: 19-32.
- Berner, R A and Raiswell R., 1984. C/S method for distinguishing freshwater from marine sedimentary rocks. Geology, 12: 365-368.
- Berner, R.A., Baldwin, T., George R., and Holden, R. Jr., 1979. Authigenic iron sulfides as paleosalinity indicators. Journal of Sedimentary Petrology, 49: 1345-1350.
- Bilodeau, G, de Vernal, A., and Hillaire-Marcel, C., 1990. Postglacial Paleoceanography of Hudson Bay: Stratigraphic, Microfaunal and Palynological Evidence Canadian Journal of Earth Sciences, 27: 946-963.
- Bilodeau, G, de Vernal, A., Hillaire-Marcel, C., and Vincent, J.S., in press.

- Stratigraphie holocène du sud-est de la baie d'Hudson: corrélations micropaléontologiques entre une coupe des terrasses de la Grande Rivière de la Baleine et une carotte marine (87-028-069) Submitted to Géographie physique et Quaternaire.
- Biron, S., 1972. Pétrographie et pétrochimie d'un gîte de pépérites spilitiques des environs de Poste-de-la-Baleine, Nouveau-Québec M.Sc. Thesis, Laval University, Quebec, 85p.
- Boulton, G.S., 1975. Processes and patterns of subglacial sedimentation: a theoretical approach. *In*: A.E. Wright and F. Moseley, ed., Ice Ages: Ancient and Modern. Geological Journal Special Issue, 6, 7-42
- Cailleux, A. and Hamelin, L.E., 1970. Poste-de-la-Baleine (Nouveau Quebec), Exemple de géomorphologie complexe. Rev geomorph dynam, 19: 129-150.
- Chamberlain, E.J., and Gow, A.J., 1979. Effect of freezing and thawing on the permeability and structure of soils. Engineering Geology, 13, 73-92.
- d'Anglejan, B. and Biskham, G, 1988 Late winter-early spring sedimentation off the Great Whale River, southeastern Hudson Bay Canadian Journal of Earth Sciences, 25: 930-933
- Dredge, L.A. and Cowan, W.R., 1989. Quaternary geology of the southwestern Canadian Shield. *In*: R.J. Fulton, ed , Quaternary Geology of Canada and Greenland, Geology of Canada no.1, Geological Survey of Canada, Ottawa, p. 214-249.

- Dyke, A.S. and Prest, V.K., 1987. Late Wisconsinian and Holocene History of the Laurentide Ice Sheet. Géographie Physique et Quaternaire, 41: 237-263.
- Eyles, N. and Miall, A.D., 1984 Glacial facies. *In*: R.G. Walker ed., Facies models, Geological Association of Canada, St-John's, p. 15-38.
- Filion, L., and Morisset, P., 1984. Eolian landforms along the eastern coast of Hudson Bay, Northern Quebec. Nordicana, 47: 73-94.
- Flodd, R.D., 1983. Classification of sedimentary furrows and a model for furrow initiation and evolution Geological Society of America Bulletin, 94: 630-639.
- Gibbs, R.J., 1965. Error due to segregation in quantitative clay mineral X-ray diffraction mounting techniques. American Mineralogist, 50: 741-751.
- Grant, A.C., and Sanford, B.V., 1988, Bedrock geological mapping and basin studies in the Hudson Bay region

 In: Current Research, Part B, Geological Survey of Canada, Paper 88-1B 287-296.
- Gray, J.T and Lauriol, B., 1985. Dynamics of the Late Wisconsin Ice Sheet in the Ungava Peninsula interpreted from geomorphological evidence. Arctic and Alpine Research, 17: 289-310.
- Haselton, G.M., 1970 Marine beach investigations in the Richmond Gulf area, eastern Hudson Bay, Quebec (Part of 34C). Geological Survey of Canada, Paper 70-1A: 174-175.
- Hamelin, L.E. and Cailleux, A., 1972. Sucession des types de rivage pendant l'Holocène à Poste-de-la-Baleine (Nouveau-Québec). Zeitschrift für

- Geomorphologie N.F., 16: 16-26.
- Hardy, L., 1976. Contribution and de géomorphologique de la portion québécoise des basses terres de la vaie James, Ph.D. Thesis, McGill University, Montreal, 264p.
- Hardy, L., 1980. Complexe Grande Baleine Détroit de Manitounuk, Étude géomorphologique des littoraux: état naturel et répercussions probables des aménagements. Report 80-07-1 of SOGEAM to Hydro-Quebec, direction de l'environnement, Longueuil, 54p.
- Henderson, P.J., 1989. Data Report Description and composition of cores and grab samples. Hudson 87-028, Hudson Bay. Geological survey of Canada, Open-File Report 2081, 157p
- Hillaire-Marcel, C., 1976. La déglaciation et le relèvement isostatique sur la côte est de la Baie d'Hudson Cahiers de géographie de Québec, 20: 185-220.
- Hillaire-Marcel, C., 1979. Les mers post-glaciaires du Québec: quelques aspects

 Ph.D Thesis, University Pierre et Marie Curie, Paris VI, 1: 293p, 2: Fig.
- Hillaire-Marcel, C. 1980. Multiple Component Postglacial Emergence, Eastern Hudson Bay, Canada In: Mörner, ed, Earth rheology and isostasy, Wiley and Sons, New York, p. 215-230
- Hillaire-Marcel, C., et de Boutray, B., 1975. Les dépôts meubles de la région du Poste-de-la-Baleine (Nouveau-Québec) Nordicana, 38: 47p.
- Hillaire-Marcel, C., and Fairbridge, R.W., 1978 Isostasy and eustasy of Hudson Bay. Geology, 6: 117-122.

- Hillaire-Marcel, C, et Vincent, J.S., 1980. Stratigraphie de l'Holocène et évolution des lignes de rivages au sud-est de la baie d'Hudson, Québec, Paléo-Québec, 11: 165p.
- Hillaire-Marcel, C., Occhietti, S., and Vincent, J.S., 1981. Sakami moraine, Quebec: a 500-km-long-moraine without climatic control. Geology, 9: 210-214.
- Ingram, R.G., 1981. Characteristics of the Great Whale River Plume. Journal of Geophysical Research, 86: 2017-2023.
- Ingram, R.G., and Larouche, P, 1987 Variability of an Under-Ice River Plume in Hudson Bay. Journal of Geophysical Research, 92: 9541-9547.
- Josenhans, H.W. and Zevenhuizen, J., 1990. Dynamics of the Laurentide Ice

 Sheet in Hudson Bay, Canada Marine geology, 92: 1-26.
- Josenhans, H.W., Zevenhuizen, J, and Klassen R.A., 1986. The Quaternary geology of the Labrador Shelf. Canadian Journal of Earth Sciences, 23: 1190-1213.
- Josenhans, H.W., Balzer, S., Henderson, P., Nielson, E., Thorliefson, H., and Zevenhuizen, J., 1988 Preliminary seismostratiraphy and geomorphic interpretations of the Quaternary sediments of Hudson Bay. *In*: Current Research, Part B, Geological Survey of Canada, Paper 88-1B: 271-286.
- Josenhans, H., Zevenhuisen, J., and Veillette J., 1991 Baseline marine geological studies off Grande Rivière de la Baleine and Petite Rivière de la Baleine, southeastern Hudson Bay, *In*: Current Research, Part E, Geological Survey

- of Canada, Paper 91-1E: 347-354.
- King, L.H., Rokoengen, K., Fader, G.B.J., and Gunleiksrud, T., 1991. Till-tongue stratigraphy. Geological Society of America Bulletin, 103: 636-659.
- Kranck, S.H., 1951. On the geology of the east coast of Hudson Bay and James Bay. Acta geographica, 11 1-77.
- Leslie, R.J., 1964. Sedimentology of Hudson Bay, District of Keewatin. Geological Survey of Canada, Paper 63-48, 31p.
- Leslie, R.J., and Pelletier, B.R., 1965 Bedrock geology beneath Hudson Bay as interpreted from submarine physiography. Bedford Institute of Oceanography, Report 65-12, 18p
- Lewis C.F.M, and Sanford B V, 1972 Marine activities in Hudson Bay, 1971. *In*:

 Report of activities, Part A: April to October, 1971 Geological survey of

 Canada, Paper 72-1. 168-169
- Markham, W.E., 1986. The ice cover In I.P Martini, ed., Canadian Island Seas, Elsevier Oceanography Series, Vol. 44, Elsevier Science Publishers, New York, p. 101-116.
- Marsters, J., 1988. Physical properties program: Hudson 87-028, Hudson Bay.

 Geological Survey of Canada, Open-File Report 1593, 85p.
- Mosher, D.C. and Asprey, K.W., 1986 A technique for slabbing fine-grained sediment in piston cores. Journal of sedimentary petrology, 56: 565-567.
- Pelletier, B.R., 1966. Hudson Bay and Approaches; Part B. Bathymetry and geology. *In*: R. Fairbridge, ed., Encyclopedia of Earth Sciences, Vol. 1,

- Rheinhold Publishing Company, New York, p. 359-363.
- Pelletier, B.R., 1986. Chapter 8: Seafloor morphology and sediments. *In*: I.P. Martini, ed., Canadian Island Seas, Elsevier Oceanography Series, Vol. 44, Elsevier Science Publishers, New York, p. 143-162.
- Pelletier, B.R., Wagner, F.J.E., and Grant, A.C., 1968. Marine Geology. *In*: C.A. Beales, ed., Science, History and Hudson Bay, Vol. 2, Canadian Department of Energy, Mines and Resources, Ottawa, p. 557-613.
- Portmann, J.P., 1970. Présence de moraine de fond à Poste-de-la-Baleine, (Nouveau-Québec). Cahier de géographie de Québec, 32: 243-251.
- Portmann, J.P., 1971. Géomorphologie de l'aire myriamétrique de Poste-de-la-Baleine (Nouveau-Québec). Cahier de géographie de Québec, 34: 53-76.
- Portmann, J.P., 1972. Les dépôts quaternaires de l'estuaire de la Grande rivière de la Baleine, Nouveau-Québec. Revue de géographie de Montréal, 26: 208-214.
- Prisenberg, S.J., 1986a. The circulation pattern and current structure of Hudson Bay. *In*: I.P. Martini, ed., Canadian Island Seas, Elsevier Oceanography Series, Vol. 44, Elsevier Science Publishers, New York, p. 187-204.
- Prisenberg, S.J., 1986b. Salinity and temperature distributions of Hudson Bay and James Bay. *In*: I.P. Martini, ed., Canadian Island Seas, Elsevier Oceanography Series, Vol. 44, Elsevier Science Publishers, New York, p. 163-186
- Sanford, B.V., and Grant, A.C., 1990, New findings relating to the stratigraphy and

- structure of the Hudson Platform. *In* Current Research, Part D, Geological Survey of Canada, Paper 90-1D: 17-30.
- Shilts, W.W., 1986. Glaciation of the Hudson Bay Region. *In*: I.P. Martini, ed.,
 Canadian Inland Seas, Elsevier Oceanoraphy Series, Vol. 44, Elsevier
 Science Publishers, New York, p. 55-78
- Smith, N.D. and Ashley, G., 1985 Proglacial lacustrine environment. *In*: G.M Ashley, J. Shaw, and N.D. Smith ed., Glacial sedimentary environments, SEPM short course no 16, Society of Economic Paleontologists and Mineralogists, Tulsa, p. 135-214.
- Stanley, G.M., 1939. Raised beaches on east of James and Hudson bays.

 Geological Society of America Bulletin, 50: 1936-1937.
- Sturm, M., 1978. Origin and composition of clastic varves. *In*: C. Schlüchter ed., Moraines and varves; origin, genesis, classification: Proceedings of an INQUA Symposium on Genesis and Lithology of Quaternary Deposits, Zurich, p. 281-285.
- Syvitski, J.P.M., and Praeg, D.B., 1989 Quaternary sedimentation in the St. Lawrence Estuary and adjoining areas, Eastern Canada: an overview based on high-resolution seismo-stratigraphy. Géographie physique et Quaternaire, 43: 291-310.
- Thibault, M.T.H., 1989. Le Québec statistique 1989. 59° ed., Les publications du Québec 1989, Québec, 1028 p.
- Thompson, E., Koudys, A., Biggar, J., and Powell, M., 1985a. Pointe Walton to

- Merry Island. Scale, 1:50,000. Canadian Hydrographic Service Field Sheet 8269.
- Thompson, E., Koudys, A., Biggar, J., and Powell, M., 1985b. Approaches to Grande Rivière de la Baleine. Scale, 1:10,000. Canadian Hydrographic Service Field Sheet 8274.
- Thompson, E., Koudys, A., Biggar, J., and Powell, M., 1985c. Bear Island to Pointe Walton. Scale, 1:50,000 Canadian Hydrographic Service Field Sheet 8270.
- Vincent, J.S., 1989. Quaternary geology of the southeastern Canadian Shield. *In*:

 R.J. Fulton, ed., Quaternary Geology of Canada and Greenland, Geology

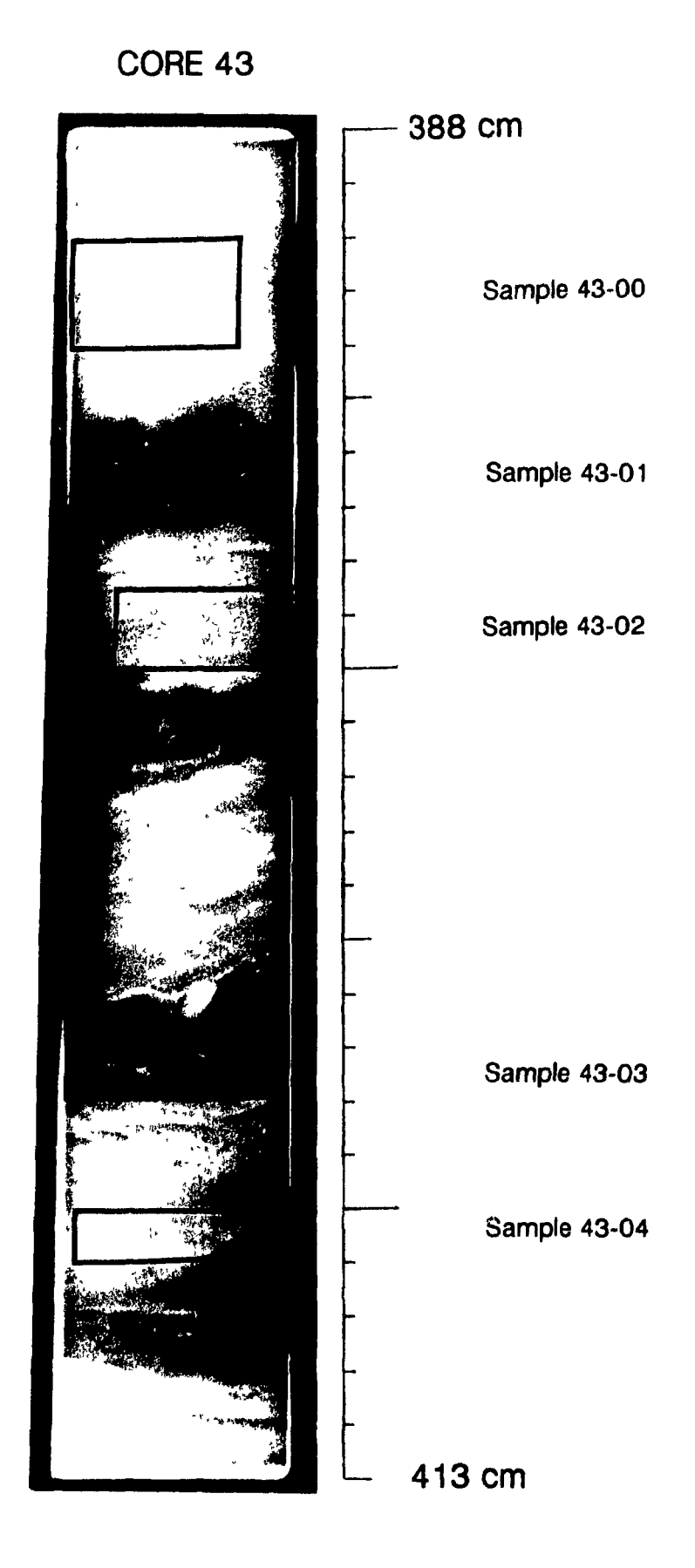
 of Canada no.1, Geological Survey of Canada, Ottawa, p. 249-275.
- Vincent, J.S., and Hardy, L., 1977 L'évolution et l'extension des lacs glaciaires Barlow et Ojibway en territoire québécois. Géographie Physique et Quaternaire, 31: 357-372.
- Vincent, J.S., Veillette, J.J., Allard, M., Richard, P.J.H., Hardy, L., and Hillaire-Marcel, C., 1987. Dernier cycle glaciaire et retrait des glaces de la vallée supérieure de l'Outaouais jusqu'au sud-est de la baie d'Hudson. 12° Congrès de l'INQUA, Excursion C-10, 87 p.
- Zevenhuizen, J., and Josenhans, H., 1988. CCGS Narwhal 1988 Eastern
 Hudson Bay nearshore survey cruise report. Geological Survey of Canada,
 Open File Report 1975, 33 p.

APPENDIX 1

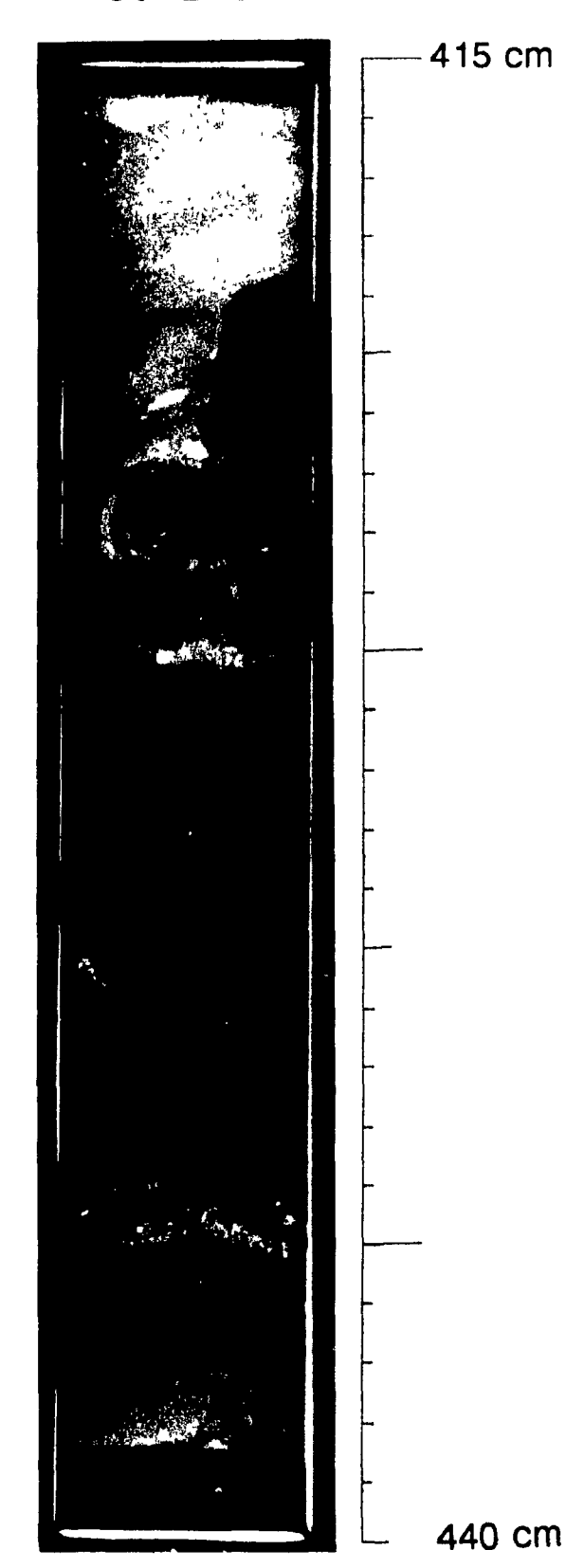
X-radiographic negative prints of core slabs from portions of cores 43, 48, and 69.

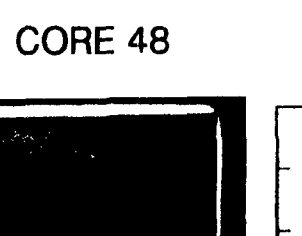
(For core localities, see Figure 5 in text).

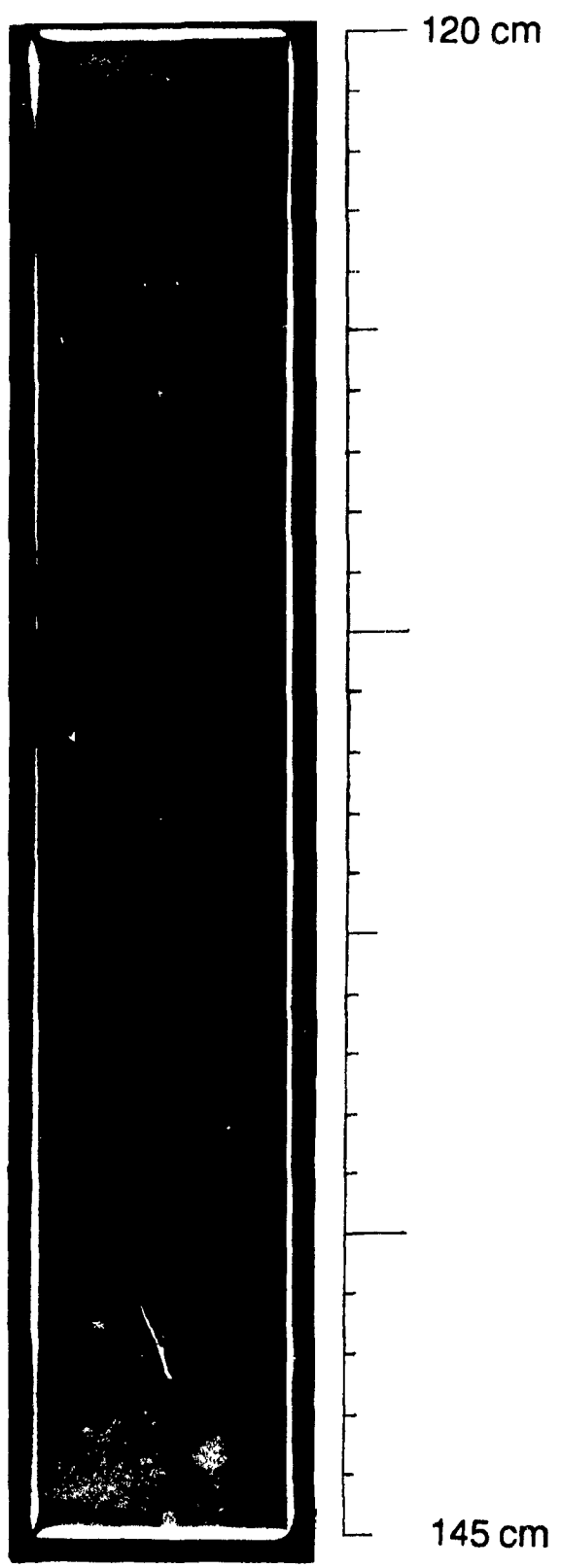
Positions of samples shown in Appendix 2 and in Tables 1, 2, and 3 are indicated beside the appropriate core slabs.

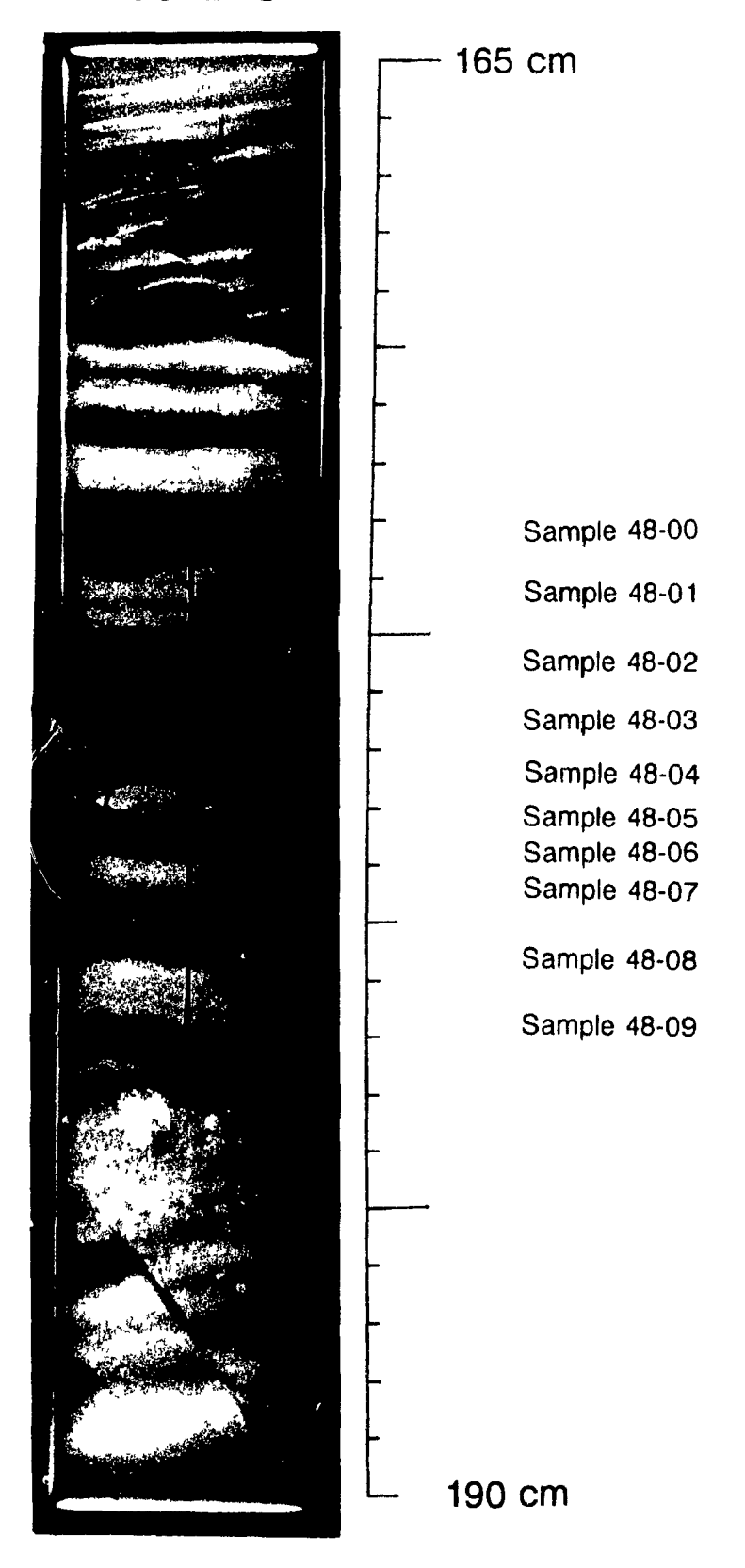


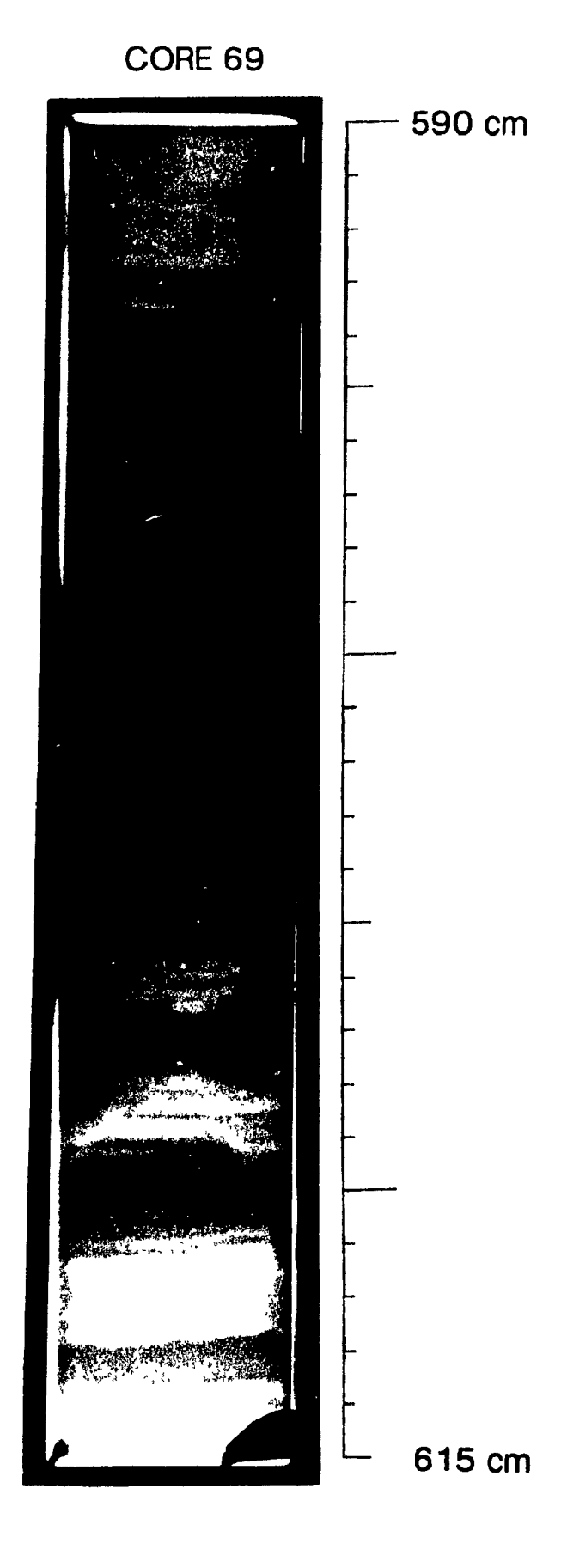




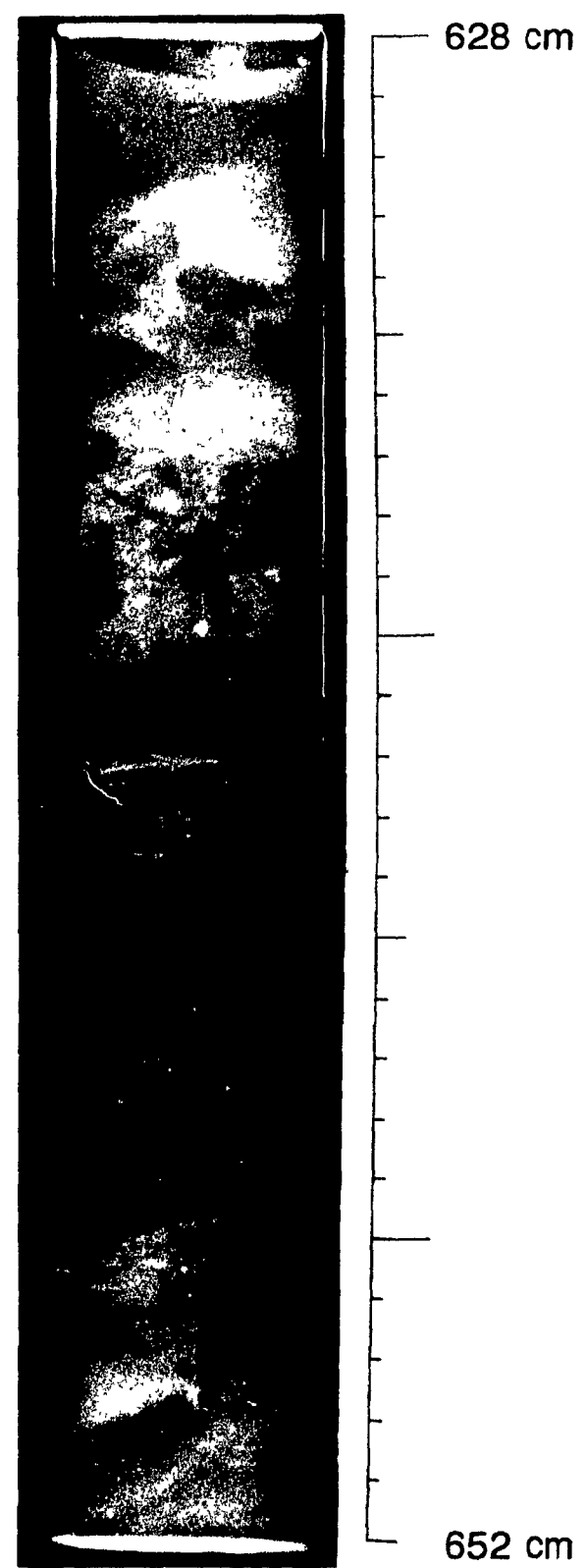




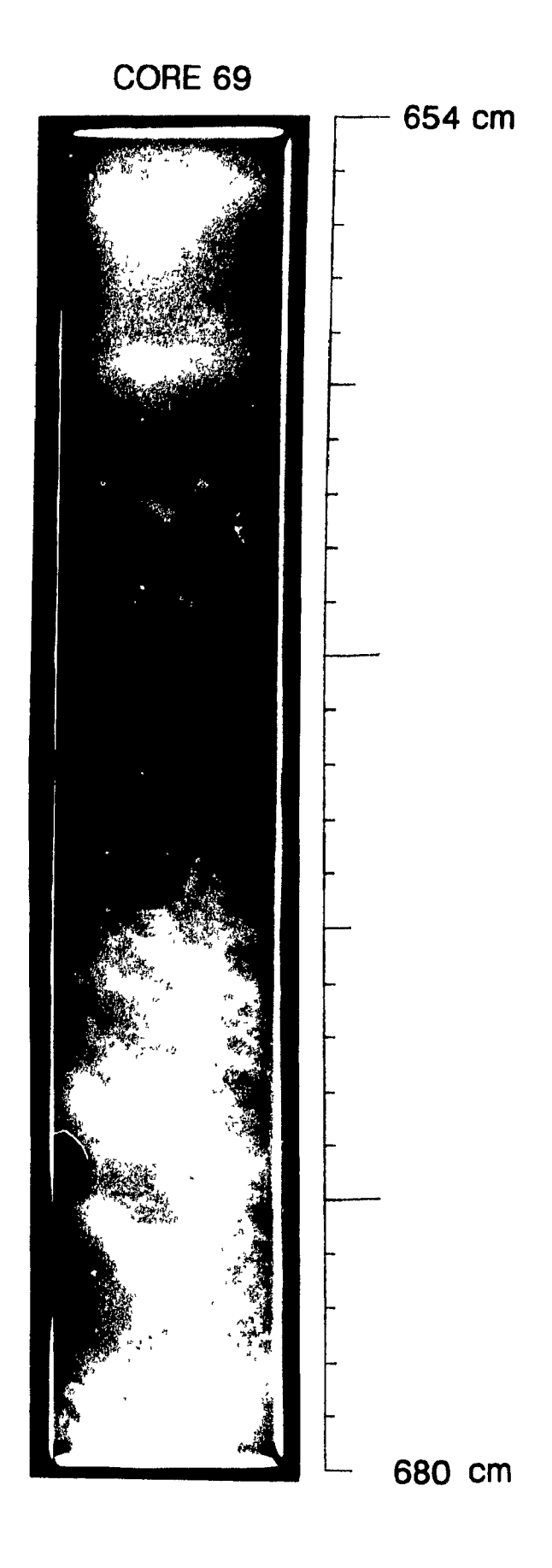












APPENDIX 2

X-ray diffractograms of samples 48-00, 48-01, and 48-02 from core 48.

(For core localities, see Figure 5 in text).

(Positions of samples are shown in Appendix 1).

Key to Symbols

C = Chlorite

V = Vermiculite

I = Illite

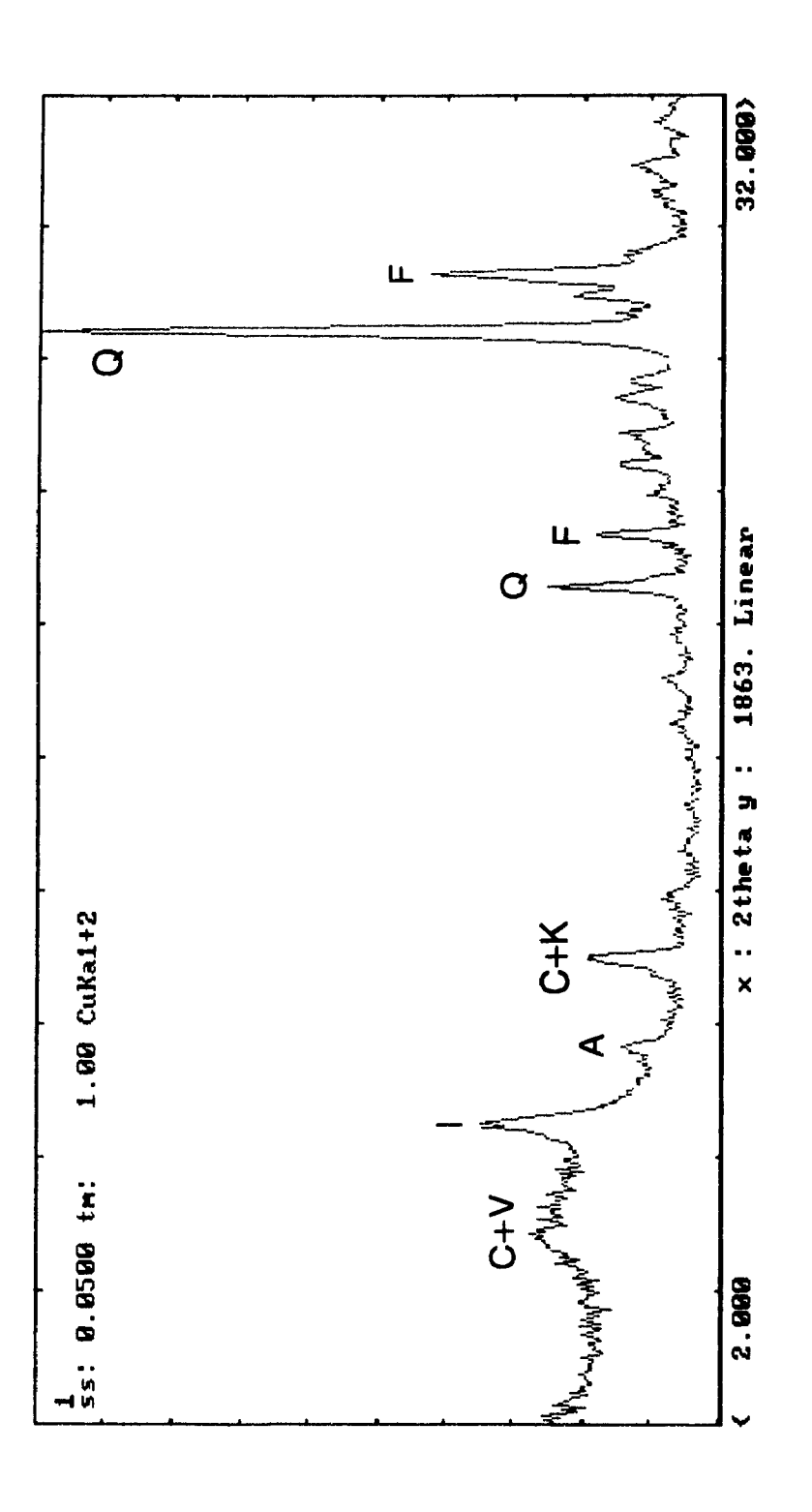
K = Kaolinite

A = Amphibole

Q = Quartz

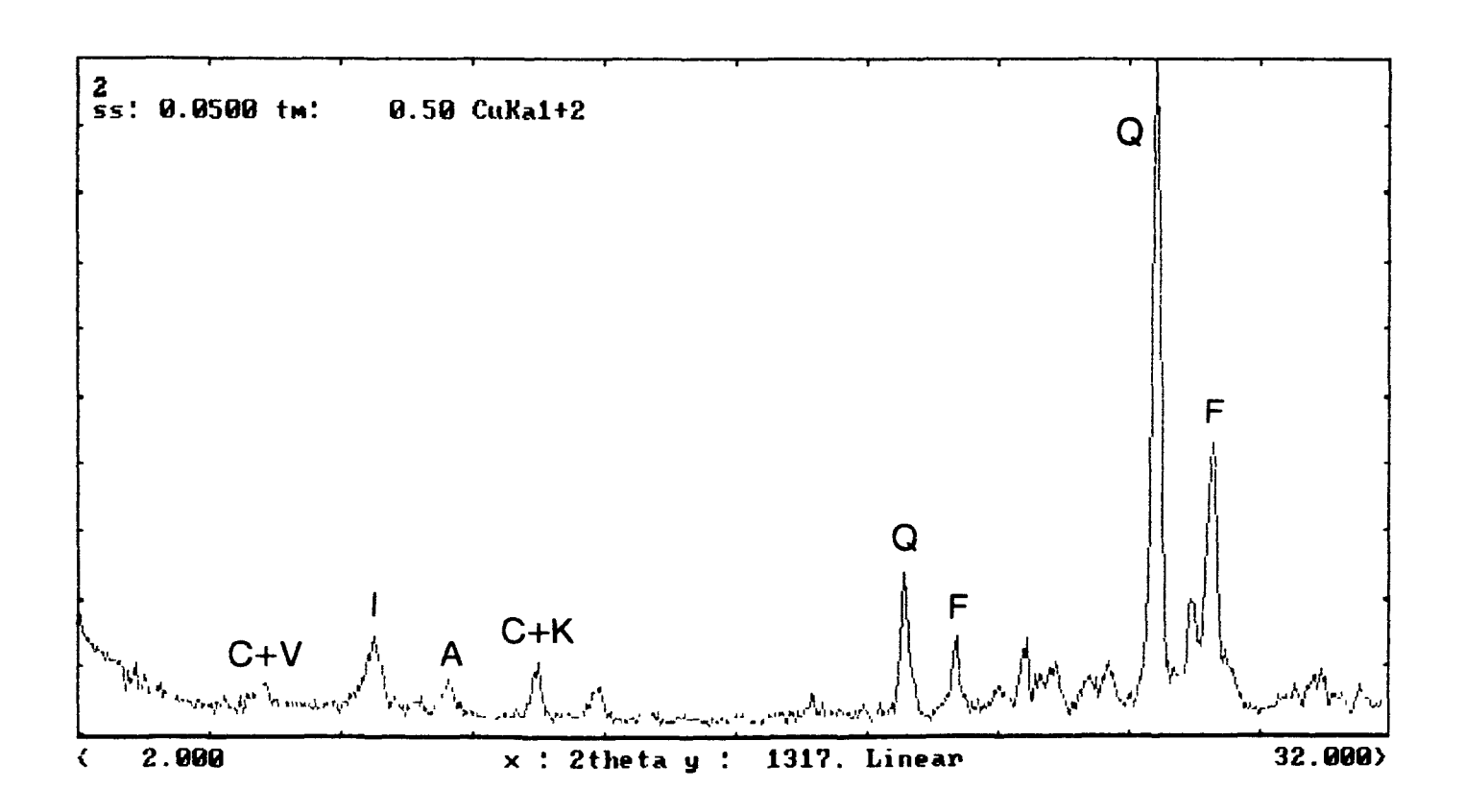
F = Feldspar

Sample 48-00 (light lamina)



Sample 48-01 (dark lamina)

1



\$ 3 F

Sample 48-02 (light lamina)

